

RESEARCH ARTICLE

10.1002/2013JD021172

Key Points:

- PM_{2.5} concentrations are estimated over Europe with a statistical algorithm
- The PM_{2.5} response to climate change is variable across Europe and complex
- It can be applied to PM_{2.5} observations from a dense monitoring network

Correspondence to:

È. Lecoœur,
eve.lecoeur@cerea.enpc.fr

Citation:

Lecoœur, È., C. Seigneur, C. Pagé, and L. Terray (2014), A statistical method to estimate PM_{2.5} concentrations from meteorology and its application to the effect of climate change, *J. Geophys. Res. Atmos.*, 119, 3537–3585, doi:10.1002/2013JD021172.

Received 12 NOV 2013

Accepted 21 FEB 2014

Accepted article online 25 FEB 2014

Published online 27 MAR 2014

A statistical method to estimate PM_{2.5} concentrations from meteorology and its application to the effect of climate change

Ève Lecoœur¹, Christian Seigneur¹, Christian Pagé², and Laurent Terray²

¹CEREA, Joint Laboratory École des Ponts ParisTech/EDF R&D, Université Paris Est, Marne-la-Vallée, France,

²CERFACS/CNRS, SUC URA1875, Toulouse, France

Abstract A statistical algorithm was developed to estimate PM_{2.5} concentrations over Europe based on a weather-type representation of the meteorology. We used modeled PM_{2.5} concentrations as pseudoobservations, because of a lack of PM_{2.5} speciated measurements over Europe, and included four meteorological variables. This algorithm was evaluated on the learning period (2000–2008) to test its ability to reproduce the pseudoobserved data set and then applied for two climatological scenarios (RCP4.5 and RCP8.5) and one historical (1975–2004) and two future periods (2020–2049 and 2070–2099). In Italy, Poland, and northern, eastern, and southeastern Europe, all future scenarios lead to decreases in PM_{2.5}, whereas in the Balkans, Benelux, the UK, and northern France, they lead to increases in PM_{2.5}. Considering each season separately shows stronger responses, which may vary for a given region and scenario. Decomposing the changes in PM_{2.5} concentrations as the sum of intertype and intratype changes, and a residual term shows that (1) the residual term is negligible; (2) intertype changes affect more the regions along the Atlantic Ocean; and (3) in most other regions, intertype and intratype changes are often on the same order of magnitude. The relationship between the atmospheric circulation and weather types evolves and therefore modifies the mean of meteorological variables and PM_{2.5} concentrations. This algorithm offers a novel approach to investigate the effect of climate change on air quality and can be applied to other pollutants, regions, and meteorological models. Furthermore, this approach can be applied using actual speciated PM_{2.5} observations, if a sufficiently dense monitoring network were available.

1. Introduction

Air pollution is strongly sensitive to meteorological conditions and is, therefore, likely to be affected by climate change. Among air pollutants of current public health concern, fine particulate matter with an aerodynamic diameter less than 2.5 μm (PM_{2.5}) is of particular interest because it is a complex mixture of particles of different sizes and chemical compositions and its relationship to meteorological variables can, therefore, be complex. PM_{2.5} includes primary components, which are directly emitted in the atmosphere from various anthropogenic and natural sources (e.g., road traffic, construction sites, sea salt, soil dust, and fires), and secondary components, which are formed in the atmosphere via chemical reactions. Nitrate (NO₃⁻), sulfate (SO₄⁼), and ammonium (NH₄⁺) are the major secondary inorganic components of PM_{2.5}; in Europe, they typically account for 3 to 8 μg m⁻³ of PM_{2.5} annual concentrations at regional sites and urban areas and up to 4 to 13 μg m⁻³ in intensively industrialized regions or heavily polluted areas [Querol *et al.*, 2004]. Carbonaceous PM includes both primary components, such as black carbon (BC) and some organic compounds, and secondary components, which comprise a large number of organic compounds of anthropogenic and biogenic origins. In Europe, carbonaceous PM_{2.5} annual concentrations range from about 1 μg m⁻³ in the rural background to over 20 μg m⁻³ at monitoring sites located near traffic [Querol *et al.*, 2004]. Many PM_{2.5} compounds are semivolatile, which implies that they partition between the gas phase and the particulate phase as a function of temperature, relative humidity, and PM_{2.5} composition and concentration.

All the studies focusing on the impact of climate change alone on PM_{2.5}, including this one, are summarized in Table 1. Jacob and Winner [2009] reviewed a number of studies that used chemical transport models (CTMs) driven by general circulation models (GCMs) to investigate the effects of climate change on air quality. Many studies pertained to North America [Steiner *et al.*, 2006; Dawson *et al.*, 2007; Zhang *et al.*, 2008; Mahmud *et al.*, 2008; Chen *et al.*, 2009; Dawson *et al.*, 2009; Tai *et al.*, 2010; Mahmud *et al.*, 2010; Jiang *et al.*,

Table 1. Review of the Studies That Have Investigated the Impact of Climate Change (Alone) on PM_{2.5} Concentrations

References	Domain Covered	GCM	CTM	Horizontal Resolution	Scenario	Projection	Averaging Period	Major Findings (μg m ⁻³ , Except Stated Otherwise)
Liao et al. [2006], Rocherla and Adams [2006]	Global	GISS GCM	GISS GCM	4° × 5°	A2	2100 versus 2000	Annual mean	Central Europe: +1 (SO ₄ ⁻), U.S.: +0.5–1 (carbonaceous) Eastern U.S.: +1 (SO ₄ ⁻)
Tagaris et al. [2007]	U.S.	GISS GCM	CMAQ	36 km	A1B	2050 versus 2000	Annual mean	U.S.: -10% (PM _{2.5})
Heald et al. [2008]	Global Urban	AGCM	CAM-Chem	2° × 2.5°	A1B	2100 versus 2000	Annual mean	Eastern U.S.: +0.5 (OM)
Zhang et al. [2008]	U.S.	PNNL-MM5	CMAQ	36 km	A1B	2050 versus 2000	JJA mean	[-8.7; 0] (PM _{2.5}), [-4.3; 0] (SO ₄ ⁻), [-1.8; 0] (OM)
Pye et al. [2009]	Global	GISS GCM III	GEOS-Chem	4° × 5°	A1B	2050 versus 2000	Annual mean	U.S.: [-0.3; 0.3] (SO ₄ ⁻), [-0.2; 0] (NO ₃ ⁻)
Dawson et al. [2009]	U.S.	GISS GCM II	CAMx	4° × 5°	A2	2050 versus 2000	January mean	-0.33 (PM _{2.5}), -0.17 (SO ₄ ⁻), -0.01 (NO ₃ ⁻), -0.04 (NH ₄ ⁺), -0.04 (SOA), -0.08 (POA)
Awise et al. [2009]	U.S.	PCM	CMAQ	36 km	A2	2050 versus 2000	July mean	+2.48 (PM _{2.5}), +1.37 (SO ₄ ⁻), +0.03 (NO ₃ ⁻), +0.5 (NH ₄ ⁺), +0.54 (SOA), +0.03 (POA)
Mahmud et al. [2010]	California	WRF	CIT-UCD	8 km	A1B	2050 versus 2000	July mean	-1 (PM _{2.5})
Kelly et al. [2012]	North America	CGCM/CRCM	AURAMS	45 km	A2	2050 versus 2000	Annual mean	[-1.1; -0.6] (PM _{2.5})
Tai et al. [2012b]	U.S.	15 IPCC AR4 GCMs			A1B	2050 versus 2000	JJA mean	[-0.5; 1.7] (PM _{2.5})
Jiménez-Guerrero et al. [2012]	Iberian Peninsula	ECHO-G/MM5	CHIMERE	3.75° × 2.5°	A2	2100 versus 2000	Annual mean	[-0.6; 0.6] (PM _{2.5})
Manders et al. [2012]	Europe	RACMO2	LOTOS-EUROS	0.44°	A1B	2050 versus 2000	Annual mean	+2 (SO ₄ ⁻), +2.5 (SOA)
Colette et al. [2013]	Europe	ISPL-CM5/WRF	CHIMERE	0.5°	RCP2.6 and RCP8.5	2050 versus 2000	Annual mean	[-1; 1] (PM ₁₀)
Hedegaard et al. [2013]	Northern Hemisphere	ECHAM5	DEHM		RCP4.5	2100 versus 2000	Annual Mean	[-4.1; -2.3] (PM _{2.5})
This work	Europe	CNRM-CM5	Polair3D	0.5°	RCP4.5 and RCP8.5	2050 versus 2000 and 2100 versus 2000	Annual and seasonal means	[-40; 15] (PM _{2.5}) See below

2010; Lam *et al.*, 2011; Kelly *et al.*, 2012; Tai *et al.*, 2012a, 2012b; Singh and Palazoglu, 2012]. This large body of studies for North America is in part due to the fact that PM_{2.5} regulations exist in the U.S. since 1997 and in Canada since 2000, whereas PM_{2.5} has only been regulated in Europe in 2008. Moreover, such research has been a priority in North America, especially in the U.S. Accordingly, an increasing number of studies now focus on Europe [Jiménez-Guerrero *et al.*, 2011, 2012; Galindo *et al.*, 2011; Manders *et al.*, 2012; Hedegaard *et al.*, 2013]. These studies agree on the effect of the major meteorological variables on PM_{2.5} concentrations. First, precipitation removes all PM_{2.5} components from the atmosphere. Second, increased wind speed leads to changes in transport and dilution resulting in lower PM_{2.5} but increases emissions of sea salt and soil dust. Third, changes in the planetary boundary layer (PBL) height affect dilution. Fourth, absolute humidity increases PM_{2.5}. Finally, temperature favors formation of sulfate and emissions of biogenic volatile organic compounds (VOC) and their oxidation to semivolatile organic compounds (SVOC) but increases SVOC volatility. When the effect of the climate change includes associated changes in anthropogenic emissions, most studies find that annual PM_{2.5} concentrations will decrease in the United States [Tagaris *et al.*, 2007; Avise *et al.*, 2009; Lam *et al.*, 2011; Kelly *et al.*, 2012]. However, the results vary when investigating the sole effect of climate change. Dawson *et al.* [2009] concluded that climate change alone leads to a decrease in January of 0.3 $\mu\text{g m}^{-3}$ and an increase in July of 2.5 $\mu\text{g m}^{-3}$ in the eastern U.S. Kelly *et al.* [2012] found that climate change will lead to worse air quality compared to current conditions, but Zhang *et al.* [2008] found a decrease in PM_{2.5} concentrations due to climate change in the U.S. Therefore, there is no consensus on the effect of climate change alone on PM_{2.5} concentrations, and the overall agreement on the decrease of PM_{2.5} concentrations in future years appears to be driven by the decrease in emissions of PM_{2.5} and its precursors.

Other studies considered climate as a succession of atmospheric situations rather than an ensemble of meteorological variables that can be examined individually. Thishan Dharshana *et al.* [2010] established connections between day-to-day variability of sea level pressure, surface air temperature, and precipitation and that of PM_{2.5} concentrations over the U.S. Ménégoz *et al.* [2010] studied the winter interactions between weather regimes and some PM_{2.5} components (SO₄²⁻, BC, and soil dust) over the North Atlantic European region and showed that atmospheric dynamic processes associated with the different weather regimes can impact sulfate and BC concentrations by up to 25% and dust concentrations by up to 80%. Tai *et al.* [2012b] studied the effect of 2000–2050 climate change on PM_{2.5} over the U.S. They first analyzed the 1999–2010 observations of eight meteorological variables to identify the dominant meteorological modes driving PM_{2.5} variability in different regions of the U.S. and their synoptic periods (PM_{2.5} observations came from the U.S. Environmental Protection Agency Air Quality System over 1999–2010). They projected the changes in frequency of these meteorological modes simulated by 15 GCM following the scenario A1B from the Intergovernmental Panel on Climate Change (IPCC) and found that general circulation affects PM_{2.5} in the eastern and northwestern U.S., temperature affects PM_{2.5} in the southeastern U.S. (organic matter and nitrate mainly), vegetation dynamics affects organic matter (OM) in the midwestern and western U.S., and wildfires affect both organic matter and BC in the northwestern U.S. These approaches are based on the relationships between patterns, such as weather regimes and PM_{2.5} concentrations. Changes in emissions are, therefore, limited to those influenced by meteorological variables (e.g., biogenic emissions, soil dust, and sea salt emissions).

Therefore, the goal of this study is to develop a statistical method, based on synoptic climatology, which estimates PM_{2.5} concentrations from a few meteorological variables and to apply it to investigate the impact of climate change on PM_{2.5} concentrations. Such an approach is based on statistics and linear regression, which allows one to perform this experimentation over 30 year periods for both climate and PM_{2.5}, to include more scenarios, and to discuss the results on both annual and seasonal bases.

Anthropogenic emissions are kept constant to isolate the effect of climate change alone, but biogenic and sea salt emissions implicitly change with changes in meteorological variables. Here the estimation of the relationships of PM_{2.5} to major meteorological variables is obtained from a model simulation because of the lack of sufficient PM_{2.5} data over Europe. However, the method is applicable to PM_{2.5} observations (if a sufficient monitoring network exists), which could remove some of the uncertainties associated with semivolatile PM.

The statistical algorithm and the necessary data are presented in section 2. The algorithm is then evaluated in section 3. It is applied to two climate scenarios from the Coupled Model Intercomparison Project Phase 5 (CMIP5) exercise in section 4. Conclusions and recommendations for future work are presented in section 5.

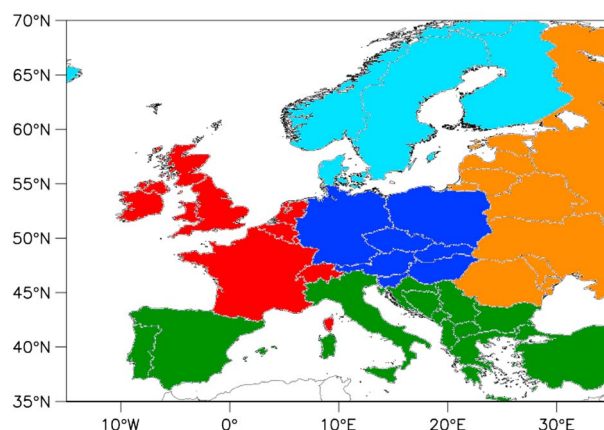


Figure 1. Study domain, with highlights of five subregions: western Europe in red, central Europe in dark blue, northern Europe in light blue, southern Europe in green, and eastern Europe in orange.

2. Data and Methods

The algorithm presented here estimates $PM_{2.5}$ concentrations over Europe (Figure 1) for any time period from some specific meteorological variables and from $PM_{2.5}$ observations (or pseudoobservations) over a long past time period. Sections 2.1 and 2.2 present the meteorological variables needed and an overview of the statistical algorithm, respectively. Finally, the algorithm is presented in section 2.3.

2.1. $PM_{2.5}$ Pseudoobservations and Meteorological Variables Over Europe

The regulation of $PM_{2.5}$ over Europe is recent and does not concern $PM_{2.5}$ speciation. Hence, there is a lack of observed $PM_{2.5}$ concentrations with speciation over a long time period, over the whole Europe, and on a daily basis. Consequently, we use here the results of the 9 year (2000–2008) simulation of *Lecœur and Seigneur* [2013] as $PM_{2.5}$ pseudoobservations for this statistical method. The long duration of the simulation allows us to assume that the effect of the interannual atmospheric variability on the $PM_{2.5}$ concentrations is taken into account, without being influenced significantly by changes in anthropogenic emissions. We have evaluated this simulation by conducting both operational and dynamic evaluations, using available observations from the European Monitoring and Evaluation Programme (EMEP) [*Lecœur and Seigneur*, 2013]. The operational evaluation showed that the concentrations of $PM_{2.5}$ and its main components (sulfate, nitrate, ammonium, and carbonaceous compounds) are well estimated. In particular, ozone (O_3), $PM_{2.5}$, and SO_4^{2-} meet the performance goal of *Boylan and Russell* [2006]. NO_3^- and NH_4^+ concentrations are overestimated, but NH_4^+ still meets the performance criteria (see Table 2). The overestimation of NO_3^- and NH_4^+ is the main drawback of the actual CTMs. In the simulation of *Lecœur and Seigneur* [2013], this overestimation results from a combination of factors. First, artifacts in the measurement methods, due to the volatilization of ammonium nitrate (NH_4NO_3) from filters, can contribute to the model overestimation. Second, the overestimation of NO_3^- could be due to the slight underestimation of SO_4^{2-} by the model, because less ammonia is then neutralized by SO_4^{2-} , favoring more formation of NH_4NO_3 . Also, there is still a significant uncertainty about ammonia emissions, including their magnitude and temporal variability. Finally, taking the mean over 5 years to generate pseudoclimatological boundary conditions for aerosols and gases is also a source of uncertainty. The comparison with other 1 year model

Table 2. Operational Evaluation of the Model Using the Correlation Coefficient ρ and the Relative Error e_r Between Simulated and Observed Data (%), and the Criteria of *Boylan and Russell* [2006] for PM and Its Components^a (Expressed in %)

Years	$PM_{2.5}$				SO_4^{2-}				NO_3^-				NH_4^+			
	ρ	e_r	MFB	MFE	ρ	e_r	MFB	MFE	ρ	e_r	MFB	MFE	ρ	e_r	MFB	MFE
2000	51	64	55	62	59	36	28	48	27	255	89	103	48	200	84	89
2001	62	18	25	42	53	4	0	45	29	89	3	93	47	27	1	55
2002	60	31	36	50	60	-7	-6	44	43	64	25	84	51	29	-7	55
2003	62	14	25	45	60	-7	-9	43	52	57	28	76	71	83	43	59
2004	60	10	22	42	57	0	-3	40	39	80	29	83	67	40	-5	52
2005	60	24	33	48	50	-9	-7	45	39	65	6	86	55	50	7	57
2006	53	5	0	40	56	-18	-12	44	51	21	5	71	56	38	23	50
2007	69	30	37	53	57	-5	-3	41	44	53	8	78	61	50	24	47
2008	51	12	25	47	56	-11	-7	39	49	41	-8	75	65	44	17	40
2000–2008	59	20	29.8	47.4	56	-4	-2.1	43.2	42	80	20.5	83.2	58	55	20.8	56

^aThe performance goal (respectively, criterion) is met when $|MFB| < 30\%$ (60%) and $MFE < 50\%$ (75%) for PM modeling. $MFB = \frac{1}{N} \sum_{i=1}^N \frac{sim - obs}{(sim + obs)/2}$ (%) and $MFE = \frac{1}{N} \sum_{i=1}^N \frac{|sim - obs|}{(sim + obs)/2}$ (%), where N is the number of observed/simulated data at a given station.

simulations over Europe showed that all models overestimate NO_3^- . The performance for $\text{PM}_{2.5}$, SO_4^{2-} , and NH_4^+ is comparable to that of the other models [Lecœur and Seigneur, 2013].

The model also shows satisfactory results for OM and Elemental Carbon (EC) [Couvidat *et al.*, 2012]. The dynamic evaluation showed that the response of the simulated $\text{PM}_{2.5}$ to changes in meteorology is correctly reproduced by the model. The evolution of $\text{PM}_{2.5}$ as a function of changes in meteorology is well represented for precipitation and wind speed overall, although the model tends to overestimate the $\text{PM}_{2.5}$ response to wind speed. This overestimation could be due to the fact that measurements at the EMEP stations respond to a very local wind speed, which cannot be captured exactly by a model which has a 0.5° (about 50 km) horizontal resolution. The relationship between $\text{PM}_{2.5}$ components and temperature is complex, and the $\text{PM}_{2.5}$ response to changes in temperature varies depending on the station and the PM component. The sign of the response is always well reproduced by the model [Lecœur and Seigneur, 2013]. Some uncertainties remain concerning semivolatile species, which is also the case for all the CTM studies mentioned above. Based on these results, we consider that $\text{PM}_{2.5}$ concentrations obtained with this simulation are suitable to be used as pseudoobservations to investigate the effects of climate change on $\text{PM}_{2.5}$ [Lecœur and Seigneur, 2013].

Four meteorological variables are used as predictors in the first step of the algorithm. We choose to use the pressure at sea level (PSL), the surface air temperature, precipitation, and the surface wind speed for the 2000–2008 period, as they are considered to be the meteorological variables that affect $\text{PM}_{2.5}$ concentrations the most [Dawson *et al.*, 2007; Mahmud *et al.*, 2010; Galindo *et al.*, 2011]. The PBL height and humidity are also influential, but the former is not a meteorological variable per se and the latter is not available in meteorological projections. For the learning period, PSL, temperature, precipitation, and wind speed are given by the ECMWF analyses and reanalyses with the following horizontal resolutions: 1.125° for 2000, 0.36° for 2001–2005, and 0.25° for 2006–2008. The reanalyses at 1.125° were interpolated, and those at 0.36° or 0.25° were aggregated to match the same grid as the $\text{PM}_{2.5}$ pseudoobservations (0.5° over Europe).

2.2. Weather Types

The concept of weather regimes was first introduced in the 1950s in synoptic climatology. Weather regimes are recurrent patterns that are representative of the large-scale circulation (LSC) over a specific region. Each weather regime defines a group of days with similar LSC and is closely related to a specific weather over the specific region. Since the atmospheric circulation is not the same over the whole year over the midlatitudes and high latitudes, these LSC depend on seasons. The four seasons are defined as follows: winter is noted as DJF for December-January-February, summer as JJA for June-July-August, spring as MAM for March-April-May, and autumn as SON for September-October-November. The most common weather regimes over the North Atlantic and Europe have been defined and analyzed by Vautard [1990]. He showed that four recurring weather regimes can be defined per season. Since the local meteorology affects $\text{PM}_{2.5}$, so should the weather regimes. For example, Ménégoz *et al.* [2010] showed that the blocking weather regime in winter, which is characterized by an anticyclonic situation over Europe, leads to more BC and SO_4^{2-} concentrations than those characterized by a cyclonic situation (e.g., Atlantic Ridge and NAO⁻). Thishan Dharshana *et al.* [2010] have found similar results over the U.S. Weather regimes are built with a classification algorithm, which is performed using the first 10 principal components of an Empirical Orthogonal Function (EOF) of a variable that is representative of the LSC (typically PSL). However, common weather regimes are not properly adequate to investigate the impacts of climate on a specific variable such as $\text{PM}_{2.5}$ because they do not reflect the meteorological variables that are the most influential for $\text{PM}_{2.5}$. In this case, the term *weather types* has been introduced. Weather types are improved weather regimes, in the sense that they are built to be more representative of the effect of meteorology on the variable of interest. We used the software package DSclim, developed by Pagé *et al.* [2009], to build these weather types (Figure 2). DSclim provides an innovative statistical downscaling methodology based on weather typing, as an alternative to dynamic downscaling methods, which are very expensive in terms of CPU and disk space. Indeed, statistical techniques do not require much computing since they rely on simple regression analyses between large-scale atmospheric fields and regional-scale fields. This methodology has already been used to provide downscaled climate scenarios over France for many groups in the climate impacts community. The building of weather types is only a part of what this package provides. The classification of the LSC variable is based on a clustering with a *k*-means automatic partitioning algorithm [Michelangeli *et al.*, 1995]. Clusters are randomly initialized in the EOF space. Each day is then attributed to one of those clusters depending on their distance to it. Clusters are then redefined by taking the barycenter of each cluster cloud. This

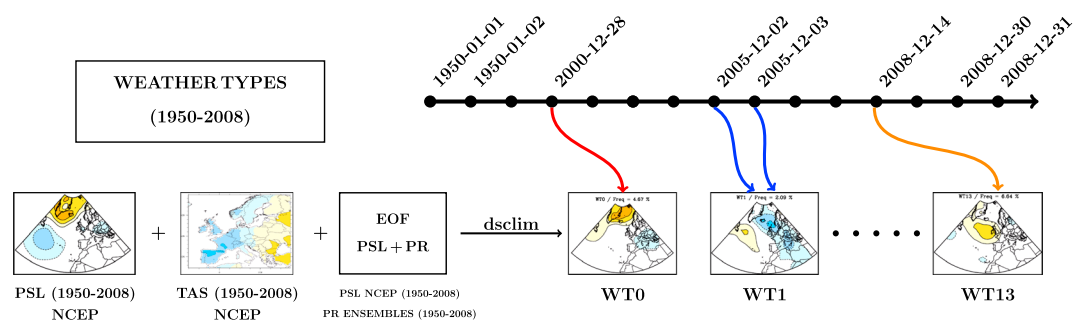


Figure 2. Building weather types over the learning period. Pressure (PSL) and temperature (TAS, only for summer) anomalies from NCEP reanalyses are projected on the space composed by the EOF of PSL and of precipitation (PR). Dsclim classifies these anomalies and attributes each day of the 1950–2008 period to one of the 14 WTs.

last step is repeated until the barycenters of each cluster cloud do not move anymore between two steps [Michelangeli *et al.*, 1995]. It is performed using the first 10 principal components of an EOF space composed of both the LSC variable (here the PSL) and a local-scale variable, which has an impact on the variable of interest. Precipitation has been chosen as this locale-scale variable, as many studies emphasize the role of changing precipitation intensity and area on $PM_{2.5}$ concentrations [Racherla and Adams, 2006; Tagaris *et al.*, 2007; Chen *et al.*, 2009; Lecœur and Seigneur, 2013]. We could have used another variable, such as temperature. This would have led to different spatial structures, but the method would have stayed the same. Furthermore, the effects of precipitation on $PM_{2.5}$ and its components are relatively straightforward and are better understood than those of temperature. In the classification algorithm, each season is treated separately. In the *k*-means partitioning algorithm, the number of clusters is chosen a priori. In this case, 14 weather types are built per season, which is in agreement with the numbers of clusters listed in the weather-type data base [Philipp *et al.*, 2010]. The 14 weather types are represented by a map of the PSL anomaly (i.e., the difference between the average PSL for a given weather type and the seasonal average PSL). These weather types are described in Appendix G, Figures G1–G4. They have each a discriminating power regarding the $PM_{2.5}$ concentrations defined as $\rho = \frac{\text{variance}(PM_{2.5})^{WT}}{\text{variance}(PM_{2.5})^{season}}$. The smaller ρ is, the more the weather type (WT) has a discriminating power on the $PM_{2.5}$ concentrations. Therefore, the discriminating power of a weather type regarding $PM_{2.5}$ can be very different from a region to another.

For this classification, we use the NCEP reanalysis over the 1950–2008 period for both PSL and temperature. Precipitation is given by the E-OBS (<http://eca.knmi.nl/download/ensembles/ensembles.php>) data set over the same period. Thus, each day of the 1950–2008 period is classified to the nearest weather type. The distance between a day and a weather type is computed in terms of PSL. As a day and a weather type are both represented here by their daily maps of pressure, these two maps can be considered as two vectors of dimensions (number of latitude points \times number of longitude points). We then compute the euclidian distance between these two vectors.

2.3. The Statistical Algorithm

The statistical algorithm consists of two steps: the regression step and the analog step. This algorithm needs to be developed and evaluated first on a past period (the learning period; here 2000–2008) before being applied to historical and future periods. The regression step for the learning period is fundamental, as it provides the basis for the regression step of historical and future periods. We recall that each season is processed independently in this algorithm.

2.3.1. The Learning Period

The algorithm is developed over the 2000–2008 learning period and subsequently for that same period to check whether the algorithm is able to reconstruct the $PM_{2.5}$ concentrations over the period. Each day of the learning period has pseudoobserved $PM_{2.5}$ concentrations, as well as a daily value of PSL, temperature, precipitation, and wind speed. Moreover, each day of this period is associated with one of the 14 weather types and is at a certain distance in terms of PSL of each one of the 14 weather types. A similar approach has already been applied to hydrology [Boé *et al.*, 2006] and to surface winds [Najac *et al.*, 2009] in France.

In the *regression step*, the variable of interest is expressed for any time step with a regression equation whose predictors are variables reflecting the weather types and some meteorological variables that impact the

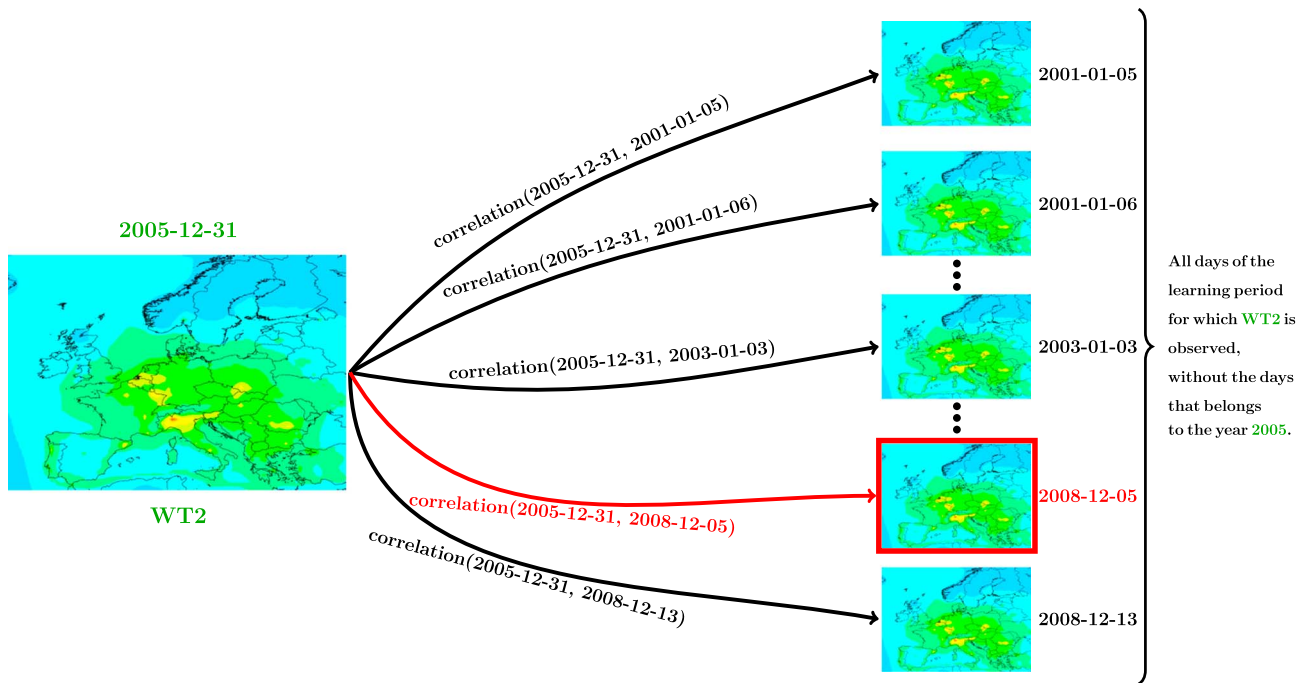


Figure 3. Resampling $PM_{2.5}$ pseudoobservations over the learning period: finding the analog day of 5 December 2005. All days of the learning period for which WT2 is observed (minus the days belonging to year 2005) are displayed on the right-hand side of the Figure. The spatial correlation between these maps are computed. The best correlation is provided by 5 December 2008 (in red).

variable of interest. The choice of the variables used in the regression equation is discussed in section 3. It is important that the variable of interest has a normal distribution to use a regression equation. $PM_{2.5}$ concentrations have a lognormal distribution (see Figure 7c). Thus, we express the logarithm of the $PM_{2.5}$ concentrations at the location (x, y) for any day t (noted $\ln(PM_{2.5}^p(t, x, y))$) as a linear combination of the distance of day t to the most discriminating weather types for the location (x, y) , noted $d(t, WT_i(x, y))$ and of the temperature $(X_1(t, x, y))$, precipitation $(X_2(t, x, y))$, wind speed $(X_3(t, x, y))$, and PSL $(X_4(t, x, y))$ (see equation (1)). The first three variables correspond to those for which the $PM_{2.5}$ model was tested in terms of its ability to reproduce changes in $PM_{2.5}$ due to changes in meteorology [Lecœur and Seigneur, 2013]. Since the discriminating power of a weather type depends on location, the number of weather types considered, noted $N(x, y)$, depends on the location (x, y) .

$$\begin{pmatrix} \ln(PM_{2.5}^p(t_0, x, y)) \\ \ln(PM_{2.5}^p(t_1, x, y)) \\ \vdots \\ \ln(PM_{2.5}^p(t_n, x, y)) \end{pmatrix} = \sum_{i=1}^{N(x,y)} a_i(x, y) \times \begin{pmatrix} d(t_0, WT_i(x, y)) \\ d(t_1, WT_i(x, y)) \\ \vdots \\ d(t_n, WT_i(x, y)) \end{pmatrix} + \sum_{j=1}^4 b_j(x, y) \times \begin{pmatrix} X_j(t_0, x, y) \\ X_j(t_1, x, y) \\ \vdots \\ X_j(t_n, x, y) \end{pmatrix}. \quad (1)$$

After solving this regression equation at each location, we obtain regression coefficients $(a_i(x, y))_{i=1, N(x,y)}$ and $(b_j(x, y))_{j=1,4}$. We use them to approximate the logarithm of the $PM_{2.5}$ concentrations on the present period, noted $\ln(PM_{2.5}^{p-REG}(t, x, y))$, since all the terms on the right-hand side of equation (1) are known.

The *analog step* consists in resampling the pseudoobserved $PM_{2.5}$ concentrations over the learning period with the following method. Let t be a day of the learning period (e.g., 31 December 2005 in Figure 3) and WT_t (WT2 in Figure 3) the associated weather type. We consider the subset E_t of days in the learning period for which WT_t is also observed, excluding all days in the same year as t (so that we make sure not to resample day t with itself). Thus, E_t contains all days with similar LSC as t . These days are represented on the right of Figure 3. The spatial correlation between the maps $\ln(PM_{2.5}^{p-REG}(t, x, y))$ and $\ln(PM_{2.5}^{p-REG}(j, x, y))$ is computed for all j in E_t . Let j_{max} be the day for which the spatial correlation with t is maximal ($j_{max} = 5$ December 2008 in Figure 3).

The pseudoobserved value of the $PM_{2.5}$ concentrations on day j_{max} is attributed to the reconstructed (REC) value of the $PM_{2.5}$ concentrations for day t (represented by the orange arrow Figure 4). By repeating this

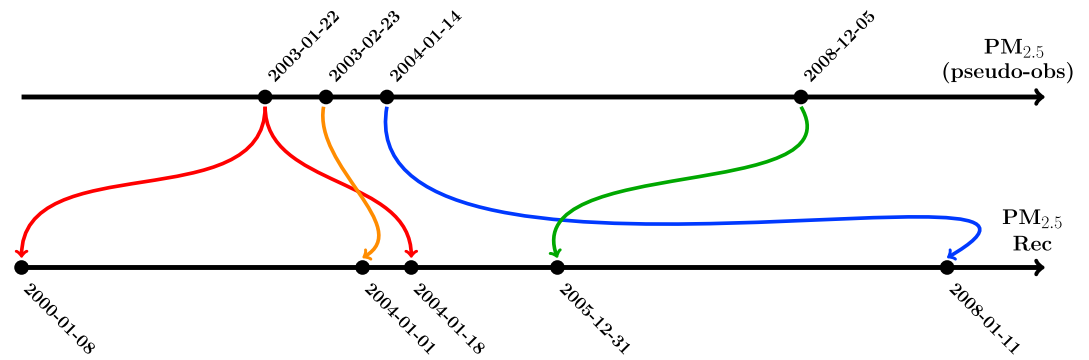


Figure 4. Resampling $PM_{2.5}$ pseudoobservations over the learning period. The analog day of 31 December 2005 is 5 December 2008 (green arrow), the analog day of both 18 January 2004 and 8 January 2000 is 22 January 2003 (red arrow).

algorithm for all days of the learning period, we reconstruct a data set of $PM_{2.5}$, denoted by $PM_{2.5}^{P-REC}(t, x, y)$. As shown in Figure 4, several days of the simulated period can be resampled to different days in the reconstructed data set (red arrows).

2.3.2. Historical Period

To avoid bias that can be present in the meteorological model, we need to apply the algorithm over a historical period from the model before applying it to the future periods. With the PSL and the temperature given by the model over the historical period, we can attribute each day of this period to one of 14 weather types built before. Using the same EOF as in the learning period (see Figure 5) ensures that we obtain the same weather types as in the learning period. PSL also allows us to compute the distance in terms of PSL between each day and each one of the 14 weather types. Thus, this algorithm implies a quasi-stationarity hypothesis on the weather types: it is assumed that climate change will only change their frequency but not the recurring patterns themselves.

The regression coefficients $(a_i(x, y))_{i=1, N(x, y)}$ and $(b_j(x, y))_{j=1, 4}$ obtained for the learning period are used to approximate the logarithm of the $PM_{2.5}$ concentrations under these historical conditions, noted $\ln(PM_{2.5}^{H-REG}(t, x, y))$.

The analog step is similar to that of the learning period. Let t be a day in the historical period (e.g., 18 February 1986 in Figure 6) and WT_t the associated weather type (e.g., WT4 in Figure 6). We consider the subset E_t of days in the learning period for which WT_t is also observed, so that we have all days in the learning period with the same LSC (represented on the right-hand side of Figure 6). The spatial correlation between the maps of $\ln(PM_{2.5}^{H-REG}(t, x, y))$ and $\ln(PM_{2.5}^{P-REG}(j, x, y))$ is computed for all j in E_t . Let j_{max} (e.g., 5 December 2008 in Figure 6) be the day for which the spatial correlation with t is the best. The pseudoobserved value of the $PM_{2.5}$ concentrations on day j_{max} is attributed to the $PM_{2.5}$ concentrations for day t in the historical

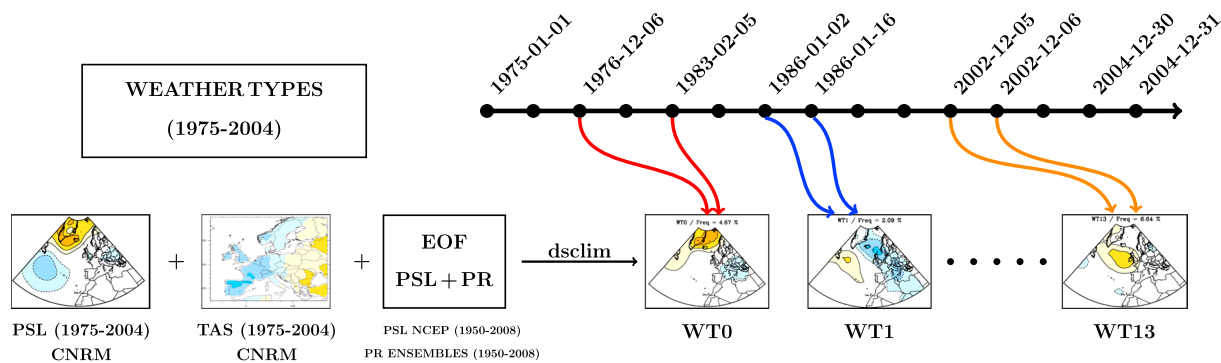


Figure 5. Building weather types over the historical period. PSL and TAS (only for summer) anomalies from Centre National des Recherches Météorologiques - Climate Model 5 (CNRM-CM5) (1975–2004) are projected on the space composed by the EOF of PSL and of PR (from the learning period). Dsclim classifies these anomalies and attributes each day of the 1975–2004 period to one of the 14 WTs of the learning period.

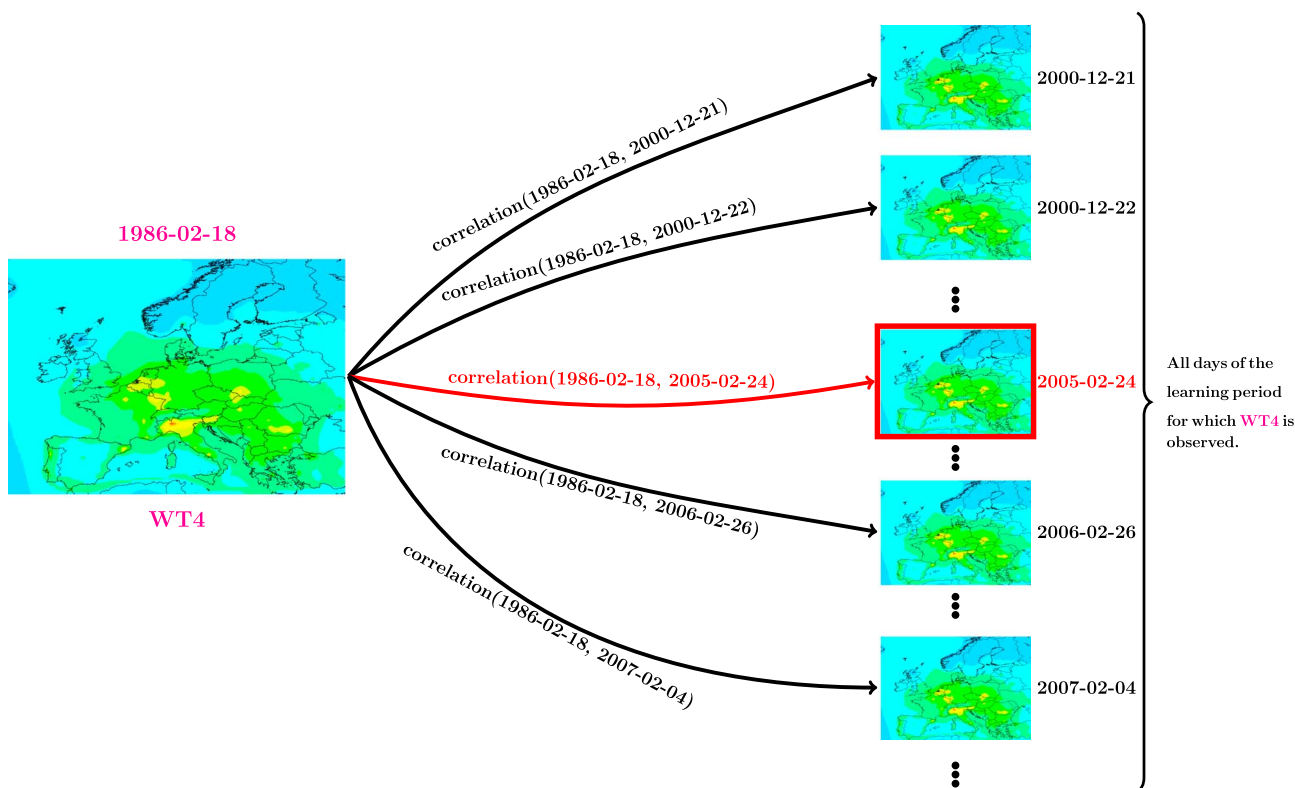


Figure 6. Resampling $PM_{2.5}$ pseudoobservations over the historical period.

period. By repeating this algorithm for all days of the historical period, we get a 30 year data set of $PM_{2.5}$ concentrations, noted $PM_{2.5}^H(t, x, y)$. Historical data sets of PSL, temperature, precipitation, and wind speed were obtained from the CNRM-CM5 model [Voltaire et al., 2013] on a $1.4^\circ \times 1.4^\circ$ horizontal grid. Since $PM_{2.5}$ pseudoobservations are on a $0.5^\circ \times 0.5^\circ$ horizontal grid and since these two data sets need to match the same grid for the regression equation, we need either to aggregate the $PM_{2.5}$ data to 1.4° or to interpolate the CNRM meteorological fields down to 0.5° . Aggregating the $PM_{2.5}$ pseudoobservations from 0.5° to 1.4° would smooth greatly the impacts of anthropogenic emissions on $PM_{2.5}$ concentrations (e.g., urban centers). The 1.4° horizontal grid for the meteorological fields is fine enough to capture synoptical and meso-alpha meteorological gradients, except perhaps in mountainous regions (e.g., the Alps). Therefore, we believe that it is preferable to interpolate the meteorological fields down to 0.5° for our analysis. Thus, the CNRM-CM5 data were interpolated to match the Polyphemus/Polair3D grid, using the `linint2` command (<http://www.ncl.ucar.edu/Document/Functions/Built-in/linint2.shtml>) from the NCAR Command Language (NCL). This command interpolates from a rectilinear grid to another rectilinear grid using bilinear interpolation.

2.3.3. Future Meteorological Conditions

Under future meteorological conditions, the building of weather types is similar to that of the historical period. The regression coefficients $(a_i(x, y))_{i=1, N(x, y)}$ and $(b_j(x, y))_{j=1, 4}$ obtained for the learning period are used to approximate the logarithm of the $PM_{2.5}$ concentrations under these future conditions, noted $\ln(PM_{2.5}^{F-REG}(t, x, y))$.

The analog step is similar to that of the historical period, with the exception that we compute the spatial correlation between the day t that we would like to estimate and all the days of the *historical period* and identify the day of the historical period corresponding to the maximal correlation. The $PM_{2.5}^H$ value for that day is then assigned to the day of the future period. By repeating this algorithm for all days of the future period, a data set of future $PM_{2.5}$ concentrations, noted $PM_{2.5}^F(t, x, y)$, is created.

Future data sets of PSL, temperature, precipitation, and wind speed were obtained from the CNRM-CM5 model [Voltaire et al., 2013] for two future scenarios RCP4.5 [Thomson et al., 2011] and RCP8.5 [Riahi et al.,

Table 3. Evaluation of the Algorithm on the Learning Period Using Different Thresholds for ρ^a

Threshold	0.2	0.3	0.4	0.5	0.6	0.7	0.8	All WTs
Simulated mean ($\mu\text{g m}^{-3}$)	12.25	12.25	12.25	12.25	12.25	12.25	12.25	12.25
Reconstructed mean ($\mu\text{g m}^{-3}$)	11.77	11.79	11.82	11.82	11.82	11.8	11.8	11.84
Mean relative error (%)	-2	-1.9	-1.7	-1.7	-1.7	-1.8	-1.8	-1.5
Monthly correlation coefficient	0.52	0.517	0.516	0.525	0.529	0.527	0.528	0.55

^aBest results are emphasized in bold.

2011], and for two 30 year periods (2020–2049 and 2070–2099). These data were interpolated using NCL to match the same grid as the $\text{PM}_{2.5}$ pseudoobservations (from 1.4° to 0.5° over Europe).

3. Evaluation of the Algorithm Over the Learning Period

Before applying the statistical algorithm to historical and future meteorological conditions given by the CNRM-CM5 model, we need to ensure that the reconstructed $\text{PM}_{2.5}$ data set over the learning period reproduces the original data set satisfactorily. To evaluate the algorithm, we must check the monthly correlation coefficient, the mean relative error (%), and the probability density function (PDF).

Several predictors for the regression equation were tested. On the one hand, we needed to choose which meteorological variables to use among PSL, surface air temperature, surface wind speed, and precipitation.

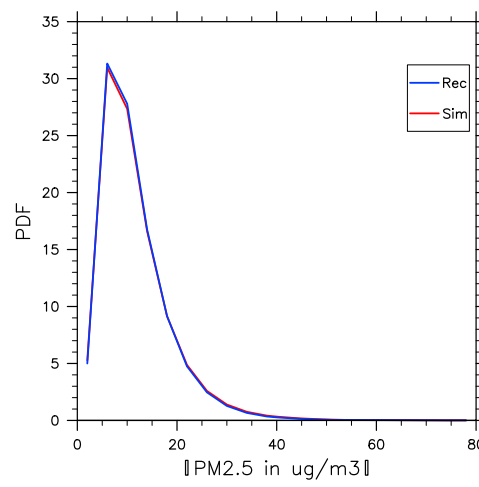
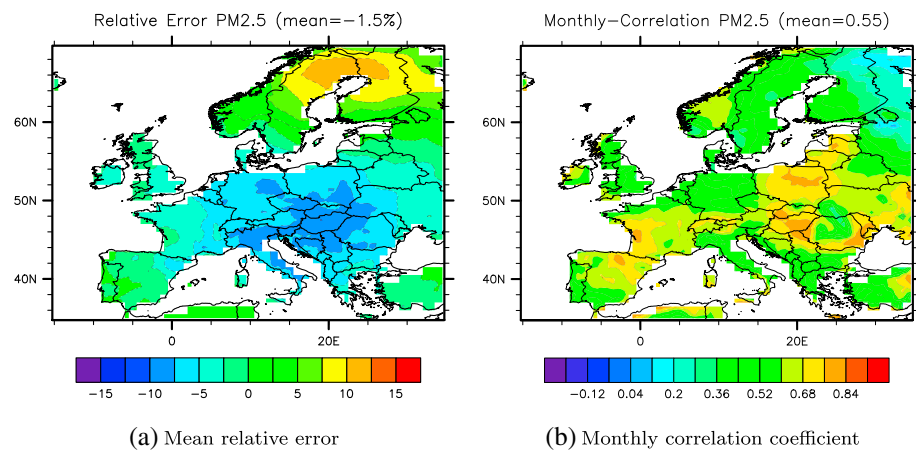


Figure 7. (a) Mean relative error and (b) monthly correlation coefficient between the reconstructed and the pseudoobserved $\text{PM}_{2.5}$ concentrations over the learning period, expressed in percent. (c) PDF of the reconstructed (Rec) and pseudoobserved (Sim) $\text{PM}_{2.5}$ concentrations ($\mu\text{g m}^{-3}$), over the learning period, in blue and red, respectively.

PSL and surface temperature were considered in every case for the regression equation. Evaluations showed that using only precipitation or surface wind speed in addition to these meteorological variables leads to a $PM_{2.5}$ data set that does not have the same PDF as the original $PM_{2.5}$, while using all four variables systematically does. On the other hand, we needed to choose how many weather types to use in the regression equation. Evaluations showed that using the same weather types for all locations is not necessarily efficient, since the discriminating power of weather types depends on location. We had to choose a number of weather types whose discriminating power ρ remains less than or equal to a certain threshold. Several thresholds were tested ranging from 0.3 to 0.8, in addition to considering all weather types.

Table 3 shows that increasing the number of weather types improves the reconstructed data set. The monthly correlation coefficient improves from 0.517 to 0.55, as well as the mean relative error (from -2% to -1.5%). Thus, we chose to use the four meteorological variables for the regression equation, as well as all the weather types, since this configuration gives the best results.

Figure 7a presents the mean relative error between the reconstructed and the pseudoobserved $PM_{2.5}$ over the learning period. The relative error is within $\pm 15\%$ over Europe and within $\pm 5\%$ in southern Scandinavia and in the westernmost and easternmost parts of Europe. The reconstructed data set tends to overestimate $PM_{2.5}$ by 5 to 12.5% in the northernmost part of Europe, which represents an error less than or equal to $1 \mu\text{g m}^{-3}$. On the contrary, the reconstructed data set underestimates $PM_{2.5}$ by -5 to -10% over central Europe (from eastern France to Romania), which represents a bias ranging between -1 and $-3 \mu\text{g m}^{-3}$. Figure 7b shows the monthly correlation coefficient between the reconstructed and the pseudoobserved $PM_{2.5}$ concentrations over the learning period. On average, this correlation coefficient is 0.55. It is less than 0.2 in some small and isolated areas in northeastern Europe and is close to 0.5 in Scandinavia, Germany, the UK, Ireland, Benelux, Portugal, southern Spain, Italy, Greece, and their surrounding countries. The monthly correlation coefficient is greater than 0.6 in western France, northern Spain, southern Norway, and eastern Europe. Figure 7c shows that the reconstructed and pseudoobserved $PM_{2.5}$ concentrations have nearly the same PDF.

The evaluation of the reconstructed $PM_{2.5}$ concentrations shows that the statistical method provides satisfactory performance to estimate $PM_{2.5}$ concentrations from meteorology and that, consequently, it can be used to study the impact of climate change on $PM_{2.5}$ concentrations.

4. Application to the Effect of Climate Change

In this section, we apply the statistical method to meteorological projections given by the CNRM-CM5 model. We first estimate $PM_{2.5}$ concentrations for the historical period (1975–2004) and then for two scenarios from the IPCC (RCP4.5 and RCP8.5) over two future periods: 2020–2049, referred to as near future, and 2070–2099, referred to as distant future. The two scenarios were selected because they depict two really different worlds. Indeed, the former is a stabilizing scenario, while in the latter, greenhouse gas (GHG) emissions and radiative forcing are the largest among the RCP family of scenarios. Moreover, they correspond closely to scenarios A1B and A2, which where the most commonly used scenarios in earlier studies. They are briefly described in section 4.1. Section 4.2 presents the estimation of future $PM_{2.5}$ concentrations, and section 4.3 discusses these results.

4.1. Climate Change Scenarios

4.1.1. RCP4.5 Scenario

RCP4.5's storyline describes a world where radiative forcing is stabilized at 4.5 Wm^{-2} in the year 2100 without ever exceeding that value. Under this scenario, the global population reaches a maximum of more than 9 billion in 2065 and then declines to 8.7 billion in 2100. It also assumes that climate policies are invoked to achieve the goal of limiting emissions and radiative forcing. RCP4.5 depicts declines in overall energy use, while substantial increases in both renewable energy forms and nuclear energy occur. In the near future, the average temperature is slightly higher than in the historical period (from $+0.5 \text{ K}$ in the westernmost part of Europe to $+4 \text{ K}$ over northern Scandinavia). Over most of Europe, the average temperature is 2 to 3 K higher than in the historical period (see Figure 8a). The average temperature in the distant future shows the same spatial distribution as in the near future (see Figure 8b) but with stronger differences compared to the historical period (from $+1 \text{ K}$ near the Atlantic Ocean to $+4 \text{ K}$ in northern and eastern Europe).

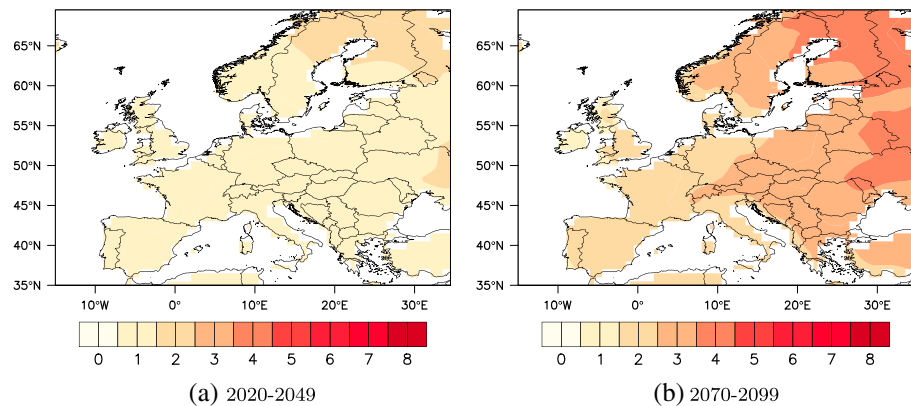


Figure 8. Difference (K) (a) between the average temperature in the near future and in the historical period and (b) between the average temperature in the distant future and in the historical period under the RCP4.5 scenario.

4.1.2. RCP8.5 Scenario

RCP8.5 is a scenario that depicts a heterogeneous world with a continuously increasing global population (12 billion by 2100) and an absence of climate change policies. At the same time, income growth, technological change, and energy improvement are relatively slow. This leads to high energy demand and increasing greenhouse gas (GHG) emissions, resulting in a radiative forcing of 8.5 Wm^{-2} by the end of the century. Among the different RPC scenarios, RCP8.5 is the scenario with the largest increase in GHG emissions. The average temperature shows similar patterns to those for the RCP4.5 scenarios, increasing from the Atlantic Ocean to northeastern Europe. In the near and distant futures, the average temperature is 1 to 3 K and 3 to 6 K, respectively, higher than in the historical period (see Figure 9).

4.2. Future PM_{2.5} Over Europe

4.2.1. Projected PM_{2.5} for the RCP4.5 Scenario in the Near Future

The difference between the projected PM_{2.5} concentrations for the near future (2020–2049) compared to those for the historical period (1975–2004) is depicted in Figure 10a. Table F1 presents the range of variation of PM_{2.5} and its components compared to the historical period for each season and each European region. The differences in annual PM_{2.5} concentrations vary within $[-0.63; 0.48] \mu\text{g m}^{-3}$. PM_{2.5} concentrations are mainly lower in northern, southern, and eastern Europe and higher in western and central Europe (see Figure 10a). For most European regions, these changes account for less than the PM_{2.5} interannual variability (the ratio of the changes due to climate change and the interannual variability varies from 10% in Scandinavia to 80% in Spain). However, in some localized areas, such as northwestern France, Denmark,

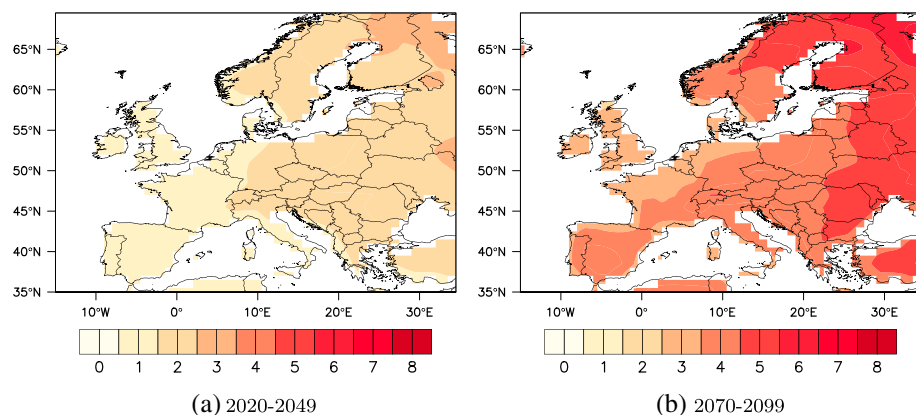


Figure 9. Difference (K) (a) between the average temperature in the near future and in the historical period and (b) between the average temperature in the distant future and in the historical period under the RCP8.5 scenario.

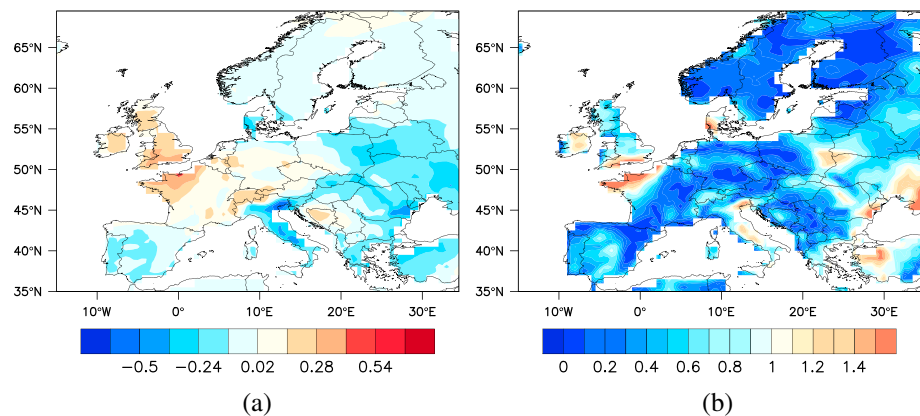


Figure 10. (a) Difference between the annual $PM_{2.5}$ concentration ($\mu g m^{-3}$) in the near future and in the historical period; (b) ratio of $PM_{2.5}$ changes due to climate change and $PM_{2.5}$ interannual variability under the RCP4.5 scenario.

Italy, Ireland, eastern Poland, and around the Black Sea, this ratio may be as high as 100% to 140% (see Figure 10b). These regions correspond to those with the largest $PM_{2.5}$ variation between the near future and historical periods.

When considering each season separately (see Appendix A, Figure A1), we see that the change in annual $PM_{2.5}$ concentrations typically results from increases in some seasons and decreases in others. The annual $PM_{2.5}$ response in northern Europe is the consequence of a decrease of $PM_{2.5}$ over southern Scandinavia in MAM and JJA (down to $-0.47 \mu g m^{-3}$) and an increase of $PM_{2.5}$ over northern Scandinavia in MAM and JJA (up to $0.34 \mu g m^{-3}$). $PM_{2.5}$ concentrations are lower in SON over northern Europe (down to $-0.45 \mu g m^{-3}$) and higher in DJF (up to $+1.05 \mu g m^{-3}$), except in Denmark (down to $-0.83 \mu g m^{-3}$). The annual response over southern Europe results from a decrease in DJF and MAM (down to $-1.5 \mu g m^{-3}$) and an increase in SON and JJA (up to $+1.03 \mu g m^{-3}$), except for Italy and northern Spain in JJA (down to $-0.47 \mu g m^{-3}$). Germany and Poland often show opposite responses among the seasons. For example, the annual $PM_{2.5}$ change in Germany results from a decrease in JJA (down to $-0.61 \mu g m^{-3}$) and from an increase in MAM and SON (up to $+0.77 \mu g m^{-3}$), while the annual $PM_{2.5}$ change in Poland results from an increase in JJA (up to $+0.58 \mu g m^{-3}$) and a decrease in MAM and SON (down to $-0.7 \mu g m^{-3}$). The response in the UK results from an increase in DJF, MAM, and JJA (up to $+0.85 \mu g m^{-3}$) and a decrease in SON (down to $-0.28 \mu g m^{-3}$). In the remaining part of western Europe, the annual $PM_{2.5}$ change results from a decrease in DJF (down to $-0.7 \mu g m^{-3}$) and an increase for the other seasons (up to $+0.85 \mu g m^{-3}$). The response is more uniform in

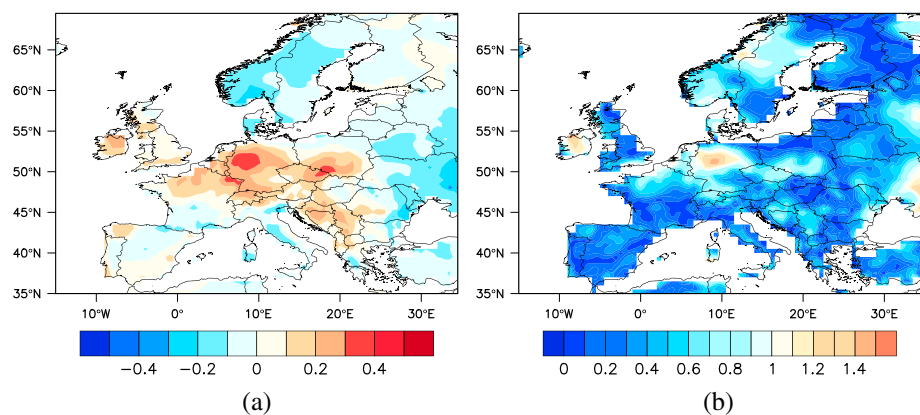


Figure 11. (a) Difference between the annual $PM_{2.5}$ concentration ($\mu g m^{-3}$) in the distant future and in the historical period; (b) ratio of $PM_{2.5}$ changes due to climate change and $PM_{2.5}$ interannual variability under the RCP4.5 scenario.

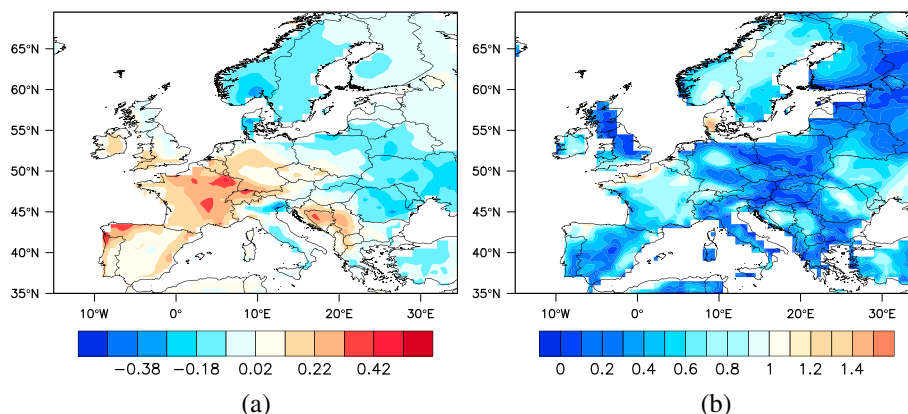


Figure 12. (a) Difference between the annual $\text{PM}_{2.5}$ concentration ($\mu\text{g m}^{-3}$) in the near future and in the historical period; (b) ratio of $\text{PM}_{2.5}$ changes due to climate change and $\text{PM}_{2.5}$ interannual variability under the RCP8.5 scenario.

eastern Europe, where the annual $\text{PM}_{2.5}$ change results from a decrease in DJF, MAM, and SON (down to $-1.01 \mu\text{g m}^{-3}$) and from an increase in JJA (up to $+0.51 \mu\text{g m}^{-3}$).

4.2.2. Projected $\text{PM}_{2.5}$ for the RCP4.5 Scenario in the Distant Future

The difference between the projected $\text{PM}_{2.5}$ concentrations for the distant future (2070–2099) compared to those for the historical period (1975–2004) is shown in Figure 11a. Table F2 presents the range of variation of $\text{PM}_{2.5}$ and its components compared to the historical period for each season and each European region. The differences in annual $\text{PM}_{2.5}$ concentrations vary within $\pm 0.4 \mu\text{g m}^{-3}$. $\text{PM}_{2.5}$ concentrations are mostly lower in northern and eastern Europe and higher in western, central, and southern Europe, except in Italy, Spain, and southern France (see Figure 11a). For most European regions, these changes account for less than the $\text{PM}_{2.5}$ interannual variability (ratio of $\text{PM}_{2.5}$ changes due to climate change and $\text{PM}_{2.5}$ interannual variability ranging from 10% in Spain to 80% in Scandinavia). In some localized areas, such as Ireland and Germany, the $\text{PM}_{2.5}$ changes due to climate change represent 100% to 140% of the $\text{PM}_{2.5}$ interannual variability (see Figure 11b).

Considering each season separately shows stronger signals (see Appendix A, Figure A2). The annual response in northern Europe results from a decrease in DJF, MAM, and SON (down to $-0.6 \mu\text{g m}^{-3}$) and an increase in JJA (up to $0.78 \mu\text{g m}^{-3}$). The annual response in southern Europe results from an increase in MAM, JJA, and SON (up to $1.13 \mu\text{g m}^{-3}$) and a decrease in DJF (down to $-0.84 \mu\text{g m}^{-3}$). $\text{PM}_{2.5}$ in central Europe results from an increase in DJF and JJA (up to $+1.22 \mu\text{g m}^{-3}$). Germany and Poland show opposite responses in MAM and SON, with a decrease of $\text{PM}_{2.5}$ concentrations in Poland (down to $-0.79 \mu\text{g m}^{-3}$) and an increase of $\text{PM}_{2.5}$ concentrations in Germany (up to $+0.97 \mu\text{g m}^{-3}$). The annual response over western Europe results from an increase in MAM and SON (up to $1.18 \mu\text{g m}^{-3}$) and from a decrease in DJF and JJA (down to $-0.92 \mu\text{g m}^{-3}$). $\text{PM}_{2.5}$ concentrations in eastern Europe result from a decrease in DJF, MAM, and SON (down to $-0.96 \mu\text{g m}^{-3}$) and from an increase in JJA (up to $0.88 \mu\text{g m}^{-3}$).

4.2.3. Projected $\text{PM}_{2.5}$ for the RCP8.5 Scenario in the Near Future

The difference between the projected $\text{PM}_{2.5}$ concentrations for the near future (2020–2049) compared to the historical period (1975–2004) is depicted in Figure 12a. Table F3 presents the range of variation of $\text{PM}_{2.5}$ and its components compared to the historical period for each season and each European region. The changes in annual $\text{PM}_{2.5}$ concentrations vary within $[-0.36; 0.48] \mu\text{g m}^{-3}$. $\text{PM}_{2.5}$ concentrations are mostly lower in northern and eastern Europe and higher in western, central, and southern Europe, except in Italy (see Figure 12a). This response of $\text{PM}_{2.5}$ to future climate change resembles more that of RCP4.5 in the distant future (see Figure 11) than that in the near future (see Figure 10). These changes account for less than the $\text{PM}_{2.5}$ interannual variability (ratio of $\text{PM}_{2.5}$ changes due to climate change and interannual variability ranging from 10% in the UK to 80% in Scandinavia) almost everywhere. However, ratios reach 100% to 140% in Denmark and near the English Channel (see Figure 12b).

As for RCP4.5, stronger responses appear when they are resolved by seasons (see Appendix B, Figure B1). The decreased $\text{PM}_{2.5}$ concentrations in northern Europe result from decreases for all seasons (down to

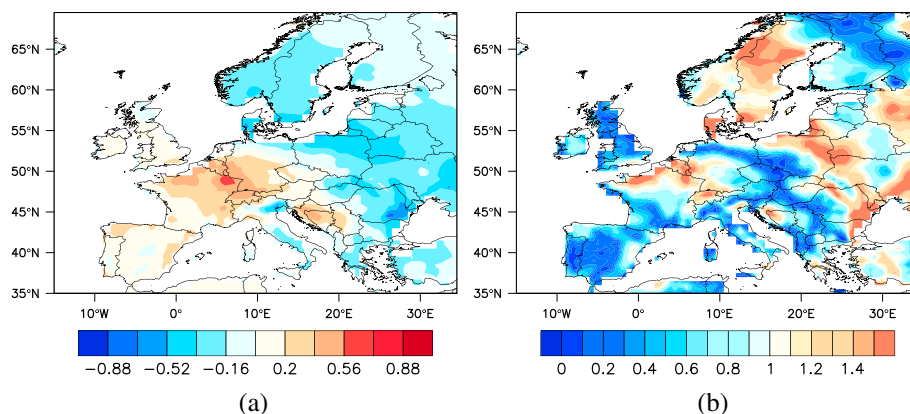


Figure 13. (a) Difference between the annual $PM_{2.5}$ concentration ($\mu g m^{-3}$) in the distant future and in the historical period; (b) ratio of $PM_{2.5}$ changes due to climate change and $PM_{2.5}$ interannual variability under the RCP8.5 scenario.

$-0.7 \mu g m^{-3}$). The $PM_{2.5}$ response in southern Europe results from increases of $PM_{2.5}$ concentrations in MAM, JJA, and SON (up to $1.17 \mu g m^{-3}$) and from a decrease in DJF (down to $-0.71 \mu g m^{-3}$). $PM_{2.5}$ in central Europe results from an increase in DJF and JJA (up to $0.85 \mu g m^{-3}$). Germany and Poland show opposite responses in MAM and SON: $PM_{2.5}$ concentrations increase in Germany (up to $0.92 \mu g m^{-3}$), while they decrease in Poland (down to $-0.87 \mu g m^{-3}$). The increased $PM_{2.5}$ in western Europe results from increasing $PM_{2.5}$ in MAM and SON (up to $0.95 \mu g m^{-3}$). The UK and the remaining part of western Europe show opposite responses in DJF and JJA. $PM_{2.5}$ concentrations in the UK increase in DJF (up to $+0.36 \mu g m^{-3}$) and decrease in JJA (down to $-0.71 \mu g m^{-3}$), while they decrease in DJF (down to $-0.45 \mu g m^{-3}$) and increase in JJA (up to $0.52 \mu g m^{-3}$) for the remaining part of western Europe. The lower $PM_{2.5}$ in eastern Europe results from a decrease in DJF, MAM, and SON (down to $-0.85 \mu g m^{-3}$) and an increase in JJA (up to $+0.64 \mu g m^{-3}$) (see Figure B1).

4.2.4. Projected $PM_{2.5}$ for the RCP8.5 Scenario in the Distant Future

The difference between the projected $PM_{2.5}$ concentrations for the near future (2070–2099) compared to the historical period (1975–2004) is presented in Figure 13a. Table F4 presents the range of variation of $PM_{2.5}$ and its components compared to the historical period for each season and each European region. The changes in annual $PM_{2.5}$ concentrations vary within $[-0.83; 0.76] \mu g m^{-3}$. $PM_{2.5}$ concentrations are mostly lower in the northernmost and westernmost parts of Europe and higher in the westernmost part (see Figure 13a). These changes exceed the $PM_{2.5}$ interannual variability (ratio of $PM_{2.5}$ changes due to climate change and interannual variability ranging from 100% to 140%) over a large part of Europe (northern France, Benelux, Switzerland, Scandinavia, Croatia, and eastern Europe) compared to the other period and scenario (see Figure 13b).

The annual decrease in northern Europe is the consequence of a decrease in MAM, JJA, and SON (down to $-1.22 \mu g m^{-3}$) and an increase in DJF (up to $0.83 \mu g m^{-3}$). The $PM_{2.5}$ response in southern Europe is the consequence of a decrease in DJF (down to $-1.78 \mu g m^{-3}$) and an increase in MAM, JJA, and SON (up to $1.53 \mu g m^{-3}$). $PM_{2.5}$ concentrations over central Europe result mostly from an increase in DJF and JJA (up to $1.54 \mu g m^{-3}$). As for the previous cases, Germany and Poland show opposite responses in MAM and SON. $PM_{2.5}$ concentrations increase in Germany (up to $1.31 \mu g m^{-3}$) and decrease in Poland (down to $-1.56 \mu g m^{-3}$). The increased $PM_{2.5}$ in western Europe results mostly from an increase in MAM and SON (up to $1.31 \mu g m^{-3}$). $PM_{2.5}$ concentrations increase in JJA over France and Benelux (up to $0.94 \mu g m^{-3}$) but decrease in the UK (down to $-0.68 \mu g m^{-3}$). In DJF, $PM_{2.5}$ concentrations increase over most of western Europe (up to $+0.47 \mu g m^{-3}$), except southern France, where they decrease (down to $-1.05 \mu g m^{-3}$). The decreased $PM_{2.5}$ concentrations over eastern Europe result from a decrease in MAM and SON (down to $-2.41 \mu g m^{-3}$) and an increase in JJA (up to $+0.89 \mu g m^{-3}$) (Figure B2).

4.2.5. Comparison of $PM_{2.5}$ Response Between the Distant and Near Futures

Figure 14 displays the difference of the $PM_{2.5}$ response between the distant and near futures for both scenarios. For the RCP4.5 scenario, $PM_{2.5}$ concentrations are higher in the distant future than in the near future in southern, central, and eastern Europe as a response to an increased temperature, compensated in part by an increased precipitation (respectively, wind speed) in southern Europe (respectively, in central Europe),

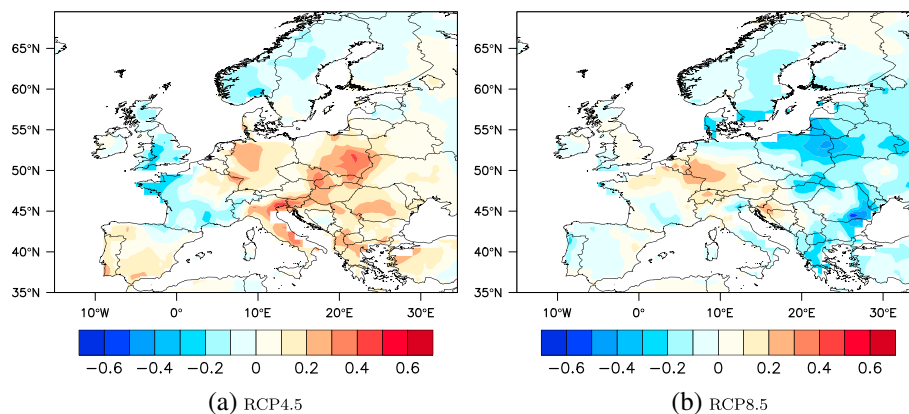


Figure 14. Difference between the annual $\text{PM}_{2.5}$ concentration ($\mu\text{g m}^{-3}$) in the distant and near futures for the (a) RCP4.5 and (b) RCP8.5 scenarios.

and enhanced by a decreased precipitation (respectively, wind speed) in central Europe (respectively, southern and eastern Europe) (see Figures E1a, E2a, and E3a). $\text{PM}_{2.5}$ concentrations are lower in the distant future than in the near future elsewhere, as a response to increased temperature and precipitation and a decreased wind speed in Scandinavia but partially compensated by increased wind speed in the UK, Ireland, Benelux, and France (see Figures E1a, E2a, and E3a).

For the RCP8.5 scenario, $\text{PM}_{2.5}$ concentrations are mostly lower in the distant future than in the near future, especially in eastern Europe, where the precipitation increases by 12% to 20% (see Figure E2b). Temperature and wind speed are higher and lower, respectively, in the distant future than in the near future (see Figures E1b, E2b, and E3b). $\text{PM}_{2.5}$ concentrations are higher in the distant future than in the near future over northern France, Benelux, Switzerland, and southern and western Germany, as a response to increased temperature and decreased wind speed, which dominate over increased precipitation.

4.2.6. $\text{PM}_{2.5}$ Components Driving the $\text{PM}_{2.5}$ Response

In this section, we identify the $\text{PM}_{2.5}$ components that influence the most the total $\text{PM}_{2.5}$ response to climate change among regions and scenarios. Tables F1–F4 provide the range of variation of $\text{PM}_{2.5}$ and their components for each scenario, future period, season, and European region. The evolution of NO_3^- and OM always contributes to the $\text{PM}_{2.5}$ response. The evolution of NH_4^+ follows that of NO_3^- but with a smaller influence because it is also associated with SO_4^{2-} . SO_4^{2-} systematically contributes to the $\text{PM}_{2.5}$ response over eastern Europe and depending on the scenarios over southern and central Europe. Sea salt contributes to the $\text{PM}_{2.5}$ response along the Atlantic coast but with a smaller influence compared to those of other components. Dust shows some influence mainly over northern and eastern Europe; it is, as for sea salt, less important than those of SO_4^{2-} , NO_3^- , and OM.

4.3. Discussion

This section aims at explaining the results and tendencies for $\text{PM}_{2.5}$ concentrations by looking at both the response of its components to changes in mean values of major meteorological variables (temperature, precipitations, and wind speed) (section 4.3.1) and the changes in weather type frequencies between the considered periods (section 4.3.2).

4.3.1. $\text{PM}_{2.5}$ Component Responses to Changes in Meteorological Variables

The relationship between precipitation and PM is straightforward. An increased precipitation generally leads to less $\text{PM}_{2.5}$, since it decreases the concentrations of most of its components (mineral dust, black carbon, organic matter, SO_4^{2-} , NO_3^- , and NH_4^+) [Lecœur and Seigneur, 2013]. Sea salt is the PM component whose presence is favored by precipitation. This result is due to the fact that increased precipitation is associated with storms that lead to sea salt particle formation as a consequence of high winds. An increased precipitation (see Figures C2, C5, D2, and D5) thus leads to more sea salt along the Atlantic, Baltic, and Mediterranean coasts. Despite the fact that sea salt represents a large fraction of $\text{PM}_{2.5}$ in those areas, an increased precipitation usually does not lead to increased $\text{PM}_{2.5}$ concentrations because of the compensating effect of precipitation scavenging on the other $\text{PM}_{2.5}$ components. In our projections, an increase in $\text{PM}_{2.5}$ happens

Table 4. Regions, Scenarios, and Projections for Which an Increased Precipitation (Compared to 1975–2004) Leads to Increased SO_4^- , Along With the Associated Changes in Precipitation (%) and SO_4^- ($\mu\text{g m}^{-3}$) Compared to 1975–2004

Scenario	Future Period	Season	Region	Increase in Precipitation (%)	Decrease in SO_4^- ($\mu\text{g m}^{-3}$)
RCP4.5	2020–2049	JJA	Baltic	[15; 30]	[0.02; 0.08]
RCP4.5	2020–2049	SON	Adriatic	[10; 20]	[0.06; 0.24]
RCP4.5	2070–2099	MAM	Adriatic	[10; 20]	[0; 0.01]
RCP4.5	2070–2099	JJA	Baltic	[15; 35]	[0; 0.19]
RCP4.5	2070–2099	SON	Adriatic	[15; 40]	[0; 0.21]
RCP8.5	2020–2049	DJF	Adriatic	[10; 15]	[0; 0.39]
RCP8.5	2020–2049	JJA	Baltic	[15; 45]	[0; 0.15]
RCP8.5	2020–2049	SON	Adriatic	[10; 30]	[0; 0.28]
RCP8.5	2070–2099	DJF	Adriatic	[15; 45]	[0; 0.45]
RCP8.5	2070–2099	SON	Adriatic	[15; 50]	[0; 0.4]

only for the RCP4.5 scenario (2070–2099, MAM) over western France and the UK Sea salt also contains a small fraction of sulfate, which explains that in some cases, more precipitation leads to more SO_4^- along the coasts (see Table 4 for details).

As for precipitation, the relationship between $\text{PM}_{2.5}$ components and wind speed is straightforward. An increased wind speed favors dispersion of most of $\text{PM}_{2.5}$ components (SO_4^- , NO_3^- , NH_4^+ , organic matter, black carbon, and mineral dust) [Lecœur and Seigneur, 2013], while a decreased wind speed leads to the accumulation of particle pollution in the atmosphere. Along the coasts, higher wind speeds (see Figures C3, C6, D3, and D6) lead to the formation of atmospheric sea salt particles and in some cases to increased SO_4^- concentrations (see Table 5 for details).

The relationship between temperature and $\text{PM}_{2.5}$ components is more complex. We only describe the relationships in DJF and JJA, as MAM and SON can be considered as intermediate seasons, in which the response can be either close to the DJF or JJA response, depending on the season and region.

For all considered scenarios and future periods, annual SO_4^- concentrations decrease over most of Europe. As temperature increases in the projections (see Figures C1, C4, D1, and D4), the decrease of SO_4^- concentrations could be explained by the decrease in winter of fuel heating, which generates the sulfate precursor SO_2 [Lecœur and Seigneur, 2013]. In JJA, SO_4^- concentrations increase over most parts of Europe. The increase in SO_4^- is a consequence of an increased temperature, which favors SO_2 oxidation. These results also suggest that other processes are involved over some regions (the UK, central Europe, northern Europe, and southeastern Europe, depending on the seasons and scenarios) where SO_4^- does not respond in terms of these major trends.

For all considered scenarios and future periods, NO_3^- and NH_4^+ concentrations mostly decrease compared to the historical period. As temperature increases in those projections, it favors the partitioning of ammonium nitrate toward the gas phase and thus a decrease in particulate ammonium nitrate concentrations [Lecœur and Seigneur, 2013]. NO_3^- and NH_4^+ concentrations increase as temperature increases over the same regions as SO_4^- (the UK and central, northern, and southeastern Europe), as higher temperatures in summer are

Table 5. Regions, Scenarios, and Projections for Which an Increased Wind Speed (Compared to 1975–2004) Leads to Increased SO_4^- , Along With the Associated Changes in Wind Speed (m s^{-1}) and SO_4^- ($\mu\text{g m}^{-3}$) Compared to 1975–2004

Scenario	Future Period	Season	Region	Increase in Wind Speed (m s^{-1})	Decrease in SO_4^- ($\mu\text{g m}^{-3}$)
RCP4.5	2020–2049	MAM	Adriatic	[0.1; 0.3]	[0.1; 0.2]
RCP4.5	2020–2049	JJA	Adriatic	[0.1; 0.3]	[0.05; 0.1]
RCP4.5	2070–2099	MAM	Adriatic	[0.1; 0.3]	[0.05; 0.1]
RCP8.5	2020–2049	MAM	Adriatic	[0.1; 0.3]	[0.1; 0.3]
RCP8.5	2020–2049	JJA	Adriatic	[0.2; 0.3]	[0; 0.15]
RCP8.5	2070–2099	MAM	Adriatic	[0.1; 0.3]	[0.1; 0.15]
RCP8.5	2070–2099	JJA	Adriatic	[0.1; 0.3]	[0.06; 0.24]

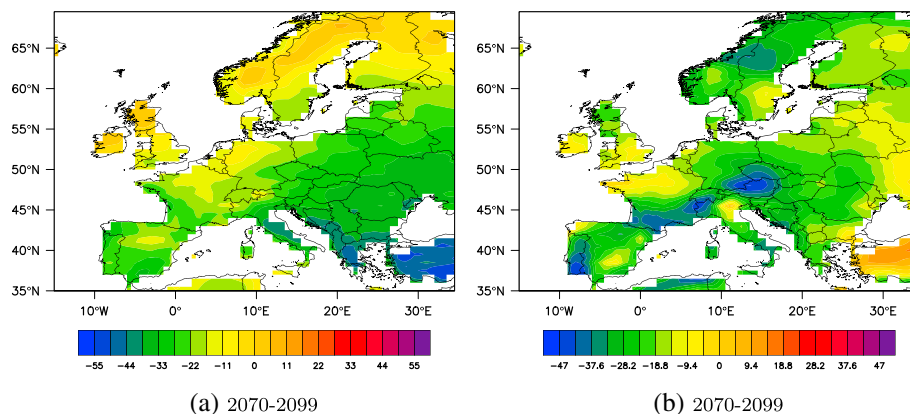


Figure 15. Correlation (%) (a) between temperature and precipitation and (b) between temperature and wind speed in JJA for the 2070–2099 period under the RCP8.5 scenario. Similar maps are obtained for all scenarios and future periods.

associated with stagnation periods in the future (see Figure 15), which dominates over the volatilization of NO_3^- and NH_4^+ at higher temperatures.

Temperature does not seem to have an impact on mineral dust concentrations, since mineral dust concentration either increases or decreases depending on the regions and the scenario considered, while temperature always increases. In DJF, black carbon concentrations decrease as temperature increases (the need of fuel heating decreases), except in some specific areas in eastern France and central Europe. In JJA, black carbon concentrations mostly increase over Europe. Sea salt decreases in Europe, especially in JJA, as higher temperatures in summer are associated with anticyclonic conditions, which lead to less precipitation and wind (see Figure 15).

In DJF, OM concentrations decrease over most of Europe (except northern and southeastern Europe) as temperature increases. This decrease is due to the volatilization of semivolatile organic compounds (SVOC) at higher temperatures, which is not compensated by increased biogenic emissions, since they are negligible in winter [Lecœur and Seigneur, 2013]. In JJA, OM concentrations increase in eastern and southeastern Europe but decrease in western, central, and northern Europe as temperature increases. This shows that opposing processes take place: increasing temperatures lead to higher biogenic emissions and faster formation of SVOC but favor SVOC partitioning toward the gas phase.

4.3.2. $\text{PM}_{2.5}$ Projections and Weather Types

The $\text{PM}_{2.5}$ response cannot be entirely explained by the mean changes in meteorological variables, which suggests that the evolution of the occurrence of the various weather types must be taken into account. We study here the impact of changes in weather type frequencies on $\text{PM}_{2.5}$ concentrations. To do so, we use the same approach as the one used by Najac [2008]. We decompose the difference of the average variable X between a future period and a historical period as follows:

$$\Delta X = X^F - X^H = \sum_{i=1}^N (f_i^F x_i^F - f_i^H x_i^H), \tag{2}$$

where X^H (X^F) is the average value of variable X over the historical (future) period, N is the number of weather types, f_i^H (f_i^F) is the frequency of weather type i over the historical (future) period, and x_i^H (x_i^F) is the average value of variable X when weather type i is observed in the historical (future) period. Equation (2) can be rewritten as follows:

$$\Delta X = \underbrace{\sum_{i=1}^N (\Delta f_i x_i^H)}_{\text{inter}} + \underbrace{\sum_{i=1}^N (\Delta x_i f_i^H)}_{\text{intra}} + \underbrace{\sum_{i=1}^N (\Delta x_i \Delta f_i)}_{\text{residual}}, \tag{3}$$

where $\Delta x_i = x_i^F - x_i^H$ and $\Delta f_i = f_i^F - f_i^H$. The first term on the right-hand side of equation (3) represents the changes that are due to modifications in weather type frequencies (intertype changes). The second

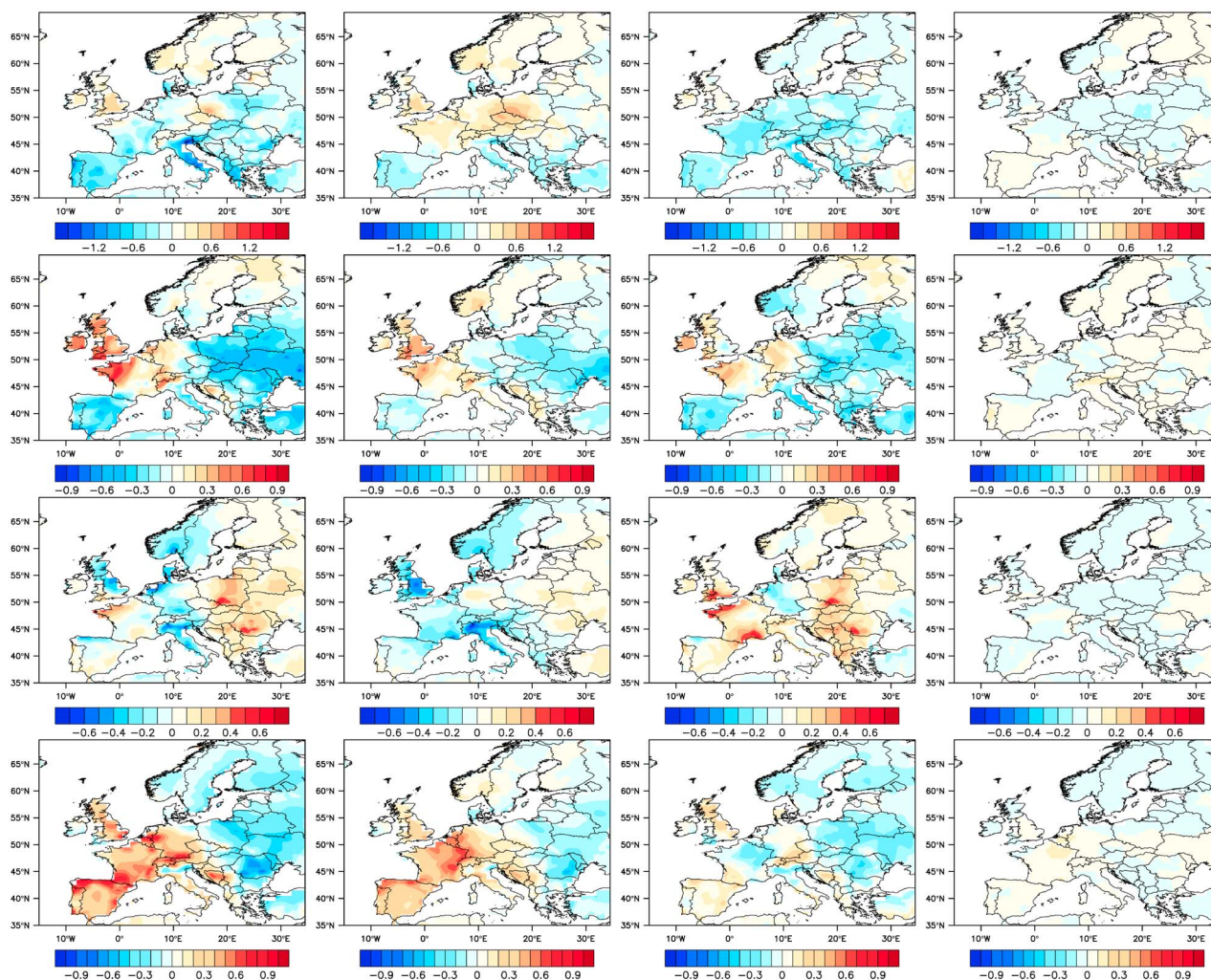


Figure 16. (first column) Total, (second column) intertype, (third column) intratype, and (fourth column) residual $PM_{2.5}$ changes between the historical (1975–2004) and near future (2020–2049) periods (scenario RCP4.5) in (first row) DJF, (second row) MAM, (third row) JJA, and (fourth row) SON. All changes are expressed in $\mu g m^{-3}$.

term represents the changes that are due to modifications of the large-scale circulation for a given weather type (intratype changes). These modifications can lead either to different inflows of $PM_{2.5}$ in the domain or to a different average value of meteorological variables within the weather type and a fortiori to a different average value of the variable X (here $PM_{2.5}$). The last term is a residual term which is related to both changes jointly (weather type frequency and variable X within a weather type and is, therefore, second order in terms of changes). We apply this decomposition to the $PM_{2.5}$ projections that were presented (see Figures 16–19 above).

This decomposition provides valuable information regarding the respective effects of changes in weather type frequencies and mean values of meteorological variables on the total changes in $PM_{2.5}$ concentrations for all seasons, scenarios, and future periods considered. The residual changes are negligible compared to the intertype and intratype changes for all scenarios, seasons, and future periods considered. Therefore, our analysis focuses on the intertype and intratype changes.

Over northern Europe, the influence of inter and intratype changes are on the same order of magnitude in DJF, MAM, and SON. In JJA, the intertype changes dominate over Scandinavia, while the intratype changes dominate over Finland. Over Scandinavia, $PM_{2.5}$ concentrations decrease between 0 and $-1.2 \mu g m^{-3}$ depending on the scenario and future period. The weather types associated with less $PM_{2.5}$ over Scandinavia are WT1, WT2, WT3, WT5, and WT8. They represent 30.5% of the days for the historical period, while they represent 37.8% to 41% of the days of the future periods (see Tables H1–H3). Finland is less influenced

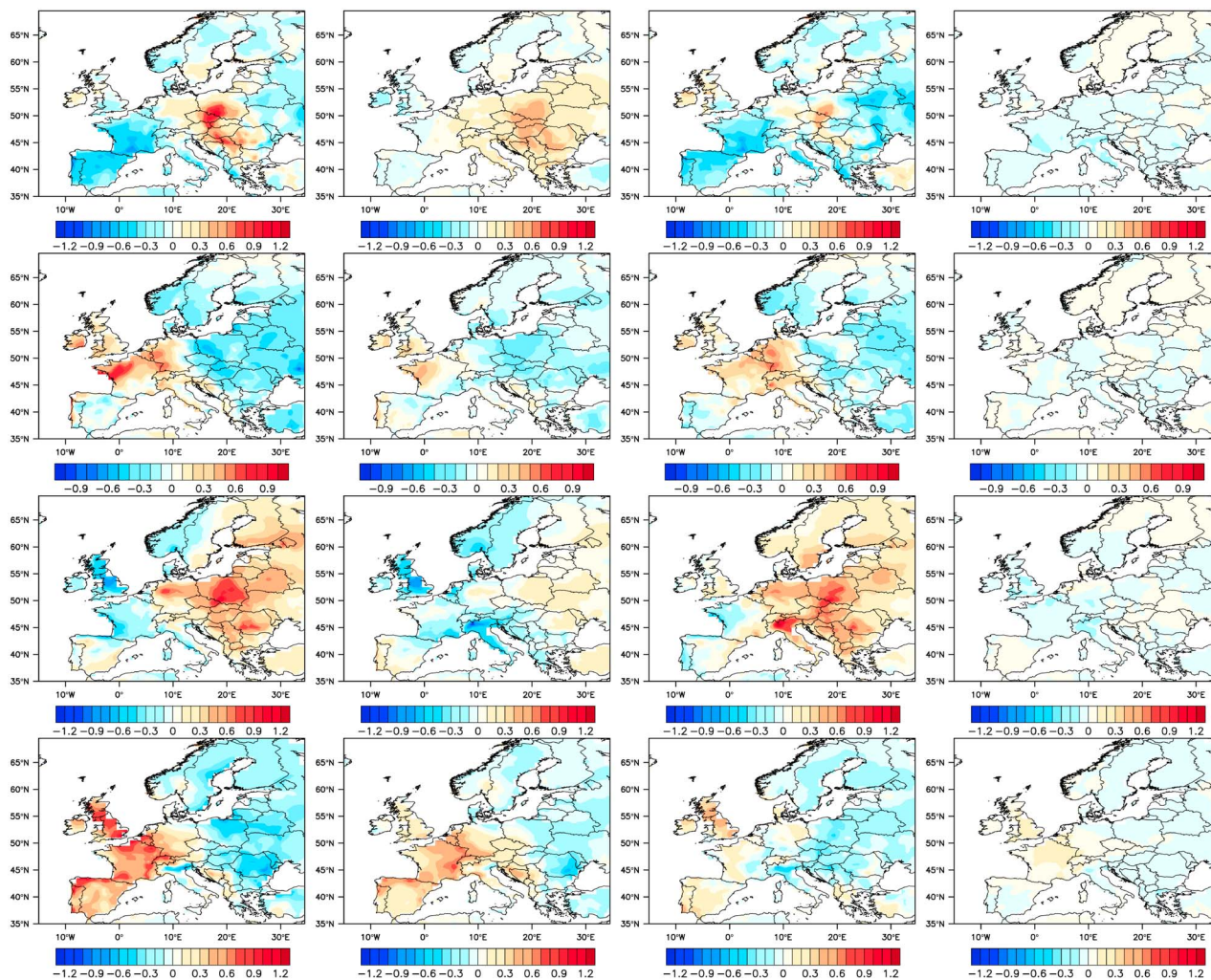


Figure 17. (first column) Total, (second column) intertype, (third column) intratype, and (fourth column) residual $PM_{2.5}$ changes between the historical (1975–2004) and distant future (2070–2099) periods (scenario RCP4.5) in (first row) DJF, (second row) MAM, (third row) JJA, and (fourth row) SON. All changes are expressed in $\mu\text{g m}^{-3}$.

by the changes of weather type frequencies, since it is located further away from the Atlantic Ocean. Moreover, the increase of temperature in JJA is stronger in northeastern Europe than in Scandinavia, which leads to greater changes in the relationship between weather type and $PM_{2.5}$ concentrations in northeastern Europe.

Over *southern Europe*, the influence of intertype and intratype changes are on the same order of magnitude in MAM. In JJA, the intertype (respectively, intratype) changes dominate in the western (respectively, eastern) part. Since the southwestern part of Europe is closer to the Atlantic Ocean than the southeastern part, it seems logical that the frequency of weather types impacts this region more. Moreover, changes in temperature are stronger in southeastern Europe than in southwestern Europe, which leads to changes in the relationship between weather types and $PM_{2.5}$ concentrations. In SON, the intertype changes dominate for the RCP4.5 scenario, while the intertype and intratype changes are on the same order of magnitude for the RCP8.5 scenario. Since the frequency of the weather types that are associated with high $PM_{2.5}$ concentrations (WT0, WT1, WT2, WT10, and WT13) does not really change between the present period (30.3% of the days) and the future periods (from 31.2% to 33.5% of the days) (see Tables H1–H3), the evolution in the fractions of total changes that are attributable to intertype and intratype changes between the RCP4.5 and RCP8.5 scenarios is due to changes in temperature, since temperature changes are stronger for the RCP8.5 scenario than for the RCP4.5 scenario. In DJF, the intratype changes dominate over the intertype ones.

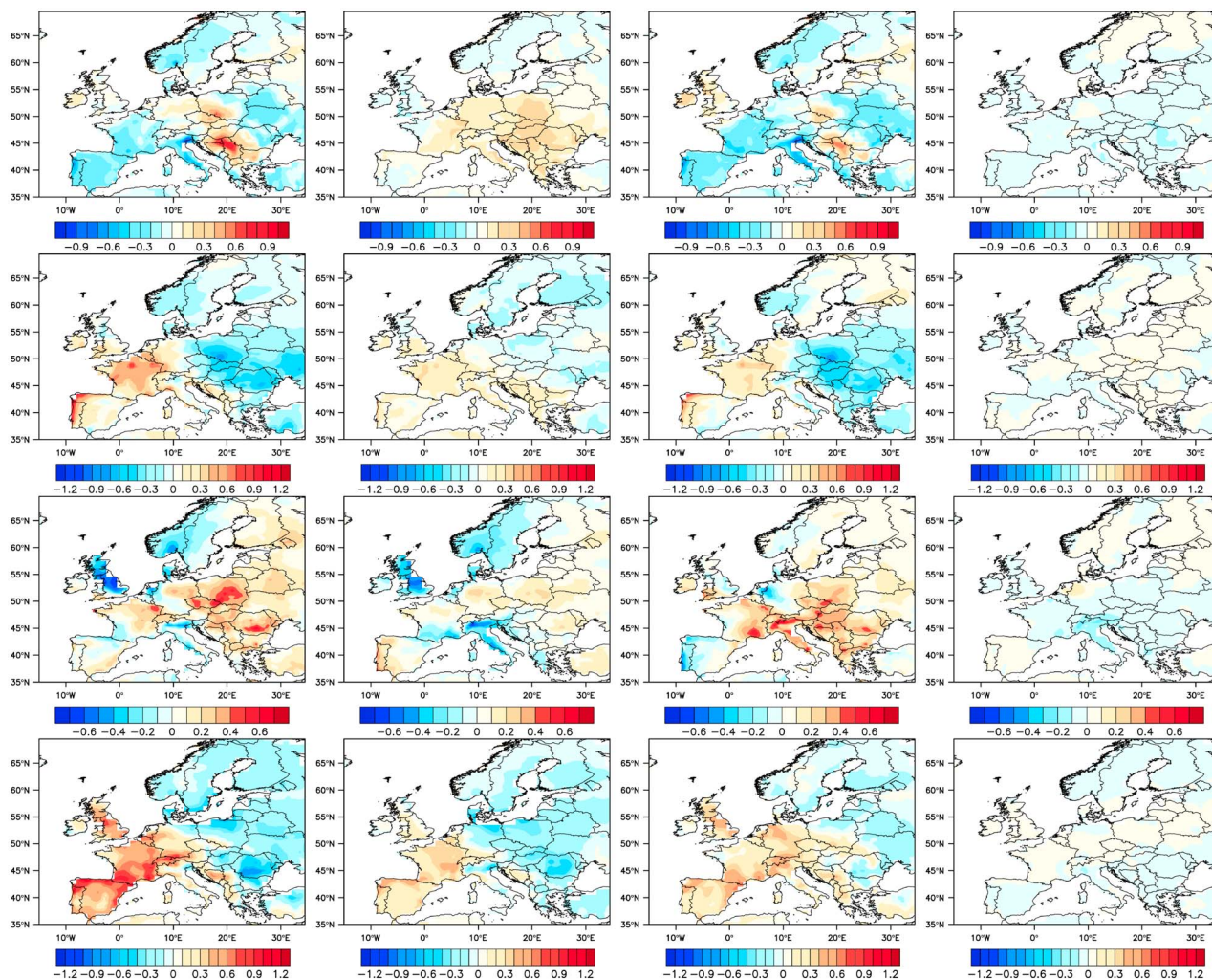


Figure 18. (first column) Total, (second column) intertype, (third column) intratype, and (fourth column) residual $PM_{2.5}$ changes between the historical (1975–2004) and near future (2020–2049) periods (scenario RCP8.5) in (first row) DJF, (second row) MAM, (third row) JJA, and (fourth row) SON. All changes are expressed in $\mu g m^{-3}$.

Over *central Europe*, the influence of intertype (respectively, intratype) changes dominates in DJF (respectively, JJA). In DJF, the frequency of the weather types associated with high $PM_{2.5}$ concentrations (WT0, WT3, WT4, and WT5) varies from 36.3% over the historical period to 38.4–42.2% for the future period (see Tables H1–H3), which explains why the intertype changes dominate. In MAM, they are on the same order of magnitude for RCP4.5, while the intratype changes dominate for RCP8.5. The increased temperature leads to changes within the weather type- $PM_{2.5}$ relationship in MAM and JJA. In SON, the intertype (respectively, intratype) changes dominate over Germany (respectively, Poland), which is due to the fact that the temperature increase is greater in Poland than in Germany.

Over *western Europe*, the influence of intertype (intratype) changes dominates in SON (DJF). In SON, the frequency of the weather types associated with high concentrations of $PM_{2.5}$ varies from 27.4% in the historical period to 30.1–43.9% in the future periods (see Tables H1–H3). In DJF, the changes in temperature lead to changes within the weather type- $PM_{2.5}$ relationships. In MAM, they are on the same order of magnitude. In JJA, the influence of intertype (intratype) changes dominates over the UK and Benelux (France).

Over *eastern Europe*, the influence of intratype changes dominates in DJF, MAM, and JJA (temperature increase), while the influences of intertype and intratype changes are on the same order of magnitude in SON.

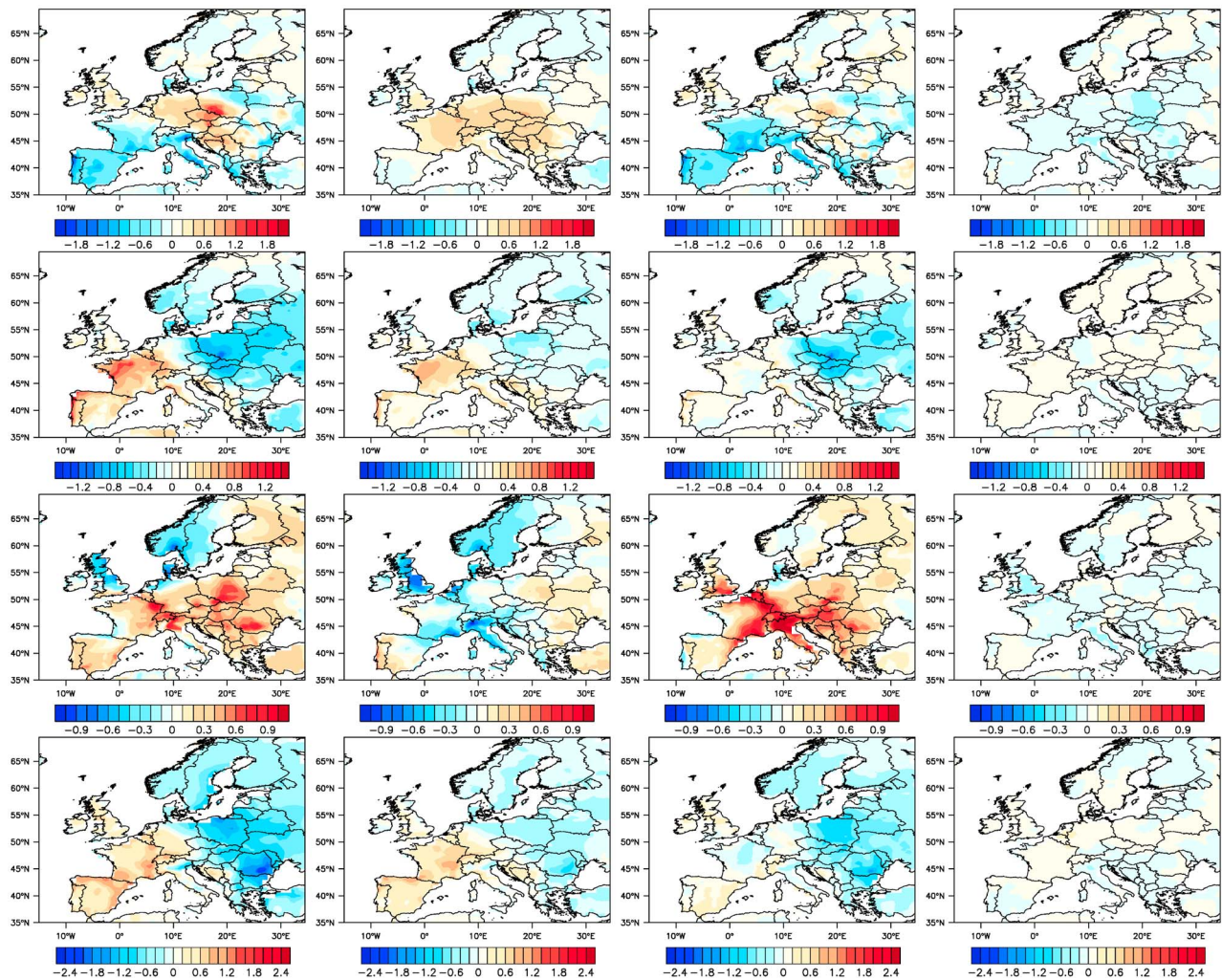


Figure 19. (first column) Total, (second column) intertype, (third column) intratype, and (fourth column) residual $PM_{2.5}$ changes between the historical (1975–2004) and distant future (2070–2099) periods (scenario RCP8.5) in (first row) DJF, (second row) MAM, (third row) JJA, and (fourth row) SON. All changes are expressed in $\mu\text{g m}^{-3}$.

5. Conclusions

A statistical algorithm was developed to estimate $PM_{2.5}$ concentrations over Europe based on a weather-type representation of the meteorology. This statistical algorithm was constructed using relationships between $PM_{2.5}$ observations and four meteorological variables (pressure at sea level, surface air temperature, precipitation, and surface wind speed). Because of a lack of $PM_{2.5}$ speciated measurements over Europe, modeled $PM_{2.5}$ concentrations were used as pseudoobservations. This algorithm resamples observed values of $PM_{2.5}$ concentrations on a given day of a given period, based on the large-scale circulation and on the similarity between the regression-based $PM_{2.5}$ estimated concentrations of that given day and that of all days with the same large-scale circulation. The algorithm was evaluated on the learning period (2000–2008) to test its ability to reproduce the pseudoobserved data set. It was then applied to the projections given by the CNRM-CM5 meteorological model: a historical period (1975–2004) and two future periods using two different climate scenarios: RCP4.5 and RCP8.5. Under RCP4.5, radiative forcing is stabilized at 4.5 W m^{-2} . Under RCP8.5, the world population continues to increase and climate change policies are lacking, which leads to high demands on food and energy, resulting in a radiative forcing of 8.5 W m^{-2} by 2100. The two future periods are 2020–2049 (near future) and 2070–2099 (distant future).

For all considered scenarios and periods, annual $PM_{2.5}$ concentrations decrease over northern Europe, eastern Europe, Italy, Poland, and southeastern Europe (down to $-0.83 \mu\text{g m}^{-3}$) compared to the historical period, while they increase over the UK, northern France, Benelux, and the Balkans (up to $0.76 \mu\text{g m}^{-3}$).

Over other regions, such as the Iberian Peninsula and central Europe, the evolution of annual $PM_{2.5}$ concentrations depends on the scenarios. Considering each season separately shows stronger responses. Those may vary among seasons for a given region and scenario.

These projections show a sign agreement with *Jiménez-Guerrero et al.* [2012] for SO_4^- and NH_4^+ in MAM and JJA, but *Jiménez-Guerrero et al.* [2012] find a stronger signal (from 0 to $+2 \mu\text{g m}^{-3}$ for SO_4^- and from 0 to $+0.4 \mu\text{g m}^{-3}$ for NH_4^+) than obtained here (from 0 to $+1 \mu\text{g m}^{-3}$ for SO_4^- and from 0 to $+0.3 \mu\text{g m}^{-3}$ for NH_4^+). The projections from this study are rather different from the ones found by *Colette et al.* [2013], whose results depict a decrease of $PM_{2.5}$ concentrations over all Europe, although the order of magnitude of this variation (about $1 \mu\text{g m}^{-3}$) is closer to the one of our projections. Finally, *Hedegaard et al.* [2013] show a similar annual response of $PM_{2.5}$ over the Iberian Peninsula. Although these studies do not show good agreement, it may not be relevant to compare these results, because the scenarios, the spatial resolutions, the years, and the number of years considered in the projected periods differ. Such differences in the numerical experiment protocols may cause these differences.

Changes in meteorological conditions between the historical and the future periods explain part of the changes found in this study. While precipitation scavenges most of $PM_{2.5}$ components, the wind disperses them. However, the formation of sea salt particles is favored by unstable weather conditions over sea (i.e., high precipitation and wind speed), and since a small fraction of sulfate is contained in sea salt, sulfate concentrations along the coasts also increase under such conditions. The relationship between $PM_{2.5}$ components and temperature is more complex. For most European regions, SO_4^- concentrations decrease in winter and increase in summer as temperature increases, as expected, since SO_2 , which is the precursor of sulfate, is generated by fuel heating in winter and since SO_2 oxidation in summer is favored at higher temperatures. As temperature increases in future scenarios, NO_3^- and NH_4^+ concentrations decrease over most of Europe, since high temperatures favor the shifting of ammonium nitrate toward the gas phase. Temperature does not impact mineral dust or black carbon concentrations much, as these components increase or decrease depending on the seasons and scenarios. Sea salt decreases in the projections, which suggests that higher temperatures will be mainly associated with anticyclonic conditions for which the formation of atmospheric sea salt particles is not favored. OM concentrations decrease mainly in winter but increase in summer, as an increased temperature leads to the volatilization of SVOC in winter but increases biogenic emissions in summer. In other regions, $PM_{2.5}$ components do not respond to changes in meteorological variables as expected, which suggests that changes in weather type frequencies must be taken into account.

We decomposed the changes in $PM_{2.5}$ concentrations as the sum of intertype changes, intratype changes, and a residual term. The first term represents the part of the $PM_{2.5}$ change, which is due to modifications in weather type frequencies. The second term combines all changes due to the modifications of the large-scale circulation for a given weather type. Such modifications affect either the $PM_{2.5}$ flow through the study domain or the average value of the meteorological variables associated with a weather type, which leads to changes in the average value of $PM_{2.5}$ concentrations within this weather type. The last term is a residual term, which includes intertype and intratype changes jointly. This decomposition provides valuable information to understand the causes of the $PM_{2.5}$ changes between the historical and future periods. It shows that the residual term is negligible. It appears that changes in regions near the ocean (Norway, the UK, the Iberian Peninsula) result mostly from changes in weather-type frequency, as changes in the large-scale circulation over the Atlantic Ocean directly impact coastal areas. In most regions, the intertype and intratype changes are on the same order of magnitude. The importance of intratype changes suggests that the relationships between weather type (meteorological variables) and $PM_{2.5}$ may evolve in the future (e.g., an increase in mean temperature will lead to lower $PM_{2.5}$ concentrations of semivolatile particulate matter for a given weather type).

Some uncertainties are associated with these results, such as the meteorological variables and the number of weather types included in the classification and in the regression equation, and the use of modeled $PM_{2.5}$ as pseudoobservations. The statistical algorithm could be expanded to include additional meteorological variables (e.g., planetary boundary layer height, relative humidity, cloud cover) to investigate whether this would lead to noticeable improvements. The effect of changes in $PM_{2.5}$ concentrations at the boundary of the domain is another uncertainty. Such effect was not taken into account in this study. The evolution of boundary conditions is negligible for most $PM_{2.5}$ components (NO_3^- , NH_4^+ , and OM) but is not for SO_4^-

[Racherla and Adams, 2006] and might be important for other components (e.g., dust, as a consequence of changes in land use). This effect could be considered by simulating the impact of climate change on $PM_{2.5}$ concentrations at a global scale.

The results of this study should be treated with caution since we used only one meteorological model. Although the predictions of this model are near the mean of a multimodel ensemble for temperature [Cattiaux et al., 2013], a multimodel analysis would be more robust to estimate the impact of climate change on $PM_{2.5}$.

This novel approach can be seen as an alternative solution to the use of PM air quality models, because it will lead to lower computational costs (see Table I1). Moreover, this approach can be used with speciated $PM_{2.5}$ observations if a sufficiently dense monitoring work were available. Thus, uncertainties associated with models could be removed, particularly those associated with semivolatile PM (although artifacts also occur with measurements).

Our analysis focused on the effect of climate change on season-averaged $PM_{2.5}$ concentrations, and larger effects were calculated for the annual averaged $PM_{2.5}$ concentrations. It would be interesting to investigate whether larger changes could yet be obtained when focusing on shorter time periods such as high- $PM_{2.5}$ episodes. Furthermore, this approach can be applied to the effect of climate change on other pollutants that are strongly linked to meteorological variables (e.g., ozone) and/or to other regions.

Appendix A: Seasonal Response of $PM_{2.5}$ Under RCP4.5

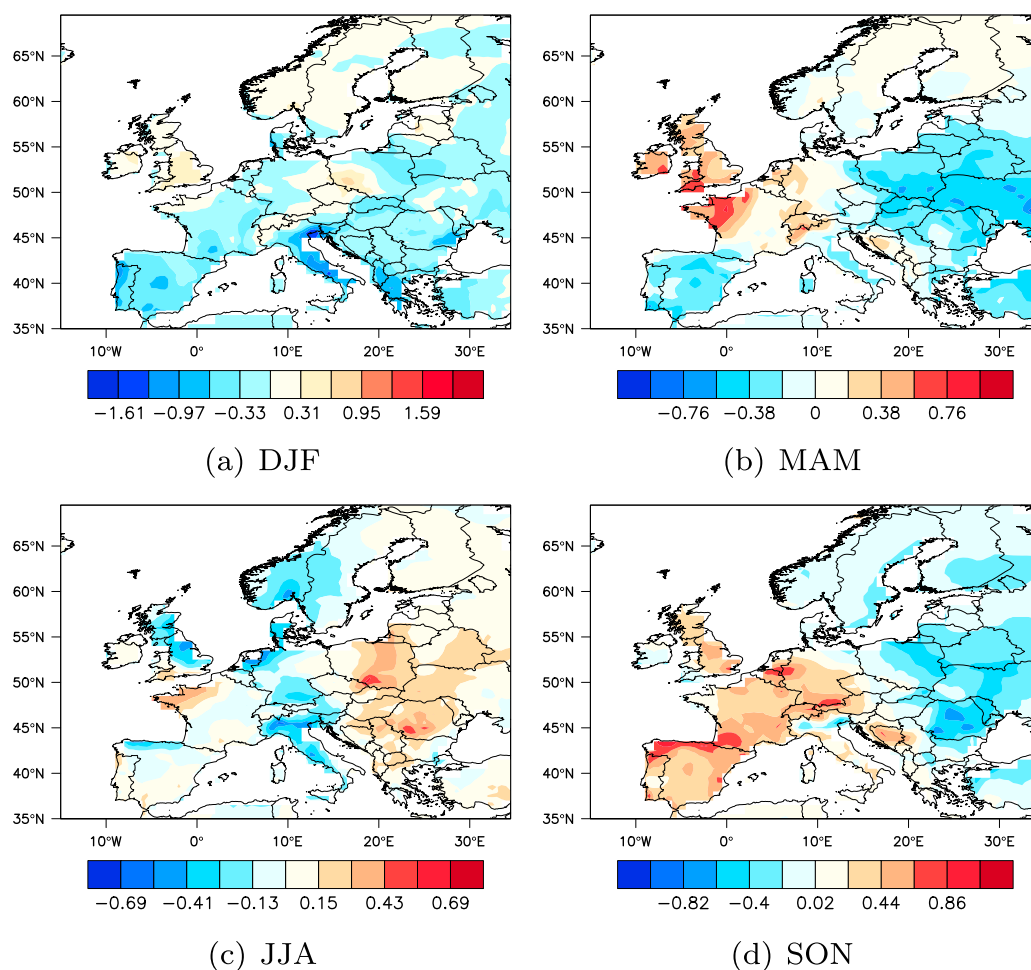


Figure A1. Difference between the average $PM_{2.5}$ in 2020–2049 and in 1975–2004 under the RCP4.5 scenario ($\mu g m^{-3}$).

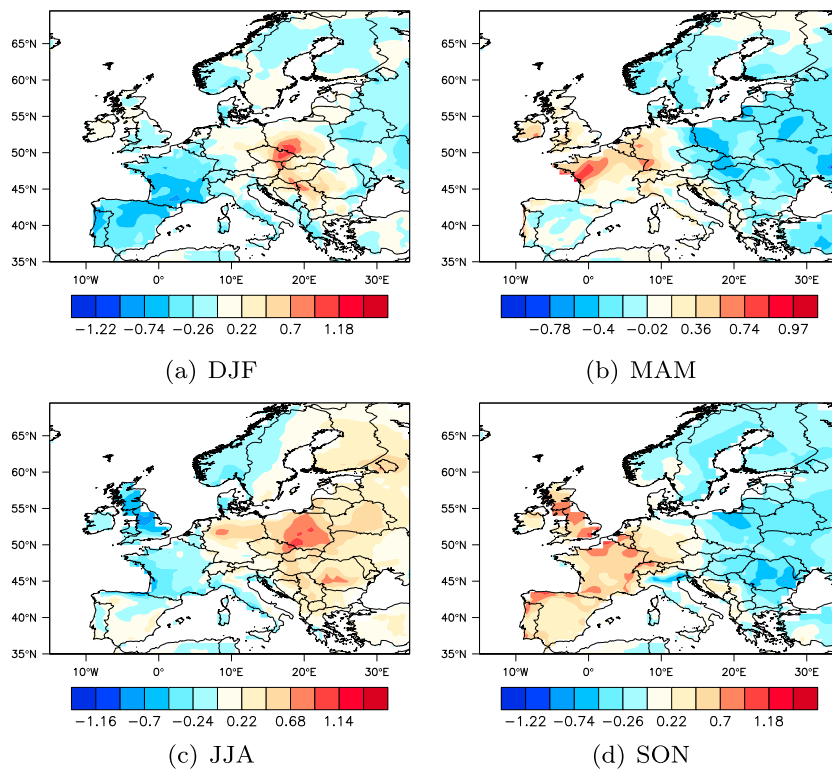


Figure A2. Difference between the average $PM_{2.5}$ in 2070–2099 and in 1975–2004 under the RCP4.5 scenario ($\mu g m^{-3}$).

Appendix B: Seasonal Response of $PM_{2.5}$ Under RCP8.5

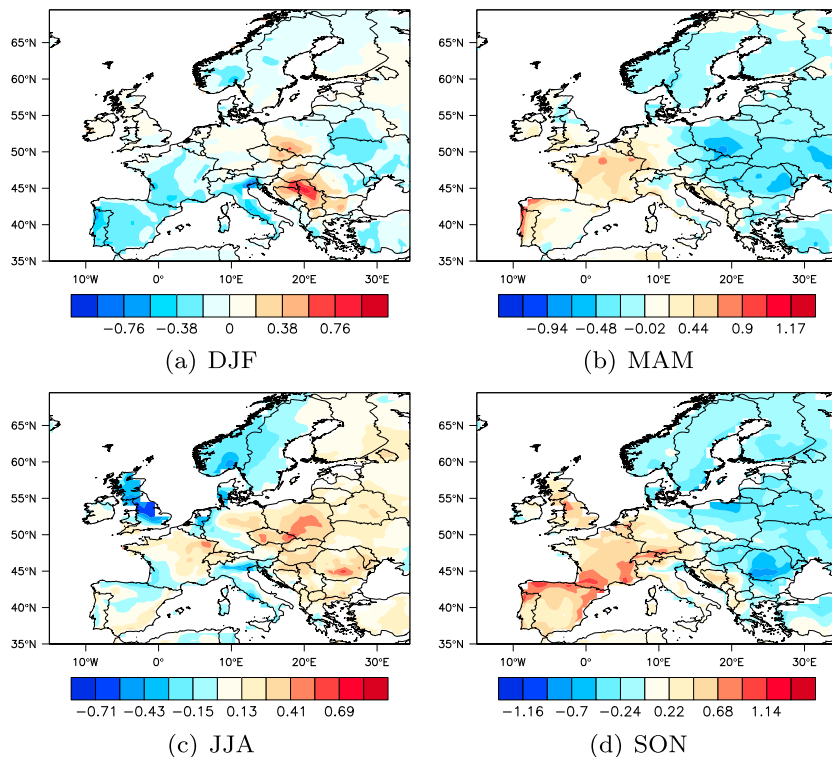


Figure B1. Difference between the average $PM_{2.5}$ in 2020–2049 and in 1975–2004 under the RCP8.5 scenario ($\mu g m^{-3}$).

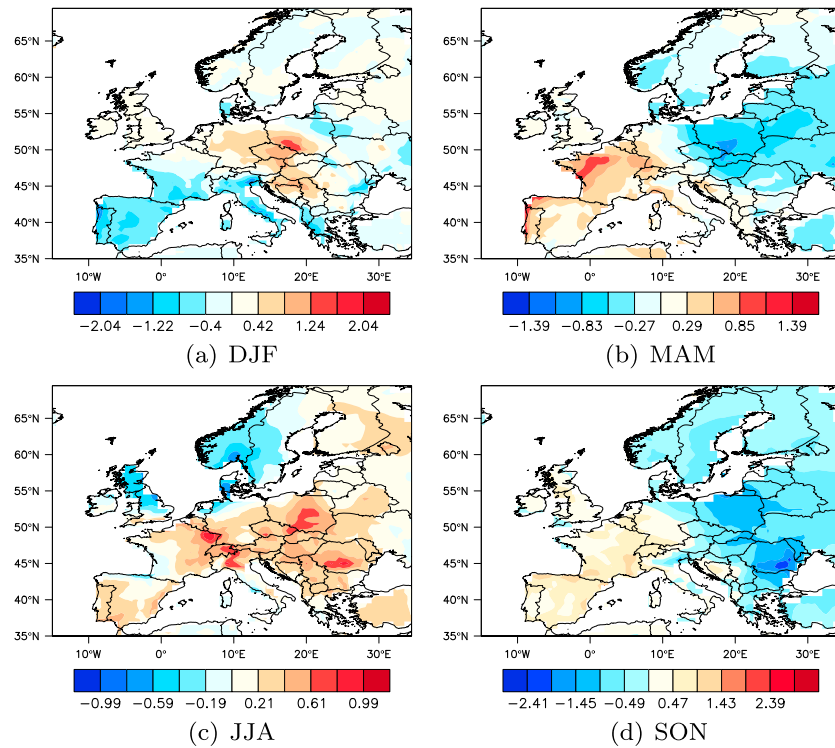


Figure B2. Difference between the average PM_{2.5} in 2070–2099 and in 1975–2004 under the RCP8.5 scenario ($\mu\text{g m}^{-3}$).

Appendix C: Seasonal Response of Meteorological Variables Under RCP4.5

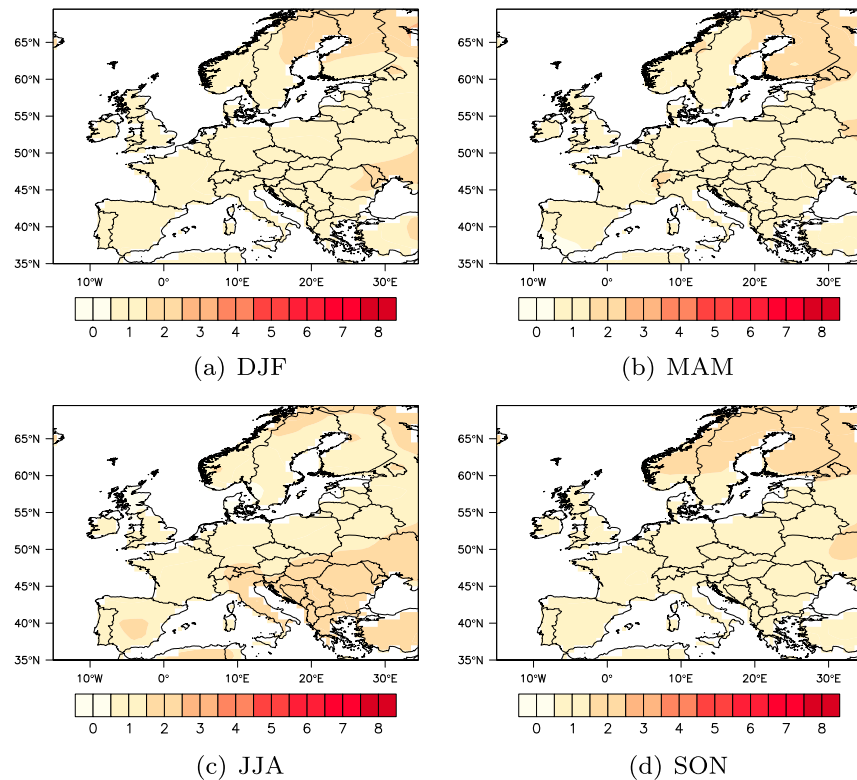


Figure C1. Difference between the average temperature in 2020–2049 and in 1975–2004 under the RCP4.5 scenario (K).

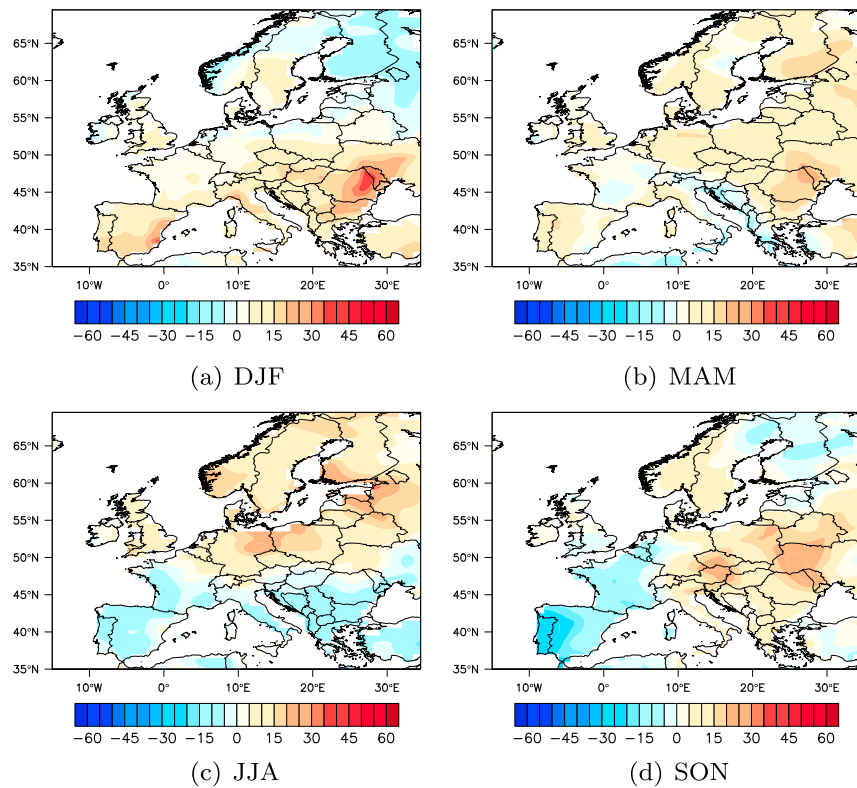


Figure C2. Evolution of the average precipitation in 2020–2049 and in 1975–2004 under the RCP4.5 scenario (%).

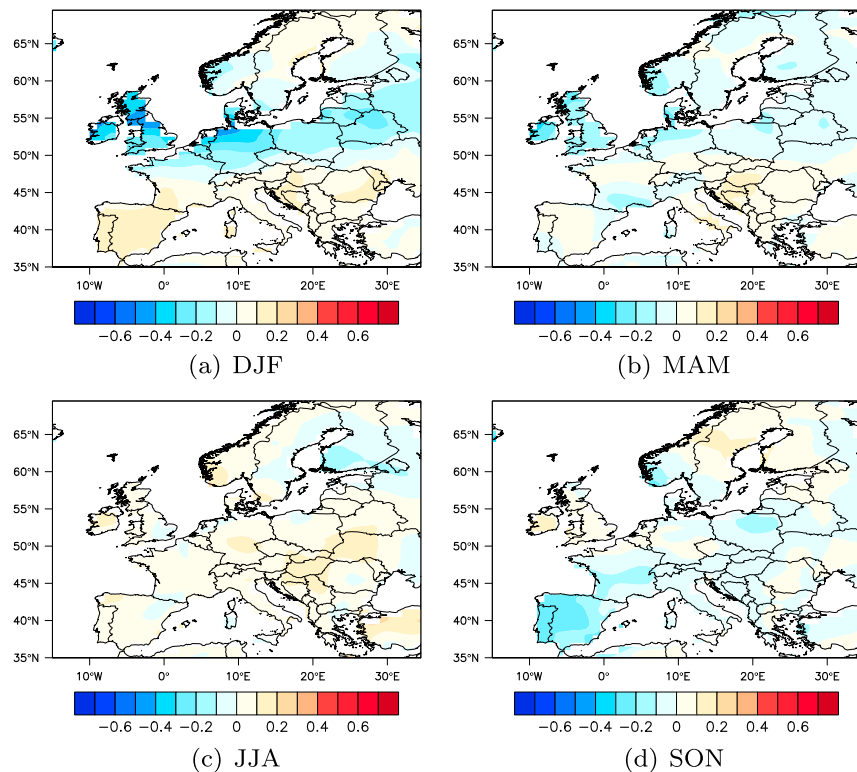


Figure C3. Difference between the average surface wind speed in 2020–2049 and in 1975–2004 under the RCP4.5 scenario ($m s^{-1}$).

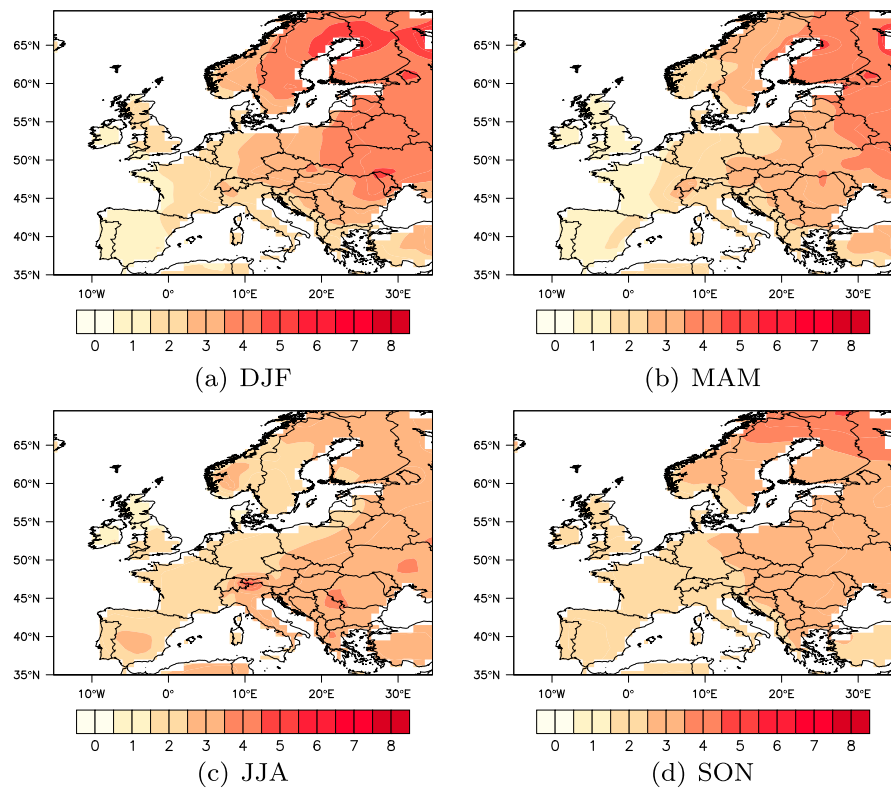


Figure C4. Difference between the average temperature in 2070–2099 and in 1975–2004 under the RCP4.5 scenario (K).

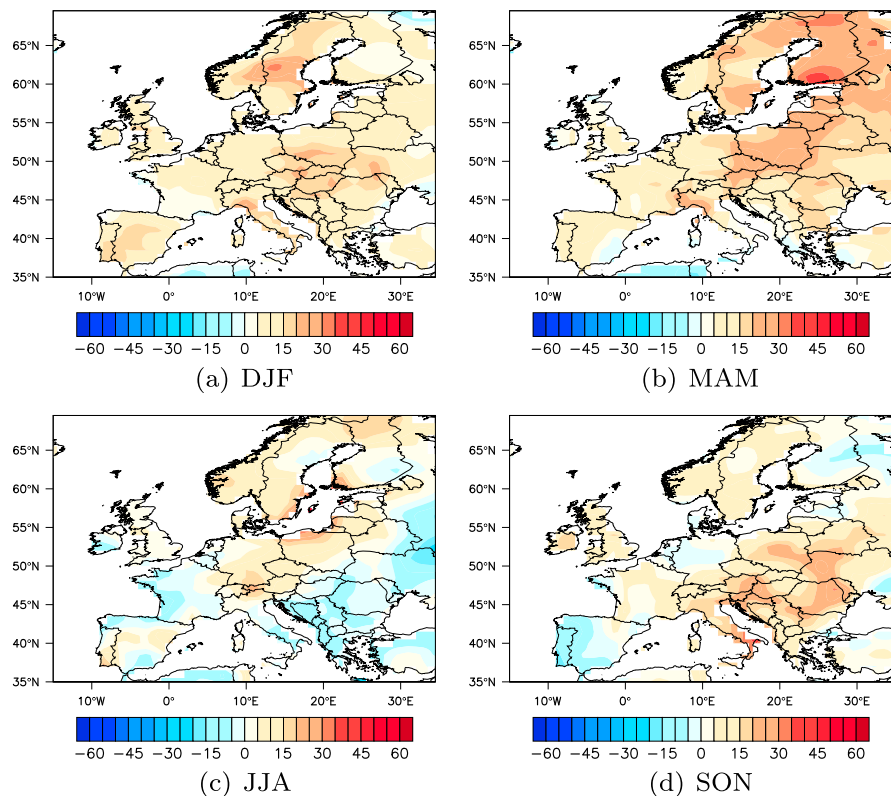


Figure C5. Evolution of the average precipitation in 2070–2099 and in 1975–2004 under the RCP4.5 scenario (%).

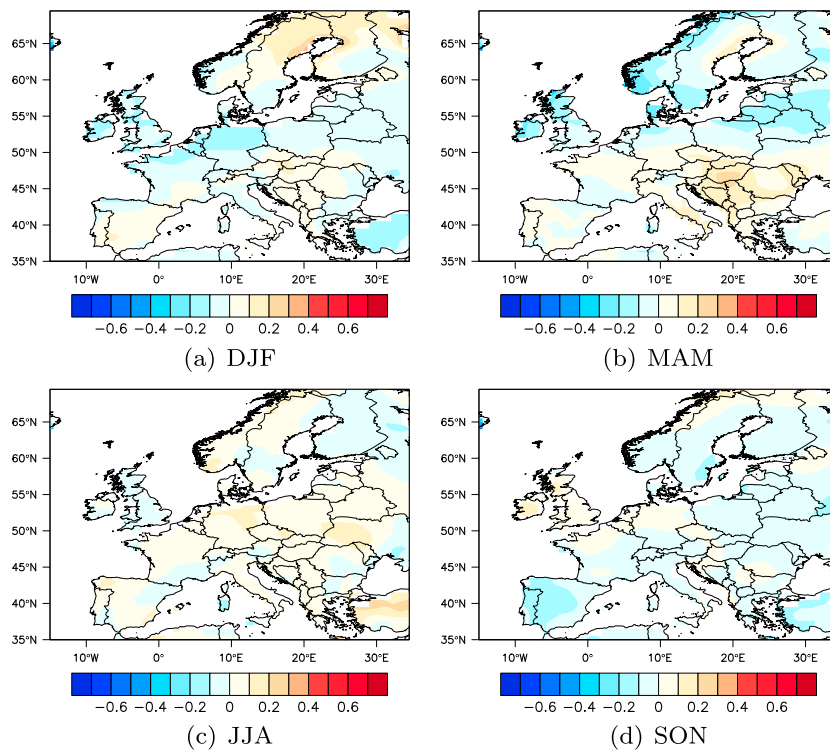


Figure C6. Difference between the average surface wind speed in 2070–2099 and in 1975–2004 under the RCP4.5 scenario (m s^{-1}).

Appendix D: Seasonal Response of Meteorological Variables Under RCP8.5

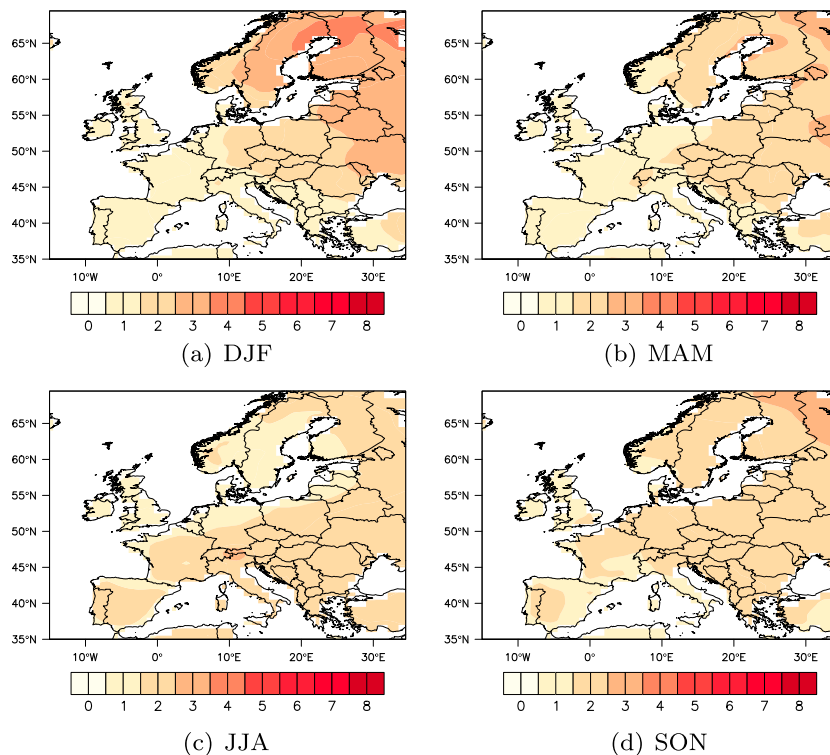


Figure D1. Difference between the average temperature in 2020–2049 and in 1975–2004 under the RCP8.5 scenario (K).

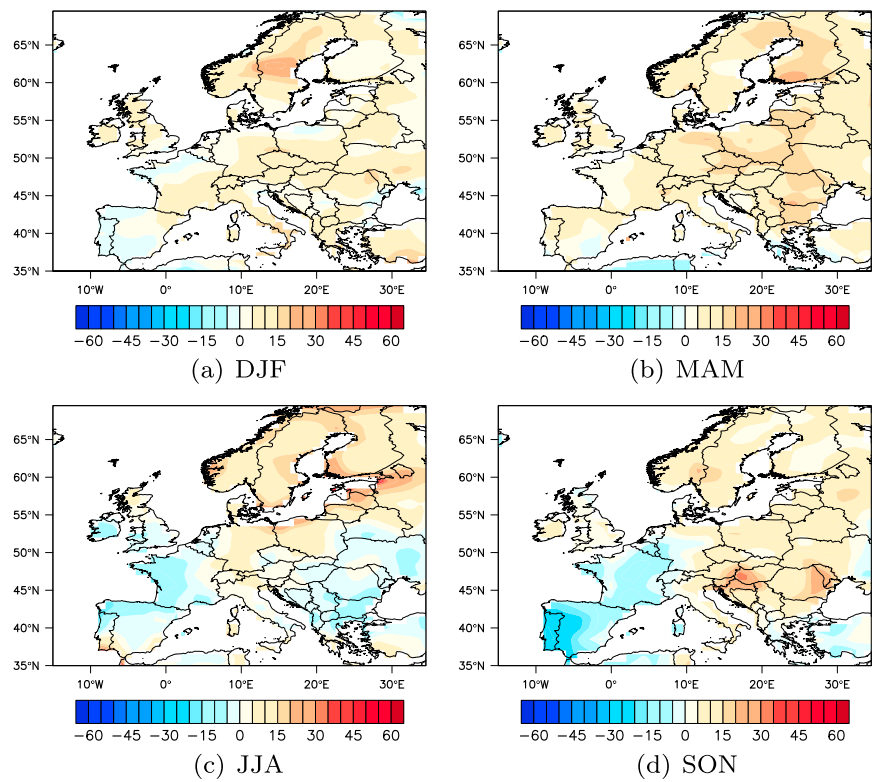


Figure D2. Evolution of the average precipitation in 2020–2049 and in 1975–2004 under the RCP8.5 scenario (%).

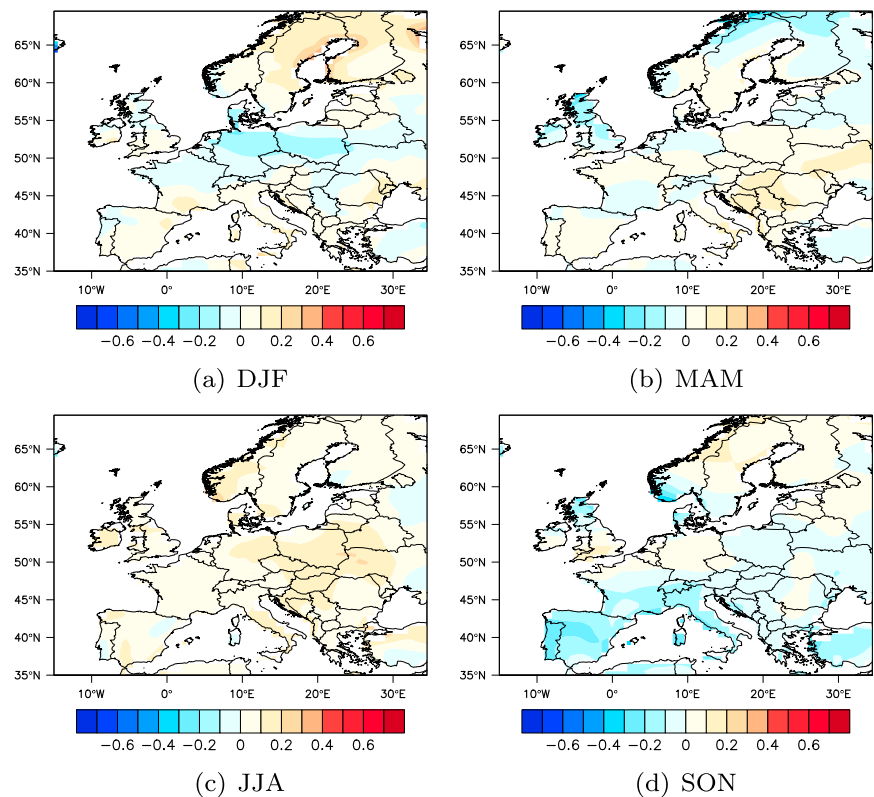


Figure D3. Difference between the average surface wind speed in 2020–2049 and in 1975–2004 under the RCP8.5 scenario ($m s^{-1}$).

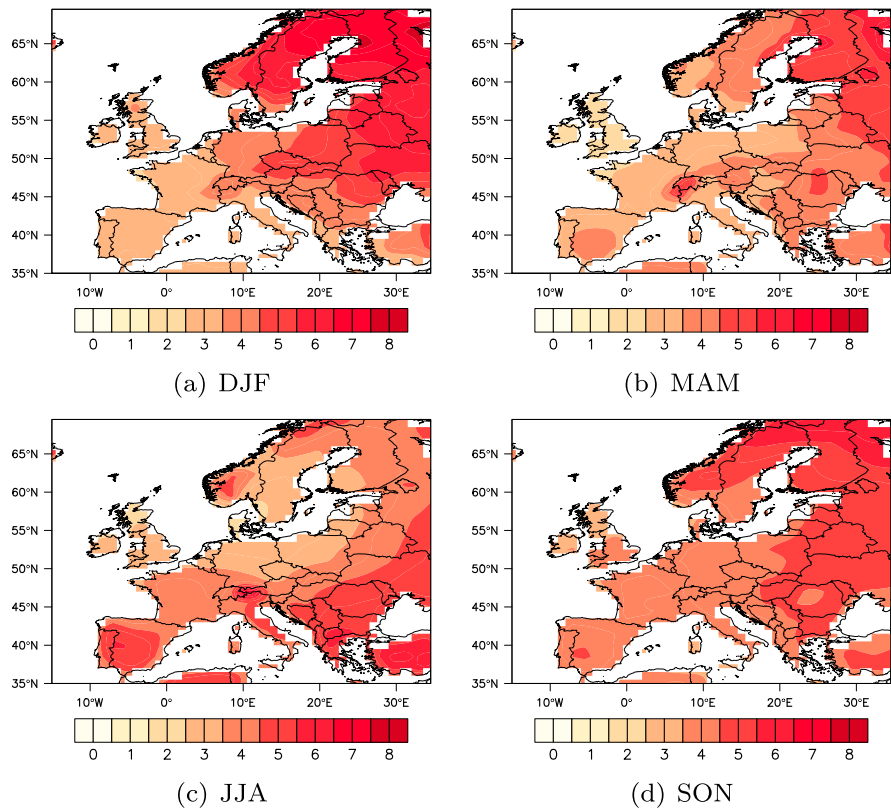


Figure D4. Difference between the average temperature in 2070–2099 and in 1975–2004 under the RCP8.5 scenario (K).

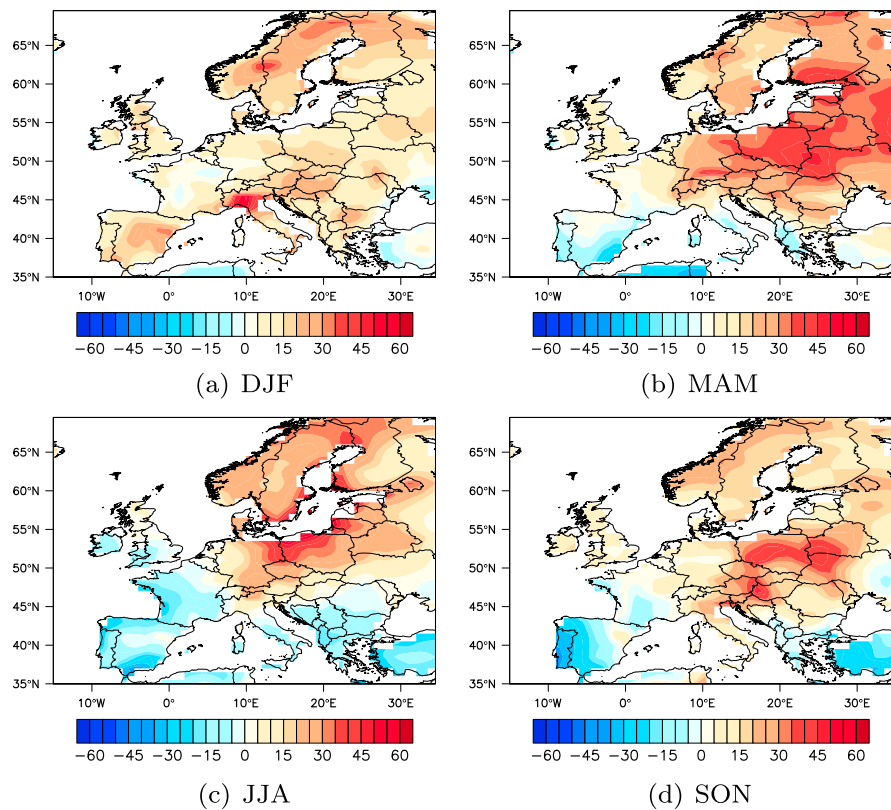


Figure D5. Evolution of the average precipitation in 2070–2099 and in 1975–2004 under the RCP8.5 scenario (%).

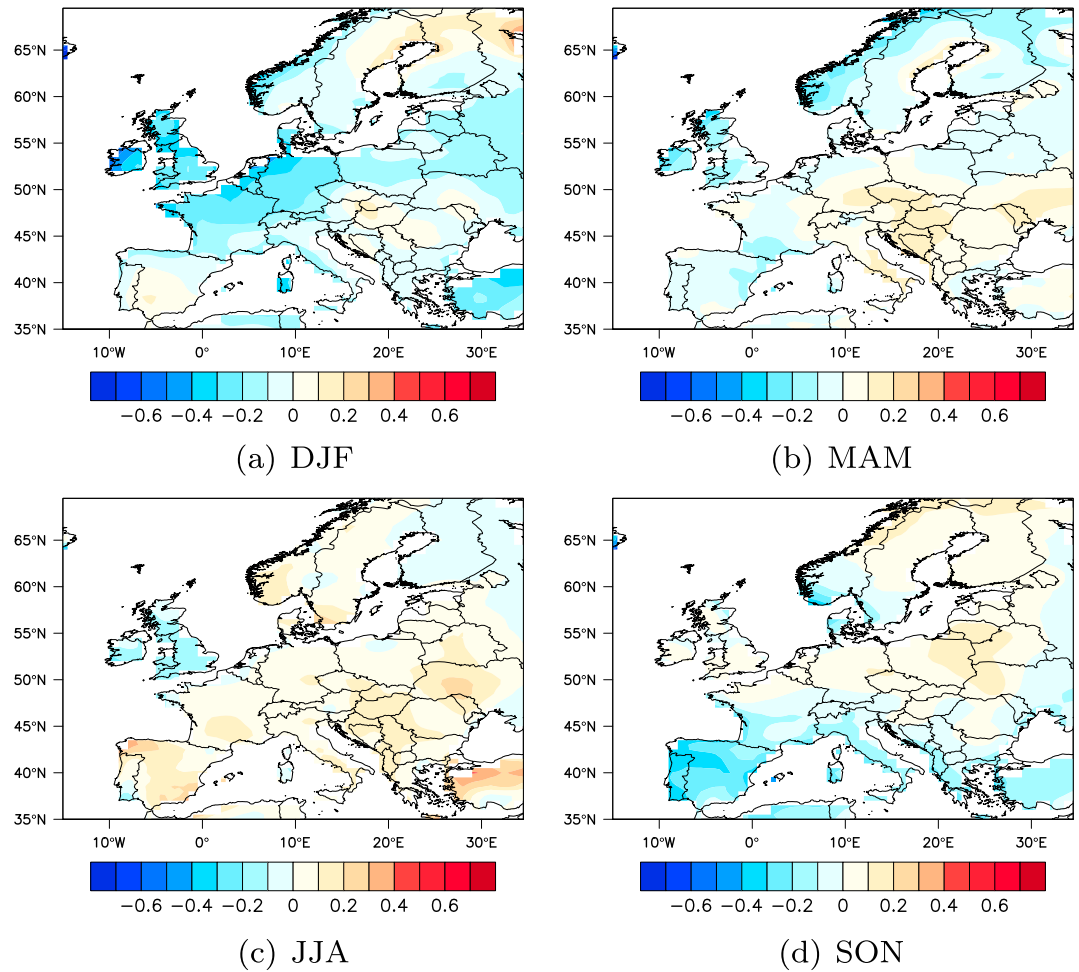


Figure D6. Difference between the average surface wind speed in 2070–2099 and in 1975–2004 under the RCP8.5 scenario (m s^{-1}).

Appendix E: Comparison in Annual Meteorological Variables Between the Distant and Near Futures

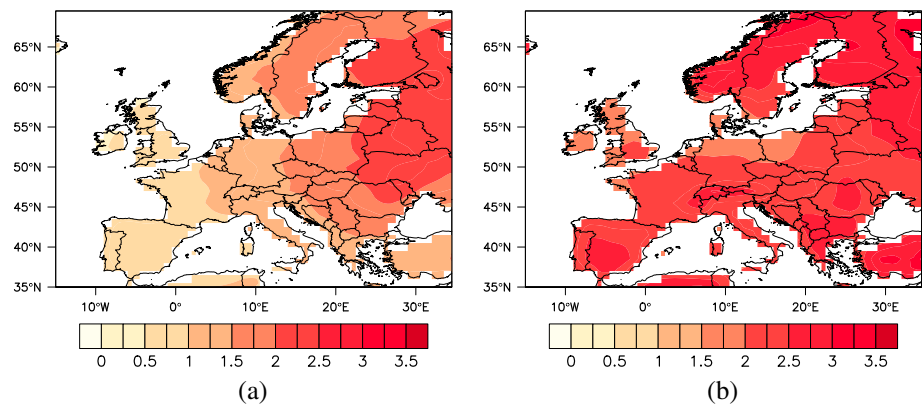


Figure E1. Difference between the annual temperature ($^{\circ}\text{C}$) in the distant and near future for the (a) RCP4.5 and (b) RCP8.5 scenarios.

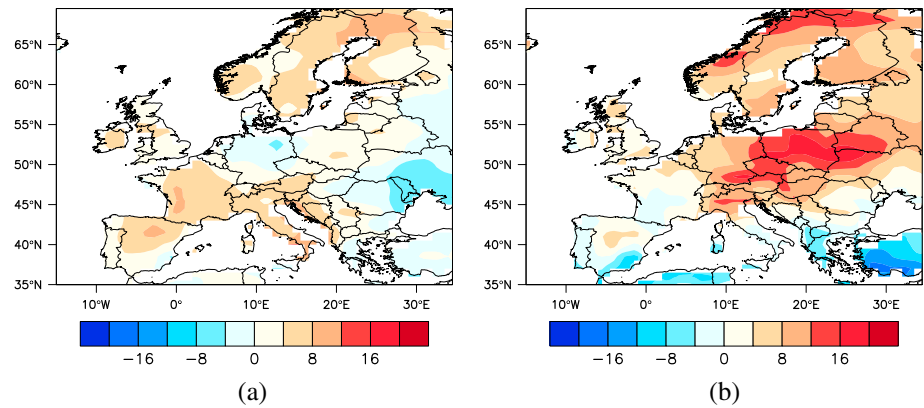


Figure E2. Difference between the annual precipitation (%) in the distant and near future for the (a) RCP4.5 and (b) RCP8.5 scenarios.

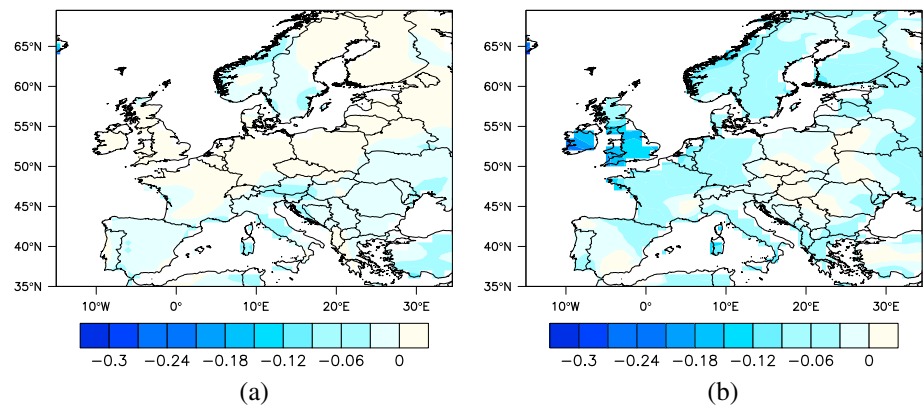


Figure E3. Difference between the annual wind speed ($m s^{-1}$) in the distant and near future for the (a) RCP4.5 and (b) RCP8.5 scenarios.

Appendix F: Range of Variation of $PM_{2.5}$ and Its Components Among Future Periods and Scenarios

Table F1. Range of Variation of $PM_{2.5}$ and Its Components^a for the RCP4.5 Scenario (2020–2049), Compared to the Historical Period ($\mu g m^{-3}$)

	DJF	MAM	JJA	SON	Annual
Northern Europe	$PM_{2.5}$ [−0.83; 1.05]	$PM_{2.5}$ [−0.4; 0.22]	$PM_{2.5}$ [−0.47; 0.34]	$PM_{2.5}$ [−0.45; 0.35]	$PM_{2.5}$ [−0.36; 0.17]
	SO_4^- [−0.07; 0.09]	SO_4^- [−0.08; 0.04]	SO_4^- [−0.05; 0.08]	SO_4^- [−0.12; 0.03]	SO_4^- [−0.04; 0.02]
	NO_3^- [−0.06; 0.16]	NO_3^- [−0.16; 0.08]	NO_3^- [−0.23; 0.12]	NO_3^- [−0.19; 0]	NO_3^- [−0.08; 0.03]
	NH_4^+ [−0.03; 0.09]	NH_4^+ [−0.07; 0.03]	NH_4^+ [−0.07; 0.06]	NH_4^+ [−0.09; 0.01]	NH_4^+ [−0.03; 0.02]
	Dust [−0.02; 0.14]	Dust [−0.03; 0.09]	Dust [−0.05; 0.06]	Dust [−0.03; 0.02]	Dust [−0.01; 0.05]
	BC [−0.01; 0.08]	BC [−0.02; 0.01]	BC [−0.01; 0]	BC [−0.01; 0.01]	BC [−0; 0.02]
	SS [−0.89; 0.09]	SS [−0.27; 0.09]	SS [−0.05; 0.15]	SS [−0.05; 0.36]	SS [−0.27; 0.11]
	OM [−0.01; 0.88]	OM [−0.11; 0.21]	OM [−0.29; 0.05]	OM [−0.09; 0.07]	OM [−0.03; 0.19]
Southern Europe	$PM_{2.5}$ [−1.5; 0.09]	$PM_{2.5}$ [−0.63; 0.3]	$PM_{2.5}$ [−0.5; 0.36]	$PM_{2.5}$ [−0.5; 1.03]	$PM_{2.5}$ [−0.5; 0.24]
	SO_4^- [−0.27; 0.14]	SO_4^- [−0.19; 0.16]	SO_4^- [−0.16; 0.15]	SO_4^- [−0.15; 0.3]	SO_4^- [−0.12; 0.16]
	NO_3^- [−0.58; 0.08]	NO_3^- [−0.25; 0.06]	NO_3^- [−0.17; 0.07]	NO_3^- [−0.16; 0.32]	NO_3^- [−0.21; 0.03]
	NH_4^+ [−0.18; 0.04]	NH_4^+ [−0.08; 0.05]	NH_4^+ [−0.06; 0.05]	NH_4^+ [−0.08; 0.16]	NH_4^+ [−0.06; 0.04]
	Dust [−0.24; 0.04]	Dust [−0.19; 0.16]	Dust [−0.11; 0.22]	Dust [−0.08; 0.2]	Dust [−0.06; 0.06]

Table F1. (continued)

	DJF	MAM	JJA	SON	Annual
	BC [−0.1; 0.01]	BC [−0.04; 0.01]	BC [−0.03; 0.02]	BC [−0.02; 0.05]	BC [−0.02; 0]
	SS [−0.06; 0.25]	SS [−0.14; 0.18]	SS [−0.05; 0.09]	SS [−0.3; 0.09]	SS [−0.06; 0.1]
	OM [−0.57; 0.04]	OM [−0.27; 0.09]	OM [−0.21; 0.12]	OM [−0.18; 0.33]	OM [−0.19; 0.04]
	PM _{2.5} [−1.61; 0.82]	PM _{2.5} [−0.62; 0.67]	PM _{2.5} [−0.61; 0.58]	PM _{2.5} [−0.7; 0.77]	PM _{2.5} [−0.63; 0.26]
	SO ₄ [−] [−0.23; 0.36]	SO ₄ [−] [−0.12; 0.19]	SO ₄ [−] [−0.05; 0.16]	SO ₄ [−] [−0.21; 0.3]	SO ₄ [−] [−0.1; 0.16]
	NO ₃ [−] [−0.66; 0.13]	NO ₃ [−] [−0.32; 0.27]	NO ₃ [−] [−0.33; 0.19]	NO ₃ [−] [−0.36; 0.39]	NO ₃ [−] [−0.35; 0.11]
Central Europe	NH ₄ ⁺ [−0.22; 0.15]	NH ₄ ⁺ [−0.11; 0.1]	NH ₄ ⁺ [−0.09; 0.08]	NH ₄ ⁺ [−0.12; 0.14]	NH ₄ ⁺ [−0.1; 0.05]
	Dust [−0.12; 0.06]	Dust [−0.02; 0.16]	Dust [−0.07; 0.09]	Dust [−0.06; 0.08]	Dust [−0.01; 0.07]
	BC [−0.09; 0.05]	BC [−0.04; 0.03]	BC [−0.04; 0.03]	BC [−0.02; 0.08]	BC [−0.04; 0.04]
	SS [−0.45; 0.05]	SS [−0.25; 0.02]	SS [−0.05; 0.05]	SS [−0.06; 0.07]	SS [−0.14; 0.03]
	OM [−0.47; 0.23]	OM [−0.17; 0.14]	OM [−0.19; 0.19]	OM [−0.16; 0.28]	OM [−0.18; 0.09]
	PM _{2.5} [−0.7; 0.6]	PM _{2.5} [−0.14; 0.85]	PM _{2.5} [−0.56; 0.44]	PM _{2.5} [−0.28; 0.77]	PM _{2.5} [−0.13; 0.48]
	SO ₄ [−] [−0.05; 0.17]	SO ₄ [−] [−0.07; 0.11]	SO ₄ [−] [−0.08; 0.05]	SO ₄ [−] [−0.03; 0.15]	SO ₄ [−] [−0.01; 0.07]
	NO ₃ [−] [−0.28; 0.24]	NO ₃ [−] [−0.15; 0.4]	NO ₃ [−] [−0.29; 0.28]	NO ₃ [−] [−0.11; 0.39]	NO ₃ [−] [−0.06; 0.22]
Western Europe	NH ₄ ⁺ [−0.08; 0.11]	NH ₄ ⁺ [−0.04; 0.14]	NH ₄ ⁺ [−0.1; 0.1]	NH ₄ ⁺ [−0.04; 0.14]	NH ₄ ⁺ [−0.01; 0.08]
	Dust [−0.02; 0.1]	Dust [0; 0.15]	Dust [−0.03; 0.06]	Dust [−0.01; 0.08]	Dust [0; 0.07]
	BC [−0.03; 0.06]	BC [−0.01; 0.03]	BC [−0.02; 0.03]	BC [−0; 0.08]	BC [−0.01; 0.04]
	SS [−0.61; 0.14]	SS [−0.24; 0.19]	SS [−0.31; 0.09]	SS [−0.39; 0.26]	SS [−0.27; 0.04]
	OM [−0.33; 0.18]	OM [−0.07; 0.26]	OM [−0.14; 0.09]	OM [−0.01; 0.28]	OM [−0.06; 0.12]
	PM _{2.5} [−1.01; 1.05]	PM _{2.5} [−0.95; 0.04]	PM _{2.5} [−0.1; 0.51]	PM _{2.5} [−0.76; −0]	PM _{2.5} [−0.44; 0.17]
	SO ₄ [−] [−0.23; 0.16]	SO ₄ [−] [−0.2; 0.06]	SO ₄ [−] [−0.04; 0.16]	SO ₄ [−] [−0.22; 0.01]	SO ₄ [−] [−0.11; 0.01]
	NO ₃ [−] [−0.23; 0.09]	NO ₃ [−] [−0.21; 0]	NO ₃ [−] [−0.03; 0.06]	NO ₃ [−] [−0.23; −0.01]	NO ₃ [−] [−0.12; −0.02]
Eastern Europe	NH ₄ ⁺ [−0.12; 0.05]	NH ₄ ⁺ [−0.11; 0.01]	NH ₄ ⁺ [−0.02; 0.07]	NH ₄ ⁺ [−0.12; 0]	NH ₄ ⁺ [−0.07; −0]
	Dust [−0.22; 0.14]	Dust [−0.22; 0.09]	Dust [−0.04; 0.1]	Dust [−0.08; 0.05]	Dust [−0.1; 0.05]
	BC [−0.08; 0.08]	BC [−0.07; 0]	BC [−0.01; 0.01]	BC [−0.03; 0.02]	BC [−0.03; 0.02]
	SS [−0.26; 0.2]	SS [−0.11; 0.14]	SS [−0.02; 0.02]	SS [−0.06; 0.07]	SS [−0.07; 0.06]
	OM [−0.42; 0.88]	OM [−0.23; 0.03]	OM [−0.06; 0.24]	OM [−0.17; 0.03]	OM [−0.14; 0.19]

^aSO₄[−]: inorganic sulfate; NO₃[−]: inorganic nitrate; NH₄⁺: inorganic ammonium; Dust: inorganic soil dust; BC: black carbon; SS: sea salt; OM: organic matter.

Table F2. Range of Variation of PM_{2.5} and Its Components^a for the RCP4.5 Scenario (2070–2099), Compared to the Historical Period (μg m^{−3})

	DJF	MAM	JJA	SON	Annual
	PM _{2.5} [−0.6; 0.55]	PM _{2.5} [−0.53; 0.19]	PM _{2.5} [−0.46; 0.78]	PM _{2.5} [−0.58; 0.58]	PM _{2.5} [−0.29; 0.25]
	SO ₄ [−] [−0.08; 0.2]	SO ₄ [−] [−0.08; 0.04]	SO ₄ [−] [−0.04; 0.17]	SO ₄ [−] [−0.12; 0.06]	SO ₄ [−] [−0.03; 0.05]
	NO ₃ [−] [−0.13; 0.13]	NO ₃ [−] [−0.18; 0.09]	NO ₃ [−] [−0.21; 0.2]	NO ₃ [−] [−0.26; 0.03]	NO ₃ [−] [−0.1; 0.01]
Northern Europe	NH ₄ ⁺ [−0.04; 0.11]	NH ₄ ⁺ [−0.07; 0.01]	NH ₄ ⁺ [−0.05; 0.1]	NH ₄ ⁺ [−0.1; 0.03]	NH ₄ ⁺ [−0.03; 0.02]
	Dust [−0.13; 0.02]	Dust [−0.09; 0.07]	Dust [−0.08; 0.11]	Dust [−0.04; 0.04]	Dust [−0.05; 0.02]
	BC [−0.04; 0.01]	BC [−0.01; 0.02]	BC [−0.01; 0.02]	BC [−0.02; 0.01]	BC [−0.01; 0]
	SS [−0.18; 0.44]	SS [−0.17; 0.12]	SS [−0.13; 0.21]	SS [−0.06; 0.62]	SS [−0.12; 0.25]
	OM [−0.37; 0.05]	OM [−0.1; 0.19]	OM [−0.32; 0.42]	OM [−0.18; 0.08]	OM [−0.12; 0.04]
	PM _{2.5} [−0.84; 0.52]	PM _{2.5} [−0.51; 0.84]	PM _{2.5} [−0.8; 0.54]	PM _{2.5} [−0.57; 1.13]	PM _{2.5} [−0.2; 0.24]
	SO ₄ [−] [−0.1; 0.32]	SO ₄ [−] [−0.09; 0.22]	SO ₄ [−] [−0.13; 0.29]	SO ₄ [−] [−0.17; 0.35]	SO ₄ [−] [−0.07; 0.13]
	NO ₃ [−] [−0.3; 0.14]	NO ₃ [−] [−0.16; 0.16]	NO ₃ [−] [−0.21; 0.21]	NO ₃ [−] [−0.16; 0.43]	NO ₃ [−] [−0.06; 0.08]
Southern Europe	NH ₄ ⁺ [−0.11; 0.14]	NH ₄ ⁺ [−0.05; 0.11]	NH ₄ ⁺ [−0.07; 0.13]	NH ₄ ⁺ [−0.1; 0.2]	NH ₄ ⁺ [−0.04; 0.05]
	Dust [−0.13; 0.02]	Dust [−0.3; 0.12]	Dust [−0.16; 0.2]	Dust [−0.09; 0.17]	Dust [−0.06; 0.02]

Table F2. (continued)

	DJF	MAM	JJA	SON	Annual
	BC [−0.04; 0.01]	BC [−0.06; 0.04]	BC [−0.04; 0.02]	BC [−0.03; 0.07]	BC [−0.01; 0.01]
	SS [−0.13; 0.23]	SS [−0.16; 0.21]	SS [−0.1; 0.13]	SS [−0.28; 0.15]	SS [−0.09; 0.08]
	OM [−0.32; 0.18]	OM [−0.12; 0.22]	OM [−0.4; 0.3]	OM [−0.22; 0.37]	OM [−0.07; 0.09]
	PM _{2.5} [−0.53; 1.22]	PM _{2.5} [−0.54; 0.64]	PM _{2.5} [−0.49; 1.16]	PM _{2.5} [−0.79; 0.97]	PM _{2.5} [−0.25; 0.4]
	SO ₄ [−] [−0.1; 0.63]	SO ₄ [−] [−0.15; 0.11]	SO ₄ [−] [−0.07; 0.28]	SO ₄ [−] [−0.17; 0.21]	SO ₄ [−] [−0.03; 0.18]
	NO ₃ [−] [−0.22; 0.16]	NO ₃ [−] [−0.18; 0.36]	NO ₃ [−] [−0.22; 0.64]	NO ₃ [−] [−0.52; 0.35]	NO ₃ [−] [−0.15; 0.28]
Central Europe	NH ₄ ⁺ [−0.08; 0.25]	NH ₄ ⁺ [−0.08; 0.11]	NH ₄ ⁺ [−0.06; 0.19]	NH ₄ ⁺ [−0.15; 0.12]	NH ₄ ⁺ [−0.04; 0.08]
	Dust [−0.06; 0.06]	Dust [−0.11; 0.08]	Dust [−0.11; 0.08]	Dust [−0.08; 0.07]	Dust [−0.04; 0.03]
	BC [−0.03; 0.04]	BC [−0.02; 0.03]	BC [−0.02; 0.04]	BC [−0.02; 0.09]	BC [−0.01; 0.03]
	SS [−0.15; 0.04]	SS [−0.08; 0.11]	SS [−0.1; 0.03]	SS [−0.11; 0.06]	SS [−0.07; 0.01]
	OM [−0.21; 0.31]	OM [−0.16; 0.14]	OM [−0.22; 0.34]	OM [−0.22; 0.39]	OM [−0.07; 0.1]
	PM _{2.5} [−0.83; 0.41]	PM _{2.5} [−0.21; 0.97]	PM _{2.5} [−0.92; 0.12]	PM _{2.5} [−0.2; 1.18]	PM _{2.5} [−0.12; 0.35]
	SO ₄ [−] [−0.15; 0.1]	SO ₄ [−] [−0.05; 0.09]	SO ₄ [−] [−0.16; 0.04]	SO ₄ [−] [−0.01; 0.23]	SO ₄ [−] [−0.02; 0.04]
	NO ₃ [−] [−0.27; 0.03]	NO ₃ [−] [−0.04; 0.5]	NO ₃ [−] [−0.44; 0.24]	NO ₃ [−] [−0.06; 0.52]	NO ₃ [−] [−0.03; 0.19]
Western Europe	NH ₄ ⁺ [−0.1; 0.04]	NH ₄ ⁺ [−0.03; 0.17]	NH ₄ ⁺ [−0.16; 0.05]	NH ₄ ⁺ [−0.02; 0.21]	NH ₄ ⁺ [−0.02; 0.05]
	Dust [−0.06; 0.04]	Dust [−0.07; 0.08]	Dust [−0.13; 0.03]	Dust [0; 0.11]	Dust [−0.03; 0.03]
	BC [−0.03; 0.02]	BC [−0; 0.02]	BC [−0.02; 0.02]	BC [−0; 0.09]	BC [−0; 0.03]
	SS [−0.23; 0.31]	SS [−0.19; 0.22]	SS [−0.4; 0.14]	SS [−0.47; 0.32]	SS [−0.22; 0.11]
	OM [−0.24; 0.09]	OM [−0.06; 0.21]	OM [−0.3; 0.03]	OM [−0.01; 0.39]	OM [−0.05; 0.09]
	PM _{2.5} [−0.54; 0.5]	PM _{2.5} [−0.96; −0.03]	PM _{2.5} [−0.05; 0.88]	PM _{2.5} [−0.77; 0]	PM _{2.5} [−0.4; 0.16]
	SO ₄ [−] [−0.17; 0.17]	SO ₄ [−] [−0.17; 0.03]	SO ₄ [−] [−0.06; 0.27]	SO ₄ [−] [−0.15; 0.01]	SO ₄ [−] [−0.09; 0.08]
	NO ₃ [−] [−0.21; 0.09]	NO ₃ [−] [−0.18; 0.09]	NO ₃ [−] [−0; 0.11]	NO ₃ [−] [−0.23; 0.02]	NO ₃ [−] [−0.1; 0.02]
Eastern Europe	NH ₄ ⁺ [−0.1; 0.08]	NH ₄ ⁺ [−0.09; 0.02]	NH ₄ ⁺ [−0.02; 0.12]	NH ₄ ⁺ [−0.11; −0]	NH ₄ ⁺ [−0.05; 0.03]
	Dust [−0.25; 0.07]	Dust [−0.28; 0.04]	Dust [−0.13; 0.11]	Dust [−0.11; 0.05]	Dust [−0.12; 0.02]
	BC [−0.06; 0.03]	BC [−0.08; 0]	BC [−0.03; 0.03]	BC [−0.03; 0.01]	BC [−0.03; 0.01]
	SS [−0.1; 0.06]	SS [−0.06; 0.2]	SS [−0.04; 0]	SS [−0.03; 0.05]	SS [−0.05; 0.06]
	OM [−0.15; 0.34]	OM [−0.27; −0]	OM [0.02; 0.38]	OM [−0.24; 0.04]	OM [−0.06; 0.11]

^aSO₄[−]: inorganic sulfate; NO₃[−]: inorganic nitrate; NH₄⁺: inorganic ammonium; Dust: inorganic soil dust; BC: black carbon; SS: sea salt; OM: organic matter.

Table F3. Range of Variation of PM_{2.5} and Its Components^a for the RCP8.5 Scenario (2020–2049), Compared to the Historical Period (μg m^{−3})

	DJF	MAM	JJA	SON	Annual
	PM _{2.5} [−0.7; 0.55]	PM _{2.5} [−0.32; 0.1]	PM _{2.5} [−0.5; 0.32]	PM _{2.5} [−0.61; 0.36]	PM _{2.5} [−0.36; 0.17]
	SO ₄ [−] [−0.07; 0.08]	SO ₄ [−] [−0.06; 0.01]	SO ₄ [−] [−0.05; 0.09]	SO ₄ [−] [−0.15; 0.05]	SO ₄ [−] [−0.04; 0.03]
	NO ₃ [−] [−0.09; 0.05]	NO ₃ [−] [−0.15; −0.01]	NO ₃ [−] [−0.19; 0.11]	NO ₃ [−] [−0.32; 0]	NO ₃ [−] [−0.14; 0]
Northern Europe	NH ₄ ⁺ [−0.04; 0.04]	NH ₄ ⁺ [−0.05; −0]	NH ₄ ⁺ [−0.06; 0.05]	NH ₄ ⁺ [−0.12; 0.01]	NH ₄ ⁺ [−0.05; 0.01]
	Dust [−0.07; 0.03]	Dust [−0.06; 0.06]	Dust [−0.06; 0.08]	Dust [−0.04; 0.03]	Dust [−0.03; 0.03]
	BC [−0.04; 0.01]	BC [−0.01; 0.01]	BC [−0.01; 0.01]	BC [−0.01; 0.01]	BC [−0.01; 0]
	SS [−0.12; 0.55]	SS [−0.17; 0.12]	SS [−0.06; 0.2]	SS [−0.1; 0.41]	SS [−0.06; 0.2]
	OM [−0.41; 0.1]	OM [−0.06; 0.12]	OM [−0.34; 0.14]	OM [−0.14; 0.07]	OM [−0.17; 0.01]
	PM _{2.5} [−0.71; 0.72]	PM _{2.5} [−0.51; 1.17]	PM _{2.5} [−0.38; 0.46]	PM _{2.5} [−0.63; 1.16]	PM _{2.5} [−0.18; 0.45]
	SO ₄ [−] [−0.09; 0.31]	SO ₄ [−] [−0.19; 0.35]	SO ₄ [−] [−0.09; 0.17]	SO ₄ [−] [−0.11; 0.35]	SO ₄ [−] [−0.06; 0.17]
	NO ₃ [−] [−0.22; 0.19]	NO ₃ [−] [−0.17; 0.25]	NO ₃ [−] [−0.08; 0.16]	NO ₃ [−] [−0.21; 0.46]	NO ₃ [−] [−0.07; 0.14]
Southern Europe	NH ₄ ⁺ [−0.08; 0.16]	NH ₄ ⁺ [−0.06; 0.16]	NH ₄ ⁺ [−0.03; 0.08]	NH ₄ ⁺ [−0.09; 0.2]	NH ₄ ⁺ [−0.03; 0.09]
	Dust [−0.13; 0.01]	Dust [−0.29; 0.17]	Dust [−0.15; 0.26]	Dust [−0.08; 0.21]	Dust [−0.05; 0.06]

Table F3. (continued)

	DJF	MAM	JJA	SON	Annual
	BC [−0.05; 0.01]	BC [−0.02; 0.04]	BC [−0.04; 0.03]	BC [−0.02; 0.1]	BC [−0.01; 0.03]
	SS [−0.1; 0.13]	SS [−0.15; 0.2]	SS [−0.09; 0.11]	SS [−0.39; 0.08]	SS [−0.11; 0.09]
	OM [−0.29; 0.15]	OM [−0.15; 0.38]	OM [−0.28; 0.19]	OM [−0.18; 0.51]	OM [−0.08; 0.16]
	PM _{2.5} [−0.95; 0.85]	PM _{2.5} [−0.81; 0.75]	PM _{2.5} [−0.49; 0.62]	PM _{2.5} [−0.87; 0.92]	PM _{2.5} [−0.36; 0.48]
	SO ₄ [−] [−0.13; 0.41]	SO ₄ [−] [−0.16; 0.07]	SO ₄ [−] [−0.06; 0.18]	SO ₄ [−] [−0.23; 0.31]	SO ₄ [−] [−0.09; 0.16]
	NO ₃ [−] [−0.44; 0.2]	NO ₃ [−] [−0.26; 0.29]	NO ₃ [−] [−0.27; 0.34]	NO ₃ [−] [−0.27; 0.42]	NO ₃ [−] [−0.22; 0.16]
Central Europe	NH ₄ ⁺ [−0.13; 0.2]	NH ₄ ⁺ [−0.12; 0.1]	NH ₄ ⁺ [−0.07; 0.1]	NH ₄ ⁺ [−0.13; 0.14]	NH ₄ ⁺ [−0.06; 0.07]
	Dust [−0.06; 0.06]	Dust [−0.07; 0.16]	Dust [−0.03; 0.09]	Dust [−0.11; 0.08]	Dust [−0.03; 0.06]
	BC [−0.03; 0.03]	BC [−0.03; 0.07]	BC [−0.03; 0.05]	BC [−0.03; 0.06]	BC [−0.01; 0.05]
	SS [−0.12; 0.05]	SS [−0.06; 0.05]	SS [−0.09; 0.06]	SS [−0.14; 0.08]	SS [−0.08; 0.01]
	OM [−0.28; 0.19]	OM [−0.25; 0.31]	OM [−0.2; 0.19]	OM [−0.2; 0.29]	OM [−0.11; 0.16]
	PM _{2.5} [−0.45; 0.36]	PM _{2.5} [−0.17; 0.82]	PM _{2.5} [−0.71; 0.52]	PM _{2.5} [−0.3; 0.95]	PM _{2.5} [−0.09; 0.48]
	SO ₄ [−] [−0.1; 0.05]	SO ₄ [−] [−0.05; 0.09]	SO ₄ [−] [−0.12; 0.06]	SO ₄ [−] [−0.04; 0.14]	SO ₄ [−] [−0.02; 0.05]
	NO ₃ [−] [−0.17; 0.07]	NO ₃ [−] [−0.08; 0.35]	NO ₃ [−] [−0.38; 0.38]	NO ₃ [−] [−0.15; 0.45]	NO ₃ [−] [−0.04; 0.21]
Western Europe	NH ₄ ⁺ [−0.07; 0.03]	NH ₄ ⁺ [−0.03; 0.12]	NH ₄ ⁺ [−0.13; 0.13]	NH ₄ ⁺ [−0.06; 0.15]	NH ₄ ⁺ [−0.02; 0.08]
	Dust [−0.02; 0.03]	Dust [−0.01; 0.14]	Dust [−0.04; 0.06]	Dust [−0.01; 0.09]	Dust [−0.01; 0.06]
	BC [−0.02; 0.03]	BC [−0; 0.06]	BC [−0.02; 0.04]	BC [−0.01; 0.06]	BC [−0; 0.05]
	SS [−0.13; 0.28]	SS [−0.22; 0.08]	SS [−0.23; 0.16]	SS [−0.46; 0.08]	SS [−0.22; 0.12]
	OM [−0.16; 0.04]	OM [−0.05; 0.31]	OM [−0.16; 0.1]	OM [−0.02; 0.36]	OM [−0.03; 0.16]
	PM _{2.5} [−0.42; 0.27]	PM _{2.5} [−0.77; −0.01]	PM _{2.5} [−0.11; 0.64]	PM _{2.5} [−0.85; 0.07]	PM _{2.5} [−0.33; −0.01]
	SO ₄ [−] [−0.15; 0.1]	SO ₄ [−] [−0.19; −0.01]	SO ₄ [−] [−0.07; 0.15]	SO ₄ [−] [−0.19; 0.02]	SO ₄ [−] [−0.09; 0.01]
	NO ₃ [−] [−0.12; 0.07]	NO ₃ [−] [−0.13; −0.01]	NO ₃ [−] [−0.04; 0.09]	NO ₃ [−] [−0.26; 0.07]	NO ₃ [−] [−0.1; −0]
Eastern Europe	NH ₄ ⁺ [−0.08; 0.03]	NH ₄ ⁺ [−0.09; −0.01]	NH ₄ ⁺ [−0.02; 0.07]	NH ₄ ⁺ [−0.12; 0.02]	NH ₄ ⁺ [−0.05; −0]
	Dust [−0.11; 0.04]	Dust [−0.18; 0.05]	Dust [−0.09; 0.14]	Dust [−0.15; 0.05]	Dust [−0.07; 0.03]
	BC [−0.04; 0.01]	BC [−0.05; 0]	BC [−0.02; 0.02]	BC [−0.04; 0.01]	BC [−0.02; 0]
	SS [−0.13; 0.03]	SS [−0.04; 0.08]	SS [−0.02; 0.01]	SS [−0.08; 0.02]	SS [−0.05; 0.01]
	OM [−0.15; 0.23]	OM [−0.23; 0.03]	OM [−0.11; 0.28]	OM [−0.21; 0.06]	OM [−0.09; 0.03]

^aSO₄[−]: inorganic sulfate; NO₃[−]: inorganic nitrate; NH₄⁺: inorganic ammonium; Dust: inorganic soil dust; BC: black carbon; SS: sea salt; OM: organic matter.

Table F4. Range of Variation of PM_{2.5} and Its Components^a for the RCP8.5 Scenario (2070–2099), Compared to the Historical Period (μg m^{−3})

	DJF	MAM	JJA	SON	Annual
	PM _{2.5} [−0.79; 0.83]	PM _{2.5} [−0.64; 0.26]	PM _{2.5} [−0.76; 0.47]	PM _{2.5} [−1.22; 0.71]	PM _{2.5} [−0.55; 0.37]
	SO ₄ [−] [−0.09; 0.13]	SO ₄ [−] [−0.14; 0.03]	SO ₄ [−] [−0.09; 0.11]	SO ₄ [−] [−0.31; 0.05]	SO ₄ [−] [−0.1; 0.04]
	NO ₃ [−] [−0.06; 0.12]	NO ₃ [−] [−0.28; 0]	NO ₃ [−] [−0.37; 0.18]	NO ₃ [−] [−0.51; −0.04]	NO ₃ [−] [−0.19; 0]
Northern Europe	NH ₄ ⁺ [−0.02; 0.07]	NH ₄ ⁺ [−0.11; 0.01]	NH ₄ ⁺ [−0.12; 0.08]	NH ₄ ⁺ [−0.24; −0.01]	NH ₄ ⁺ [−0.08; 0.01]
	Dust [−0.08; 0.06]	Dust [−0.08; 0.06]	Dust [−0.09; 0.05]	Dust [−0.1; 0.04]	Dust [−0.06; 0.02]
	BC [−0.02; 0.03]	BC [−0.03; 0.01]	BC [−0.01; 0.01]	BC [−0.04; 0.01]	BC [−0.02; 0]
	SS [−0.82; 0.66]	SS [−0.08; 0.35]	SS [−0.06; 0.2]	SS [−0.06; 0.81]	SS [−0.18; 0.37]
	OM [−0.11; 0.42]	OM [−0.2; 0.09]	OM [−0.5; 0.21]	OM [−0.25; −0.02]	OM [−0.19; 0.02]
	PM _{2.5} [−1.78; 0.67]	PM _{2.5} [−0.5; 1.39]	PM _{2.5} [−0.44; 0.59]	PM _{2.5} [−1.66; 1.53]	PM _{2.5} [−0.53; 0.43]
	SO ₄ [−] [−0.25; 0.41]	SO ₄ [−] [−0.12; 0.37]	SO ₄ [−] [−0.13; 0.3]	SO ₄ [−] [−0.5; 0.37]	SO ₄ [−] [−0.17; 0.21]
	NO ₃ [−] [−0.53; 0.18]	NO ₃ [−] [−0.19; 0.38]	NO ₃ [−] [−0.09; 0.21]	NO ₃ [−] [−0.43; 0.62]	NO ₃ [−] [−0.16; 0.17]
Southern Europe	NH ₄ ⁺ [−0.18; 0.16]	NH ₄ ⁺ [−0.06; 0.21]	NH ₄ ⁺ [−0.04; 0.12]	NH ₄ ⁺ [−0.28; 0.24]	NH ₄ ⁺ [−0.09; 0.09]
	Dust [−0.23; 0.02]	Dust [−0.34; 0.26]	Dust [−0.13; 0.25]	Dust [−0.18; 0.27]	Dust [−0.09; 0.06]

Table F4. (continued)

	DJF	MAM	JJA	SON	Annual
	BC [−0.09; 0.02]	BC [−0.02; 0.07]	BC [−0.02; 0.02]	BC [−0.05; 0.14]	BC [−0.02; 0.04]
	SS [−0.26; 0.2]	SS [−0.21; 0.18]	SS [−0.12; 0.19]	SS [−0.48; 0.2]	SS [−0.15; 0.1]
	OM [−0.75; 0.3]	OM [−0.14; 0.44]	OM [−0.3; 0.27]	OM [−0.47; 0.7]	OM [−0.16; 0.2]
	PM _{2.5} [−1.49; 1.54]	PM _{2.5} [−1.15; 0.76]	PM _{2.5} [−0.58; 0.97]	PM _{2.5} [−1.56; 1.31]	PM _{2.5} [−0.59; 0.76]
	SO ₄ [−] [−0.26; 0.62]	SO ₄ [−] [−0.24; 0.11]	SO ₄ [−] [−0.09; 0.23]	SO ₄ [−] [−0.4; 0.37]	SO ₄ [−] [−0.14; 0.24]
	NO ₃ [−] [−0.7; 0.16]	NO ₃ [−] [−0.31; 0.35]	NO ₃ [−] [−0.24; 0.51]	NO ₃ [−] [−0.65; 0.52]	NO ₃ [−] [−0.32; 0.25]
Central Europe	NH ₄ ⁺ [−0.2; 0.25]	NH ₄ ⁺ [−0.16; 0.13]	NH ₄ ⁺ [−0.09; 0.15]	NH ₄ ⁺ [−0.28; 0.16]	NH ₄ ⁺ [−0.09; 0.1]
	Dust [−0.11; 0.14]	Dust [−0.09; 0.13]	Dust [−0.05; 0.09]	Dust [−0.19; 0.14]	Dust [−0.05; 0.07]
	BC [−0.06; 0.09]	BC [−0.05; 0.05]	BC [−0.03; 0.09]	BC [−0.05; 0.1]	BC [−0.02; 0.07]
	SS [−0.57; 0.05]	SS [−0.07; 0.08]	SS [−0.12; 0.09]	SS [−0.18; 0.22]	SS [−0.15; 0.03]
	OM [−0.43; 0.65]	OM [−0.39; 0.19]	OM [−0.22; 0.36]	OM [−0.42; 0.42]	OM [−0.15; 0.24]
	PM _{2.5} [−1.05; 0.47]	PM _{2.5} [−0.22; 1.08]	PM _{2.5} [−0.68; 0.94]	PM _{2.5} [−0.34; 1.31]	PM _{2.5} [−0.16; 0.76]
	SO ₄ [−] [−0.09; 0.28]	SO ₄ [−] [−0.04; 0.13]	SO ₄ [−] [−0.13; 0.09]	SO ₄ [−] [−0.07; 0.14]	SO ₄ [−] [−0.04; 0.09]
	NO ₃ [−] [−0.34; 0.19]	NO ₃ [−] [−0.1; 0.6]	NO ₃ [−] [−0.35; 0.47]	NO ₃ [−] [−0.23; 0.52]	NO ₃ [−] [−0.08; 0.26]
Western Europe	NH ₄ ⁺ [−0.12; 0.14]	NH ₄ ⁺ [−0.05; 0.19]	NH ₄ ⁺ [−0.13; 0.15]	NH ₄ ⁺ [−0.09; 0.15]	NH ₄ ⁺ [−0.04; 0.1]
	Dust [−0.06; 0.11]	Dust [−0.07; 0.1]	Dust [−0.07; 0.05]	Dust [−0; 0.14]	Dust [−0.02; 0.07]
	BC [−0.04; 0.08]	BC [−0.01; 0.05]	BC [−0.01; 0.07]	BC [−0.01; 0.1]	BC [−0; 0.07]
	SS [−0.73; 0.08]	SS [−0.31; 0.2]	SS [−0.43; 0.11]	SS [−0.6; 0.64]	SS [−0.44; 0.17]
	OM [−0.39; 0.25]	OM [−0.04; 0.3]	OM [−0.16; 0.25]	OM [−0.08; 0.45]	OM [−0.05; 0.24]
	PM _{2.5} [−1.3; 0.62]	PM _{2.5} [−1.04; −0]	PM _{2.5} [−0.16; 0.89]	PM _{2.5} [−2.41; −0.18]	PM _{2.5} [−0.83; −0.02]
	SO ₄ [−] [−0.26; 0.21]	SO ₄ [−] [−0.2; −0.03]	SO ₄ [−] [−0.05; 0.22]	SO ₄ [−] [−0.48; −0.04]	SO ₄ [−] [−0.16; −0]
	NO ₃ [−] [−0.25; 0.12]	NO ₃ [−] [−0.28; 0.07]	NO ₃ [−] [−0.02; 0.13]	NO ₃ [−] [−0.64; −0.04]	NO ₃ [−] [−0.22; 0.01]
Eastern Europe	NH ₄ ⁺ [−0.14; 0.08]	NH ₄ ⁺ [−0.13; 0.01]	NH ₄ ⁺ [−0.02; 0.1]	NH ₄ ⁺ [−0.32; −0.03]	NH ₄ ⁺ [−0.1; 0]
	Dust [−0.36; 0.09]	Dust [−0.3; 0.03]	Dust [−0.12; 0.17]	Dust [−0.38; 0.04]	Dust [−0.17; 0.01]
	BC [−0.11; 0.04]	BC [−0.09; 0]	BC [−0.03; 0.03]	BC [−0.12; 0.01]	BC [−0.05; 0]
	SS [−0.34; 0.08]	SS [−0.03; 0.14]	SS [−0.02; 0.03]	SS [−0.04; 0.09]	SS [−0.07; 0.05]
	OM [−0.34; 0.53]	OM [−0.28; −0.02]	OM [−0.12; 0.38]	OM [−0.61; −0.06]	OM [−0.23; 0.06]

^aSO₄[−]: inorganic sulfate; NO₃[−]: inorganic nitrate; NH₄⁺: inorganic ammonium; Dust: inorganic soil dust; BC: black carbon; SS: sea salt; OM: organic matter.

Appendix G: Weather Type Description

G1. DJF Weather Types

WT0 is characterized by a positive anomaly of PSL over Greenland and a negative one that extends from northern America to eastern Europe. Such a positive anomaly favors northern flows, which lead to below average temperatures over the northern half of Europe. The negative anomaly of PSL favors southern flows, which lead to above average precipitations over all Europe, except over the Norwegian coast, which is protected by the anticyclone. PM_{2.5} concentrations are below average over the southern half of Europe (0 to −6 μg m^{−3}) and above average over the northern half of Europe (0 to +6 μg m^{−3}).

WT1 is characterized by a positive anomaly of PSL over Greenland and a negative one over the British Isles. Such a negative anomaly favors unstable meteorological conditions and above average precipitations over Europe, except for the southeasternmost part. It also favors above average temperatures. PM_{2.5} concentrations are below average (0 to −10 μg m^{−3}) over all Europe, except in the east (0 to +6 μg m^{−3}).

WT2 is characterized by a negative anomaly of PSL over Denmark and a positive one over the Azores. Such a WT is associated with above average precipitation over the largest part of Europe, with below average temperatures over the northern half of Europe, and with above average temperatures over southeastern Europe. PM_{2.5} concentrations are below average (0 to −10 μg m^{−3}) over western, central, and southern Europe and above average (0 to +4 μg m^{−3}) over northern and eastern Europe.

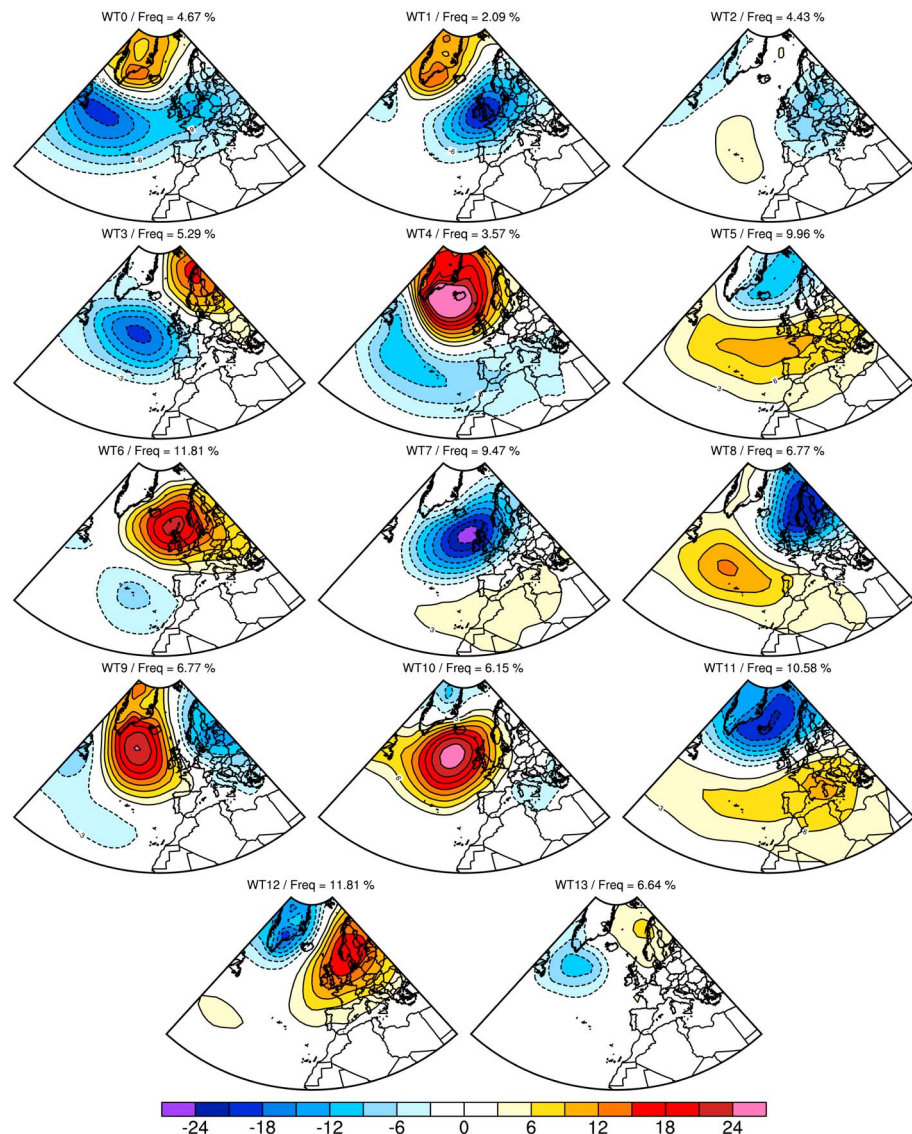


Figure G1. PSL anomalies (expressed in hPa) of the 14 WTs in DJF, built on the learning period (2000–2008). The frequency of each WT is stated above the corresponding WT.

WT3 is characterized by a positive anomaly of PSL over northern Scandinavia and a negative one over the North Atlantic Ocean. Such a positive anomaly favors northern flows, which leads to below average temperatures and precipitations over northern, central, and eastern Europe. The negative anomaly of PSL favors ocean flows, which lead to above average temperatures and precipitations. $PM_{2.5}$ concentrations are below average over France, the Iberian Peninsula, and eastern Europe (0 to $-6 \mu g m^{-3}$) and are above average over the UK, central Europe, and Scandinavia (0 to $+10 \mu g m^{-3}$).

WT4 is characterized by a strong positive anomaly of PSL over Iceland and a negative one that extends from the Quebec coasts to Greece. Such a positive anomaly leads to below average temperatures over Europe. Precipitations are also below average, except in southern Europe, where precipitations are above average because this region is under the influence of the negative anomaly of PSL. $PM_{2.5}$ concentrations are below average over Europe (0 to $-6 \mu g m^{-3}$), except in France and in the UK where they are above average (0 to $+8 \mu g m^{-3}$).

WT5 is characterized by a negative anomaly of PSL over the Greenland sea and a positive one that extends from the Quebec coasts to southeastern Europe. Such a positive anomaly leads to below average precipitation over Europe, except over the UK and the Norwegian coasts. Temperatures are above average, except in

the southeast. $PM_{2.5}$ concentrations are above average (0 to $+10 \mu\text{g m}^{-3}$) over central, eastern, and southern Europe. $PM_{2.5}$ concentrations are below average over northern Europe and the UK (0 to $-4 \mu\text{g m}^{-3}$).

WT6 is characterized by a positive anomaly of PSL over northern UK. Such a positive anomaly favors northern flows, which lead to below average temperatures and precipitations over the main part of Europe, except for northern Scandinavia, where there are above average temperatures and precipitations. $PM_{2.5}$ concentrations are above average over western and central Europe (0 to $+6 \mu\text{g m}^{-3}$) and below average elsewhere (0 to $-6 \mu\text{g m}^{-3}$).

WT7 is characterized by a strong negative anomaly of PSL over the northern part of the British Isles. Such a negative anomaly leads to above average temperatures and precipitations over most of Europe. Precipitations are below average over southeastern Europe and the Norwegian coasts. $PM_{2.5}$ concentrations are below average over western and central Europe (0 to $-10 \mu\text{g m}^{-3}$) and above average elsewhere (0 to $+8 \mu\text{g m}^{-3}$).

WT8 is characterized by a strong negative anomaly of PSL over Scandinavia and a positive one over the Atlantic Ocean. Such a negative anomaly leads to above average precipitation over most of Europe (except for the Iberian Peninsula, which is protected by the positive anomaly of PSL). This WT is associated with above average temperatures. $PM_{2.5}$ concentrations are below average (0 to $-12 \mu\text{g m}^{-3}$) over most of Europe, except over some localized areas (northern Italy and southeastern Romania).

WT9 is characterized by a positive anomaly of PSL over the North Atlantic Ocean and two negative anomalies: one over the Baltics and one over the Quebec coasts. This WT is associated with below average temperatures and with above average precipitations over most of Europe. Precipitations are below average only in western Europe. $PM_{2.5}$ concentrations are below average over most of Europe (0 to $+6 \mu\text{g m}^{-3}$). They are above average over northern Europe and in some localized areas of the Iberian Peninsula (0 to $+4 \mu\text{g m}^{-3}$).

WT10 is characterized by a positive anomaly of PSL over the North Atlantic region. Such a positive anomaly favors northern flows, which leads to below average temperatures over Europe and to below average precipitations over the western half of Europe. $PM_{2.5}$ concentrations are above average over France (0 to $+6 \mu\text{g m}^{-3}$) and below average elsewhere (0 to $-6 \mu\text{g m}^{-3}$).

WT11 is characterized by a strong negative anomaly of PSL over Iceland and a positive anomaly over the Mediterranean Sea. This WT is associated with above average temperatures over most of Europe and with below average precipitations, except in Scandinavia, the northern UK, and Ireland. $PM_{2.5}$ concentrations are above average in France and in southern Europe (0 to $+8 \mu\text{g m}^{-3}$) and are below average elsewhere (0 to $-4 \mu\text{g m}^{-3}$).

WT12 is characterized by a positive anomaly of PSL over southern Scandinavia and negative anomaly over Greenland. This WT is associated with below average temperatures and precipitations over most of Europe, except over northern Norway, where precipitations are above average. $PM_{2.5}$ concentrations are above average (0 to $+8 \mu\text{g m}^{-3}$) on the western half of Europe and are below average over the eastern half (0 to $-8 \mu\text{g m}^{-3}$).

WT13 is characterized by a positive anomaly of PSL over Norway and a negative one over the Greenland and Quebec coasts. This WT is associated with below average precipitations over western and northern Europe and the Iberian Peninsula and with above average precipitations over eastern and southern Europe. Temperatures are below average over most of Europe, except over the Iberian Peninsula and southeastern Europe. $PM_{2.5}$ concentrations are below average in southern Europe (0 to $-2 \mu\text{g m}^{-3}$) and are above average elsewhere (0 to $+2 \mu\text{g m}^{-3}$).

G2. MAM Weather Types

WT0 is characterized by a positive anomaly of PSL over the North Atlantic Ocean and a negative one over Scandinavia. This WT is associated with above average temperatures over eastern and southern Europe and with below average temperatures over northern and western Europe. Such a negative anomaly favors unstable meteorological conditions, leading to above average precipitations over most of Europe, except over some localized regions over southern Europe and Norway. $PM_{2.5}$ concentrations are above average over eastern Europe (0 to $+2 \mu\text{g m}^{-3}$) and are below average elsewhere (0 to $-6 \mu\text{g m}^{-3}$).

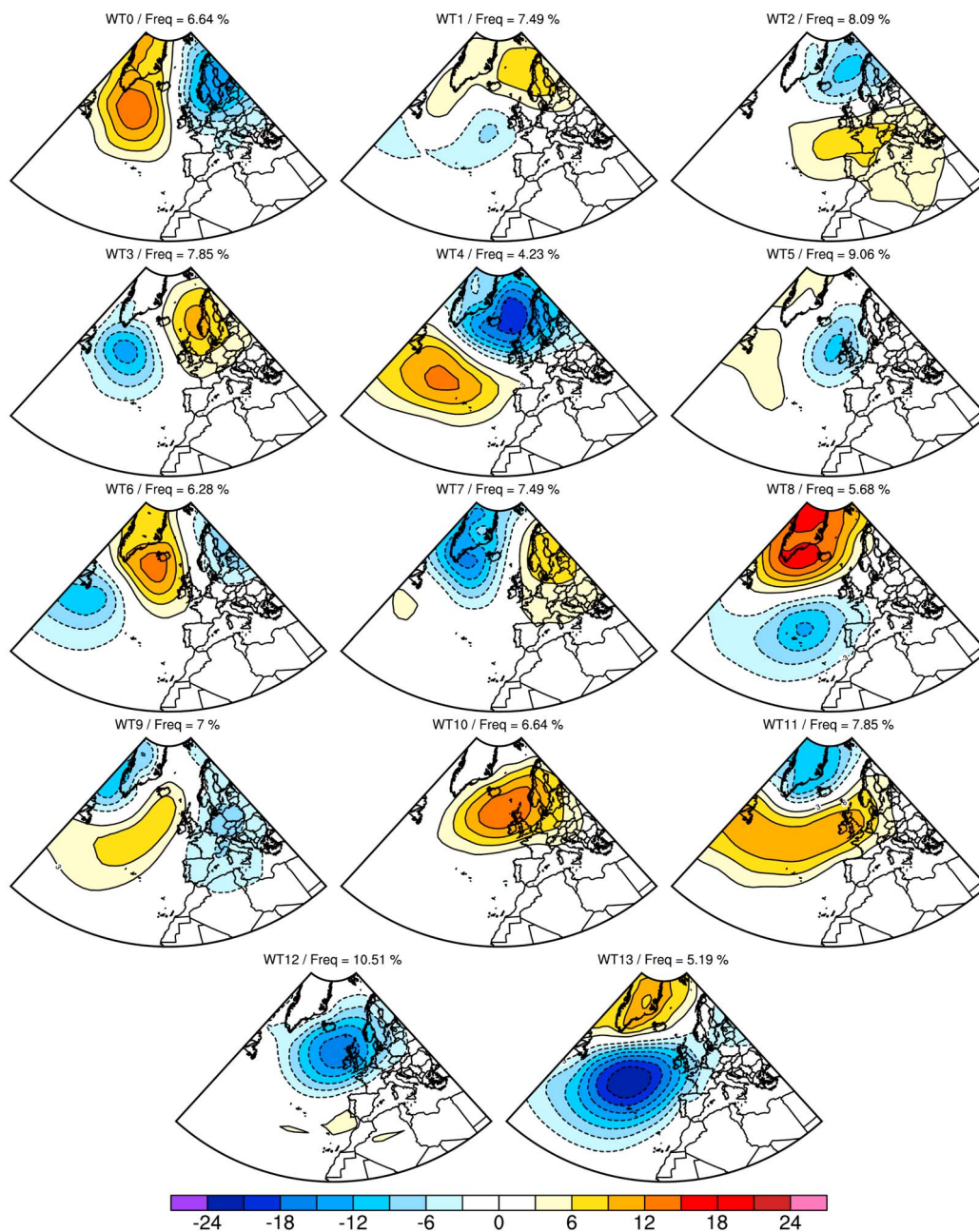


Figure G2. PSL anomalies (expressed in hPa) of the 14 WTs in MAM, built on the learning period (2000–2008). The frequency of each WT is stated above the corresponding WT.

WT1 is characterized by a positive anomaly of PSL over the Greenland Sea and a negative one over western Ireland. This WT is associated with above average precipitations over France, the Iberian Peninsula, and Italy and with below average precipitations elsewhere. Temperatures are below average over Portugal and the eastern half of Europe and are above average elsewhere. PM_{2.5} concentrations are above average over the UK and central Europe (0 to +6 μg m⁻³) and below average elsewhere (0 to -4 μg m⁻³).

WT2 is characterized by a negative anomaly of PSL over the Greenland Sea and a positive one over western Europe. This WT is associated with above average precipitation over the northern half of Europe and with below average precipitations over the southern half. Temperatures are above average. PM_{2.5} concentrations are above average over France and southern Europe (0 to +6 μg m⁻³). They are below average elsewhere (0 to -4 μg m⁻³).

WT3 is characterized by a positive anomaly of PSL over the Norwegian Sea and a negative one over the northern part of the Atlantic Ocean. This WT is associated with below average temperatures over most of Europe, except in some localized regions in Scandinavia, and in western and southeastern Europe. This WT favors below average precipitations over most of Europe, except in the southeast. $PM_{2.5}$ concentrations are above average over western Europe (0 to $+10 \mu\text{g m}^{-3}$) and are below average elsewhere (0 to $-2 \mu\text{g m}^{-3}$).

WT4 is characterized by a strong negative anomaly of PSL over Greenland and by a positive one over the Atlantic Ocean. This WT is associated with above average temperatures over most of Europe, except in France. Precipitations are above average over most of Europe, except over France, the Iberian Peninsula, and Turkey. $PM_{2.5}$ concentrations are below average in western and central Europe, in Norway, and in Italy (0 to $-6 \mu\text{g m}^{-3}$). They are above average elsewhere (0 to $+4 \mu\text{g m}^{-3}$).

WT5 is characterized by a negative anomaly of PSL over the north of the British Isles. Such a negative anomaly leads to above average precipitations over the western half of Europe. Precipitations are below average over southern and eastern Europe. Temperatures are above average, except in some localized areas (over the British Isles, the Iberian Peninsula, and northern Europe). $PM_{2.5}$ concentrations are above average in central Europe and Italy (0 to $+6 \mu\text{g m}^{-3}$) and below average elsewhere (0 to $-4 \mu\text{g m}^{-3}$).

WT6 is characterized by a positive anomaly of PSL over Iceland and by two negative anomalies: one over the Quebec coasts and one over Finland. This WT is associated with below average temperatures. Precipitations are below average over the western part of Europe and above average over the eastern part. $PM_{2.5}$ concentrations are below average (0 to $-8 \mu\text{g m}^{-3}$).

WT7 is characterized by a negative anomaly of PSL over Greenland and by a positive one over Scandinavia. Such a positive anomaly leads to below average precipitations. Temperatures are below average over southeastern Europe and is above average elsewhere. $PM_{2.5}$ concentrations are above average over western Europe (0 to $+4 \mu\text{g m}^{-3}$) and are below average over southern, central, and eastern Europe (0 to $-2 \mu\text{g m}^{-3}$).

WT8 is characterized by a strong positive anomaly of PSL over Greenland and by a negative anomaly over the Azores. This WT is associated with below average temperatures over most of Europe, except over southwestern France and Spain. Precipitations are above average in Portugal and eastern Europe, while they are below average elsewhere. $PM_{2.5}$ concentrations are above average in southeastern Europe, Scandinavia, and over the British Isles (0 to $+4 \mu\text{g m}^{-3}$). They are below average elsewhere (0 to $-4 \mu\text{g m}^{-3}$).

WT9 is characterized by a positive anomaly of PSL over the northern part of the Atlantic Ocean and by two negative anomalies: one over the Quebec coasts and one over northern Europe. This weather type is associated with below average temperatures over the western half of Europe and with above average temperatures over the eastern half. Precipitations are below average over the UK and over the Norwegian coasts. They are above average elsewhere. $PM_{2.5}$ concentrations are below average over the western half of Europe and in the south (0 to $-2 \mu\text{g m}^{-3}$). They are above average in central Europe (0 to $+2 \mu\text{g m}^{-3}$).

WT10 is characterized by a positive anomaly of PSL over the northern part of the British Isles. This WT is associated with above average temperatures in northern Europe and with below average temperatures elsewhere. Precipitations are below average over most of Europe, except in the south. $PM_{2.5}$ concentrations are above average in western Europe (0 to $+6 \mu\text{g m}^{-3}$) and below average elsewhere (0 to $-6 \mu\text{g m}^{-3}$).

WT11 is characterized by a negative anomaly of PSL over Greenland and a positive one that extends from the Quebec coasts to Scandinavia. This WT is associated with above average temperatures over Scandinavia and eastern Europe and with below average temperatures elsewhere. Precipitations are below average in western Europe and in southern Scandinavia. They are above average elsewhere. $PM_{2.5}$ concentrations are above average in France and Spain (0 to $+6 \mu\text{g m}^{-3}$). They are below average elsewhere (0 to $-6 \mu\text{g m}^{-3}$).

WT12 is characterized by a strong negative anomaly over the northern part of the British Isles. This WT is associated with below average temperatures, except over the westernmost part of Europe (Portugal, Ireland, etc.). Precipitations are above average over western, central, and northern Europe. They are below average in the south and the east. $PM_{2.5}$ concentrations are below average in western, southern, and central Europe (0 to $-8 \mu\text{g m}^{-3}$) and above average in the north and in the east (0 to $+2 \mu\text{g m}^{-3}$).

WT13 is characterized by a strong negative anomaly of PSL over the Atlantic Ocean and by a positive one over Greenland. This WT is associated with above average temperatures over the southern half of Europe and with below average temperatures over the northern half. Precipitations are above average over

most of Europe. They are below average over the Norwegian coasts and in southeastern Europe. $PM_{2.5}$ concentrations are below average over most of Europe (0 to $-6 \mu\text{g m}^{-3}$).

G3. JJA Weather Types

WT0 is characterized by a negative anomaly of PSL over Ireland. This WT is associated with above average precipitations over western and central Europe, over the Iberian Peninsula, and Scandinavia. Precipitations are below average over the Norwegian coasts and in southeastern Europe. Temperatures are below average in westernmost and easternmost parts of Europe. They are above average elsewhere. $PM_{2.5}$ concentrations are above average (0 to $+2 \mu\text{g m}^{-3}$) in northern Europe and below average elsewhere (0 to $-6 \mu\text{g m}^{-3}$).

WT1 is characterized by a positive anomaly of PSL over the north of the Atlantic Ocean. This WT is associated with above average temperatures in southern and southeastern Europe, and with below average temperatures elsewhere. Precipitations are above average in central Europe, Italy, Spain, and central Scandinavia. $PM_{2.5}$ concentrations are above average in central Europe and northern France (0 to $+8 \mu\text{g m}^{-3}$). They are below average elsewhere (0 to $-4 \mu\text{g m}^{-3}$).

WT2 is characterized by a negative anomaly of PSL over Scandinavia. Such a positive anomaly leads to above average precipitations over northern and eastern Europe. Temperatures are below average over most of Europe, except over the easternmost part. $PM_{2.5}$ concentrations are below average (0 to $-10 \mu\text{g m}^{-3}$) over most of Europe, except in the east (0 to $-2 \mu\text{g m}^{-3}$).

WT3 is characterized by a positive anomaly of PSL over Greenland and by a negative anomaly over the North Sea. This WT is associated with below average temperatures and above average precipitations over most of Europe, except in southern and eastern Europe, where temperatures are above average and precipitations are below average. $PM_{2.5}$ concentrations are below average (0 to $-10 \mu\text{g m}^{-3}$).

WT4 is characterized by a negative anomaly of PSL which extends from Greenland to the Azores and by a positive anomaly over Scandinavia. Such a positive anomaly leads to below average precipitations, except in southeastern Europe. Temperatures are above average over most of Europe, except in southeastern and eastern Europe. $PM_{2.5}$ concentrations are above average over most of Europe (0 to $+10 \mu\text{g m}^{-3}$). They are below average (0 to $-2 \mu\text{g m}^{-3}$) over some localized areas in central, eastern, and southern Europe.

WT5 is characterized by a negative anomaly of PSL over Greenland. Temperatures are below average in southeastern and central Europe and in the westernmost parts of Europe. Precipitations are above average over France and southern Scandinavia and from Slovakia to Ukraine. $PM_{2.5}$ concentrations are below average over most of Europe (0 to $-4 \mu\text{g m}^{-3}$). They are above average (0 to $+2 \mu\text{g m}^{-3}$) over some localized areas in central, southern, and northern Europe.

WT6 is characterized by a positive anomaly of PSL which extends from Greenland to the UK. This WT is associated with above average temperatures in northern, central, and western Europe and with below average temperatures in southern and eastern Europe. Precipitations are below average in Scandinavia, Italy, and over the southeast. $PM_{2.5}$ concentrations vary at $\pm 2 \mu\text{g m}^{-3}$ around the average.

WT7 is characterized by a negative anomaly of PSL over the northern part of the Atlantic Ocean. Such a negative anomaly leads to above average precipitations over the western half of Europe and to below average precipitations in the east and southeast. Temperatures are below average in western, eastern, and southern Europe. They are above average in northern and central Europe. $PM_{2.5}$ concentrations have a similar response: they are above average in central and northern Europe (0 to $+4 \mu\text{g m}^{-3}$) and below average in western and eastern Europe (0 to $-4 \mu\text{g m}^{-3}$).

WT8 is characterized by a negative anomaly of PSL over the Greenland Sea and by a positive anomaly which extends from the Quebec coasts to France. This WT is associated with above average precipitations in northern Europe, Italy, Austria, and Czech Republic. Precipitations are below average elsewhere. Temperatures are below average over the Atlantic coasts and above average elsewhere. $PM_{2.5}$ concentrations are above average in central Europe (0 to $+6 \mu\text{g m}^{-3}$) and below average elsewhere (0 to $-6 \mu\text{g m}^{-3}$).

WT9 is characterized by a positive anomaly over the North Sea and by a negative one over the Labrador Sea. This WT is associated with above average temperatures over the westernmost and northernmost parts of Europe. Precipitations are above average over southwestern Norway and western and eastern Europe. $PM_{2.5}$ concentrations are above average over northwestern France, Benelux, Germany, Portugal, and northern Italy (0 to $+8 \mu\text{g m}^{-3}$). They are below average elsewhere (0 to $-2 \mu\text{g m}^{-3}$).

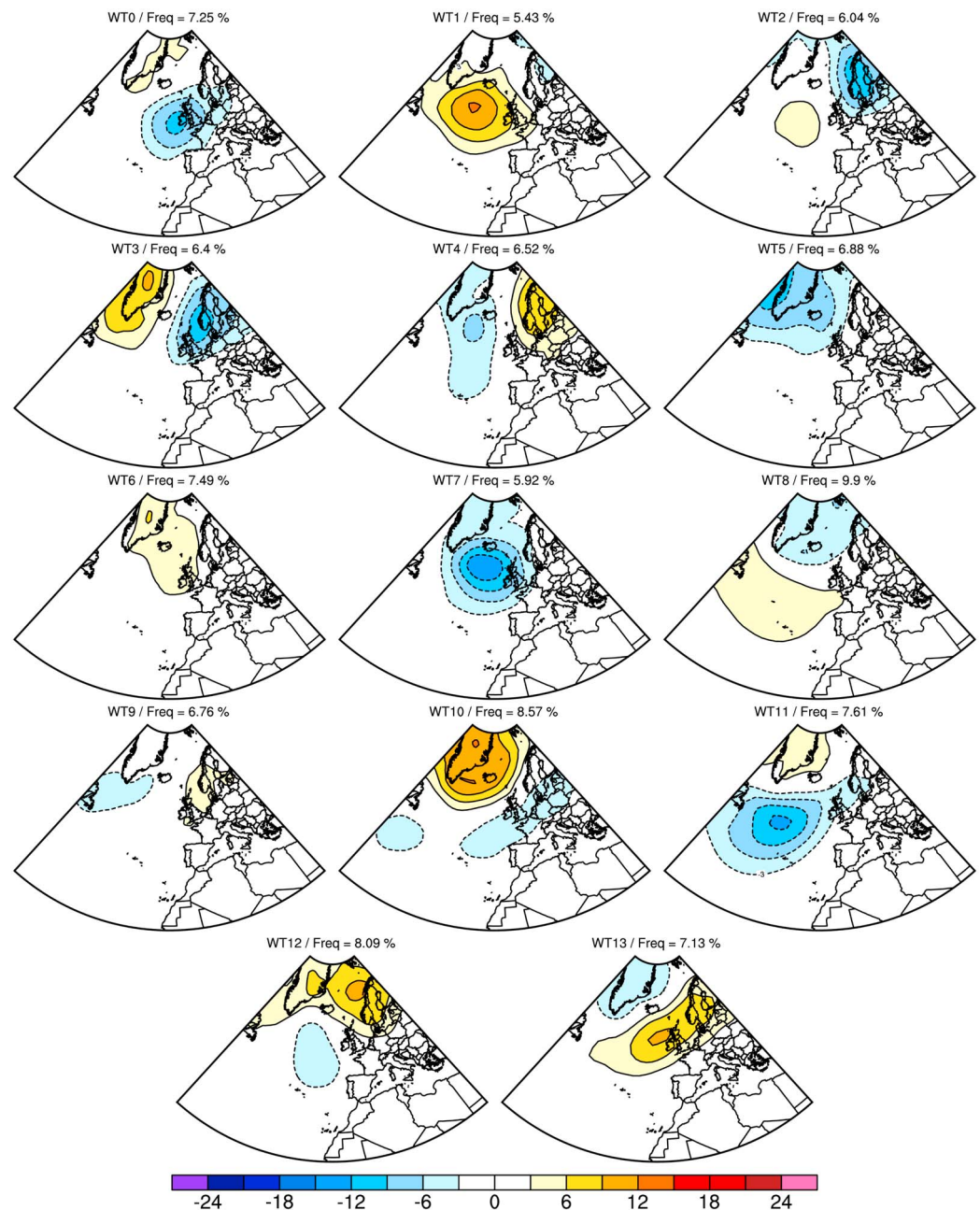


Figure G3. PSL anomalies (expressed in hPa) of the 14 WTs in JJA, built on the learning period (2000–2008). The frequency of each WT is stated above the corresponding WT.

WT10 is characterized by a positive anomaly of PSL over Greenland and by a negative one over Europe. Such a negative anomaly leads to above average precipitations over most of Europe, except over the Norwegian coasts, southeastern Europe, and the Iberian Peninsula. Temperatures are below average over most of Europe, except over southern Norway and southeastern Europe. $PM_{2.5}$ concentrations are above average in the UK, in southeastern Europe, and over some localized areas in northern and central Europe (0 to $+6 \mu g m^{-3}$). They are below average elsewhere (0 to $-6 \mu g m^{-3}$).

WT11 is characterized by a positive anomaly of PSL over Greenland and by a negative one over the Atlantic Ocean. This WT is associated with below average precipitations over southeastern and southwestern Europe, northern Scandinavia, and from France to Poland. Temperatures are above average in southern,

southeastern, central, and western Europe. $PM_{2.5}$ concentrations are above average from Italy to Greece (0 to $+6 \mu\text{g m}^{-3}$) and are below average in central Europe (0 to $-6 \mu\text{g m}^{-3}$).

WT12 is characterized by a positive anomaly of PSL which extends from Greenland to Scandinavia. Such a positive anomaly leads to below average precipitations in western, central, and northern Europe. Temperatures are above average over most of Europe, except in Portugal and in the southeast. $PM_{2.5}$ concentrations are above average in western, northern, and southwestern Europe (0 to $+8 \mu\text{g m}^{-3}$). They are below average elsewhere (0 to $-2 \mu\text{g m}^{-3}$).

WT13 is characterized by a negative anomaly of PSL over Greenland and by a positive one over the north of the British Isles. This WT is associated with below average precipitations over the northern half of Europe and with above average precipitations over the southern half. Temperatures are below average over the southern half of Europe and above average elsewhere. $PM_{2.5}$ concentrations are above average in northwestern Europe (0 to $+6 \mu\text{g m}^{-3}$) and below average elsewhere (0 to $-2 \mu\text{g m}^{-3}$).

G4. SON Weather Types

WT0 is characterized by a strong negative anomaly of PSL over the Atlantic Ocean. This WT is associated with above average precipitations over western Europe and southern Scandinavia. Precipitations are below average in central, eastern, and southern Europe. Temperatures are above average over most of Europe, except in the northeast. $PM_{2.5}$ concentrations are above average in western and southeastern Europe (0 to $+8 \mu\text{g m}^{-3}$) and are below average elsewhere (0 to $-6 \mu\text{g m}^{-3}$).

WT1 is characterized by a negative anomaly of PSL over the Atlantic Ocean and by a positive one over the Norwegian Sea. Precipitations are below average over northern, central, and northeastern Europe and over France, Benelux, the UK, and Ireland. They are above average over southern and southeastern Europe. Temperatures are above average over western and southeastern Europe. They are below average in central, northern, and northeastern Europe and over the Iberian Peninsula. $PM_{2.5}$ concentrations are above average over western Europe (0 to $+6 \mu\text{g m}^{-3}$) and are below average elsewhere (0 to $-2 \mu\text{g m}^{-3}$), especially in the east.

WT2 is characterized by a positive anomaly of PSL over the northern part of the British Isles. This WT is associated with below average temperatures over Europe, except over Ireland, Portugal, and the northern UK. Precipitations are below average in western Europe, over the Iberian Peninsula, northern Italy, and over southern and eastern Scandinavia. They are above average in eastern and southeastern Europe. $PM_{2.5}$ concentrations are below average over most of Europe (0 to $-8 \mu\text{g m}^{-3}$). They are above average (0 to $+6 \mu\text{g m}^{-3}$) in western Europe.

WT3 is characterized by a strong negative anomaly of PSL over the North Sea. Precipitations are above average over northern, central, and western Europe. They are below average over southern and eastern Europe. Temperatures are above average over most of Europe. $PM_{2.5}$ concentrations are below average (0 to $-8 \mu\text{g m}^{-3}$) over most of Europe. They are above average over northern Italy and Ukraine (0 to $+6 \mu\text{g m}^{-3}$).

WT4 is characterized by a strong negative anomaly of PSL over the North Sea and a positive one over southern Greenland. This WT is associated with above average precipitations over Europe, except over the Norwegian coasts and in the southeast. Temperatures are above average over southeastern, central, and eastern Europe. They are below average in western Europe. $PM_{2.5}$ concentrations are below average (0 to $-10 \mu\text{g m}^{-3}$) over northern, central, and southwestern Europe. They are above average over eastern and southeastern Europe (0 to $+10 \mu\text{g m}^{-3}$).

WT5 is characterized by a negative anomaly of PSL over Scandinavia and a positive one over the Atlantic Ocean. Precipitations are below average over western, southern, and eastern Europe. They are above average over central, northern, and northeastern Europe. Temperatures are below average over most of Europe, except over some localized areas in northern, central, and western Europe. $PM_{2.5}$ concentrations are below average over most of Europe (0 to $-6 \mu\text{g m}^{-3}$).

WT6 is characterized by a positive anomaly of PSL over the Atlantic Ocean and by a positive one over Greenland. Temperatures are below average over Europe. Precipitations are above average over southern and eastern Europe and over the Norwegian coasts. They are below average elsewhere. $PM_{2.5}$

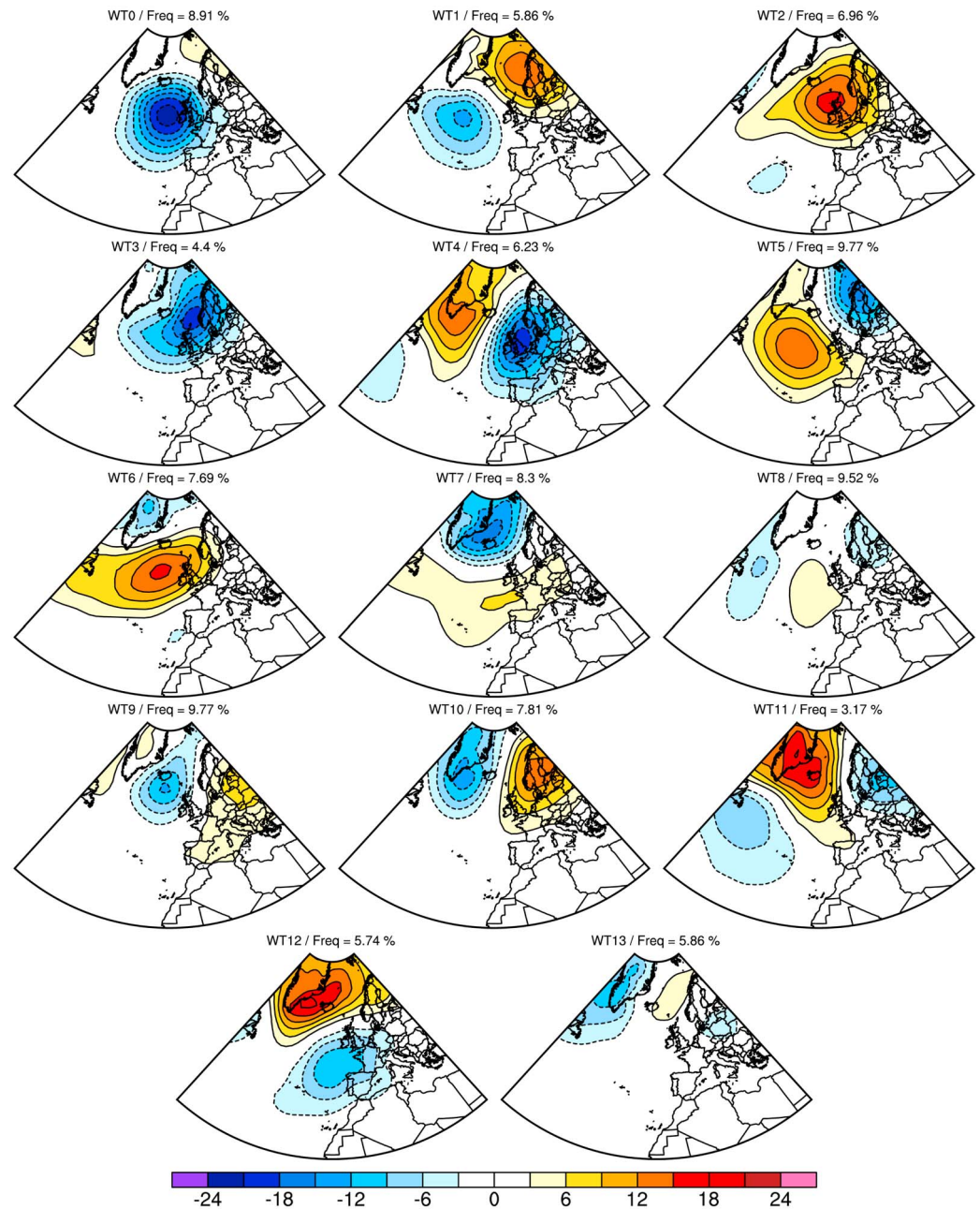


Figure G4. PSL anomalies (expressed in hPa) of the 14 WTs in SON, built on the learning period (2000–2008). The frequency of each WT is stated above the corresponding WT.

concentrations are below average over most of Europe (0 to $-8 \mu\text{g m}^{-3}$), except over France and the UK (0 to $+2 \mu\text{g m}^{-3}$).

WT7 is characterized by a strong anomaly of PSL over the Denmark Strait and by a negative one which extends from the Quebec coasts to eastern Europe. Precipitations are below average over western, central, and southwestern Europe. They are above average in northern and southeastern Europe. Temperatures are above average over northern Europe, the British Isles, and the western part of the Iberian Peninsula. They are below average elsewhere. $\text{PM}_{2.5}$ concentrations vary at $\pm 2 \mu\text{g m}^{-3}$ around the average.

WT8 is characterized by a positive anomaly of PSL over the Atlantic Ocean and by two negative anomalies: one over the Labrador Sea and one over Scandinavia. Precipitations are below average over the Iberian Peninsula, southeastern Europe, Italy, and the British Isles. They are above average elsewhere. Temperatures

are below average over France and over southern, eastern, and northern Europe. They are above average elsewhere. $PM_{2.5}$ concentrations are around the average values over Europe.

WT9 is characterized by a negative anomaly of PSL over Iceland and by two positive anomalies: one over eastern Europe and one over North America. This WT is associated with below average precipitations over Europe, except over the Norwegian coasts, Italy, and the British Isles. Temperatures are above average over Europe, except over southeastern Europe. $PM_{2.5}$ concentrations are above average in central Europe, the southern UK, and Scandinavia (0 to $+6 \mu g m^{-3}$). They are below average elsewhere (0 to $-2 \mu g m^{-3}$).

WT10 is characterized by a positive anomaly of PSL over Scandinavia and by negative one over Greenland. This WT is associated with below average precipitations in western, central, and northern Europe and with above average precipitations in southern and eastern Europe. Temperatures are below average. $PM_{2.5}$ concentrations are above average over western Europe, the Iberian Peninsula, and southern Scandinavia (0 to $+6 \mu g m^{-3}$). They are below average in central, eastern, and southeastern Europe (0 to $-4 \mu g m^{-3}$).

WT11 is characterized by a positive anomaly of PSL over Scandinavia and by two negative anomalies: one over the Quebec coasts and one over the Baltics. This WT is associated with above average precipitations over most of Europe. Such precipitations are below average over the Iberian Peninsula, Scandinavia, and over the Mediterranean Sea. Temperatures are below average over Europe, except over southeastern and southwestern Europe. $PM_{2.5}$ concentrations are below average over Europe (0 to $-10 \mu g m^{-3}$), except over northern Scandinavia and the westernmost part of Europe (0 to $+2 \mu g m^{-3}$).

WT12 is characterized by a positive anomaly over the Denmark Strait and by a negative one over western Europe. This WT is associated with above average precipitations over eastern and western Europe, southern Scandinavia, Italy, and the Iberian Peninsula. They are below average over northern, central, and southwestern Europe. Temperatures are below average over Europe, except over France, Spain, and southeastern Europe. $PM_{2.5}$ concentrations are above average over northern Scandinavia and Germany (0 to $+2 \mu g m^{-3}$). They are below average elsewhere (0 to $-4 \mu g m^{-3}$).

WT13 is characterized by a negative anomaly over the Davis Strait and by a positive one over the Norwegian Sea. This WT is associated with below average temperatures over northern and western Europe and with above average temperatures over eastern, central, and southern Europe. Precipitations are above average in western and southeastern Europe and over the Norwegian coasts. They are below average elsewhere. $PM_{2.5}$ concentrations are above average over southwestern, southeastern, and eastern Europe and in eastern Scandinavia (0 to $+6 \mu g m^{-3}$). They are below average elsewhere (0 to $-4 \mu g m^{-3}$).

Appendix H: Weather Type Frequencies

Table H1. Frequency of the Weather Types Over the Historical Period (1975–2004) for the CNRM-CM5 Model (%)

	DJF	MAM	JJA	SON
WT0	3.7	3.3	14.3	7.3
WT1	5.2	10.8	6	7.2
WT2	11.7	17.4	14.4	3.4
WT3	6.7	10.5	0.8	4.7
WT4	9.7	5.8	5.5	7
WT5	16.2	2.1	1.4	8
WT6	5.4	6.8	2.4	4.3
WT7	6.9	6.3	7.2	7.6
WT8	5.4	4.4	7.9	3.5
WT9	5.1	15.4	9.6	12.6
WT10	3.7	6.4	3.7	4.2
WT11	8.2	1.5	6.1	7.6
WT12	3.8	7.1	15.9	14.4
WT13	8.3	2.2	4.8	8.2

Table H2. Frequency of the Weather Types for the RCP4.5 Scenario From the CNRM-CM5 Model (%) Over Two Future Periods (2020–2049 and 2070–2099)

	2020–2049				2070–2099			
	DJF	MAM	JJA	SON	DJF	MAM	JJA	SON
WT0	4.7	4.4	12.9	6.6	5	5.6	12	6.4
WT1	5.4	12.4	8.4	8	6.5	9.8	8.6	7.1
WT2	11.6	17.2	15.9	4.4	10.2	18	17.7	4
WT3	9.1	9.1	1.3	3.6	7.6	9.6	0.9	4.8
WT4	11.9	3.3	4.5	4.9	8.7	3.3	5.8	5.5
WT5	12.7	2.3	1.5	6.6	19.1	3	2.1	7.3
WT6	6.2	4.9	2.1	4.4	5.5	6.1	1.9	5.5
WT7	6	6.9	6.3	11	5.9	3.8	6	10.9
WT8	3.4	3.3	10.7	2.8	4.4	4.2	11.7	2.5
WT9	5	13.5	9.8	14.9	4.6	15.1	11.2	16
WT10	5.9	10.2	4.7	5	5.4	10.7	2.5	5.2
WT11	5.3	1.5	3.3	7.2	6.6	1.4	3.3	5
WT12	4.5	7.1	13.4	11.1	2.8	5.5	10.1	10.1
WT13	8.3	3.9	5.2	9.5	7.7	3.9	6.2	9.7

Table H3. Frequency of the Weather Types for the RCP8.5 Scenario From the CNRM-CM5 Model (%) Over Two Future Periods (2020–2049 and 2070–2099)

	2020–2049				2070–2099			
	DJF	MAM	JJA	SON	DJF	MAM	JJA	SON
WT0	3.9	4	11.4	4.9	4.1	4.4	9.6	5.2
WT1	4.6	11.9	8	7.3	5.8	10.7	7.9	6.3
WT2	12	18.7	15.7	4.7	9.7	20.9	17.8	5.3
WT3	7.8	10.4	1	4.4	8.6	9.6	1.2	5.2
WT4	9.3	3.9	5.1	6.5	10.6	3.3	4.7	3.9
WT5	18.8	3.2	2	7.8	18.3	2.6	1.9	9.2
WT6	5.4	6.7	1.7	6.3	7.2	5.9	1.7	6.5
WT7	6.1	3.8	6.5	8.8	5.1	3.2	5.8	11.6
WT8	4.5	5.3	11.2	3.3	3	4.7	11.3	1.9
WT9	5.1	13.3	13.4	14.4	4.7	13.8	13.4	15.7
WT10	4.5	9.2	2.6	4.7	5.2	10.8	3.3	4.9
WT11	8	1.1	4.1	7	6	2.1	4.5	5.3
WT12	2.7	5.5	11.3	10.3	3.8	5.1	9.5	8.9
WT13	7.3	3	6	9.6	7.9	2.9	7.4	10.1

Appendix I: Computational Cost

Table I1. Differences Between the Computational Costs for a Simulation With Polyphemus/Polair3D CTM and This Statistical Model Over Europe

	Polyphemus/Polair3D	Statistical approach
Length of simulated period	1 year	30 years
Preprocessing	5 days	1 day
Processing	19 days	3 h
Postprocessing	1 day	1 day
Total	25 days	2 to 3 days

Acknowledgments

The authors would like to thank the World Climate Research Programme's Working Group on Coupled Modelling for their role in making available the CNRM-CM5 data obtained in the context of the Coupled Model Intercomparison Project Phase 5.

References

- Avise, J., J. Chen, B. Lamb, C. Wiedinmyer, A. Guenther, E. Salathé, and C. Mass (2009), Attribution of projected changes in summertime US ozone and PM_{2.5} concentrations to global changes, *Atmos. Chem. Phys.*, *9*(4), 1111–1124.
- Boé, J., L. Terray, F. Habets, and E. Martin (2006), A simple statistical-dynamical downscaling scheme based on weather types and conditional resampling, *J. Geophys. Res.*, *111*, D23106, doi:10.1029/2005JD006889.
- Boylan, J. W., and A. G. Russell (2006), PM and light extinction model performance metrics, goals, and criteria for three-dimensional air quality models, *Atmos. Environ.*, *40*(26), 4946–4959.
- Cattiaux, J., H. Douville, and Y. Peings (2013), European temperatures in CMIP5: Origins of present-day biases and future uncertainties, *Clim. Dyn.*, *41*, 2889–2907, doi:10.1007/s00382-013-1731-y.
- Chen, J., et al. (2009), The effects of global changes upon regional ozone pollution in the United States, *Atmos. Chem. Phys.*, *9*(4), 1125–1141.
- Colette, A., et al. (2013), European atmosphere in 2050, a regional air quality and climate perspective under CMIP5 scenarios, *Atmos. Chem. Phys.*, *13*(15), 7451–7471.
- Couvidat, F., É. Debry, K. Sartelet, and C. Seigneur (2012), A hydrophilic/hydrophobic organic (H₂O) aerosol model: Development, evaluation and sensitivity analysis, *J. Geophys. Res.*, *117*, D10304, doi:10.1029/2011JD017214.
- Dawson, J., P. Adams, and S. Pandis (2007), Sensitivity of PM_{2.5} to climate in the eastern US: A modeling case study, *Atmos. Chem. Phys.*, *7*(16), 4295–4309.
- Dawson, J. P., P. N. Racherla, B. H. Lynn, P. J. Adams, and S. N. Pandis (2009), Impacts of climate change on regional and urban air quality in the eastern United States: Role of meteorology, *J. Geophys. Res.*, *114*, D05308, doi:10.1029/2008JD009849.
- Galindo, N., M. Varea, J. Gil-Moltó, E. Yubero, and J. Nicolás (2011), The influence of meteorology on particulate matter concentrations at an urban Mediterranean location, *Water Air Soil Pollut.*, *215*(1-4), 365–372.
- Heald, C., et al. (2008), Predicted change in global secondary organic aerosol concentrations in response to future climate, emissions, and land use change, *J. Geophys. Res.*, *113*, D05211, doi:10.1029/2007JD009092.
- Hedegaard, G. B., J. H. Christensen, and J. Brandt (2013), The relative importance of impacts from climate change vs. emissions change on air pollution levels in the 21st century, *Atmos. Chem. Phys.*, *13*(7), 3569–3585.
- Jacob, D. J., and D. A. Winner (2009), Effect of climate change on air quality, *Atmos. Environ.*, *43*(1), 51–63.
- Jiang, X., Z.-L. Yang, H. Liao, and C. Wiedinmyer (2010), Sensitivity of biogenic secondary organic aerosols to future climate change at regional scales: An online coupled simulation, *Atmos. Environ.*, *44*(38), 4891–4907.
- Jiménez-Guerrero, P., J. Jose Gomez-Navarro, S. Jerez, R. Lorente-Plazas, J. A. Garcia-Valero, and J. P. Montavez (2011), Isolating the effects of climate change in the variation of secondary inorganic aerosols (SIA) in Europe for the 21st century (1991–2100), *Atmos. Environ.*, *45*(4), 1059–1063.
- Jiménez-Guerrero, P., J. P. Montávez, J. J. Gómez-Navarro, S. Jerez, and R. Lorente-Plazas (2012), Impacts of climate change on ground level gas-phase pollutants and aerosols in the Iberian Peninsula for the late XXI century, *Atmos. Environ.*, *55*, 483–495.
- Kelly, J., P. Makar, and D. Plummer (2012), Projections of mid-century summer air-quality for North America: Effects of changes in climate and precursor emissions, *Atmos. Chem. Phys.*, *12*(12), 5367–5390.
- Lam, Y., J. Fu, S. Wu, and L. Mickley (2011), Impacts of future climate change and effects of biogenic emissions on surface ozone and particulate matter concentrations in the United States, *Atmos. Chem. Phys.*, *11*(10), 4789–4806.
- Lecœur, É., and C. Seigneur (2013), Dynamic evaluation of a multi-year model simulation of particulate matter concentrations over Europe, *Atmos. Chem. Phys.*, *13*(8), 4319–4337.
- Liao, H., W.-T. Chen, and J. H. Seinfeld (2006), Role of climate change in global predictions of future tropospheric ozone and aerosols, *J. Geophys. Res.*, *111*, D12304, doi:10.1029/2005JD006852.
- Mahmud, A., M. Tyree, D. Cayan, N. Motallebi, and M. J. Kleeman (2008), Statistical downscaling of climate change impacts on ozone concentrations in California, *J. Geophys. Res.*, *113*, D21103, doi:10.1029/2007JD009534.
- Mahmud, A., M. Hixson, J. Hu, Z. Zhao, S.-H. Chen, and M. Kleeman (2010), Climate impact on airborne particulate matter concentrations in California using seven year analysis periods, *Atmos. Chem. Phys.*, *10*(22), 11,097–11,114.
- Manders, A., E. van Meijgaard, A. Mues, R. Kranenburg, L. van Ulft, and M. Schaap (2012), The impact of differences in large-scale circulation output from climate models on the regional modeling of ozone and pm, *Atmos. Chem. Phys.*, *12*(20), 9441–9458.
- Ménégoz, M., V. Guemas, D. Salas y Melia, and A. Voldoire (2010), Winter interactions between aerosols and weather regimes in the North Atlantic European region, *J. Geophys. Res.*, *115*, D09201, doi:10.1029/2009JD012480.
- Michelangeli, P.-A., R. Vautard, and B. Legras (1995), Weather regimes: Recurrence and quasi stationarity, *J. Atmos. Sci.*, *52*(8), 1237–1256.
- Najac, J. (2008), Impacts du changement climatique sur le potentiel éolien en France : Une étude de régionalisation, PhD thesis, Université Toulouse III - Paul Sabatier.
- Najac, J., J. Boé, and L. Terray (2009), A multi-model ensemble approach for assessment of climate change impact on surface winds in France, *Clim. Dyn.*, *32*(5), 615–634.
- Pagé, C., L. Terray, and J. Boé (2009), dsclim: A software package to downscale climate scenarios at regional scale using a weather-typing based statistical methodology, *Tech. Rep.* SUC au CERFACS, URA CERFACS/CNRS No1875, Toulouse, France.
- Philipp, A., et al. (2010), Cost733cat—A database of weather and circulation type classifications, *Phys. Chem. Chem. Phys.*, *35*(9), 360–373.
- Pye, H., H. Liao, S. Wu, L. J. Mickley, D. J. Jacob, D. K. Henze, and J. Seinfeld (2009), Effect of changes in climate and emissions on future sulfate-nitrate-ammonium aerosol levels in the United States, *J. Geophys. Res.*, *114*, D01205, doi:10.1029/2008JD010701.
- Querol, X., et al. (2004), Speciation and origin of PM₁₀ and PM_{2.5} in selected European cities, *Atmos. Environ.*, *38*(38), 6547–6555.
- Racherla, P. N., and P. J. Adams (2006), Sensitivity of global tropospheric ozone and fine particulate matter concentrations to climate change, *J. Geophys. Res.*, *111*, D24103, doi:10.1029/2005JD006939.
- Riahi, K., S. Rao, V. Krey, C. Cho, V. Chirkov, G. Fischer, G. Kindermann, N. Nakicenovic, and P. Rafaj (2011), RCP8.5—A scenario of comparatively high greenhouse gas emissions, *Clim. Change*, *109*(1-2), 33–57.
- Singh, A., and A. Palazoglu (2012), Climatic variability and its influence on ozone and PM pollution in 6 non-attainment regions in the United States, *Atmos. Environ.*, *51*, 212–224.
- Steiner, A. L., S. Tonse, R. C. Cohen, A. H. Goldstein, and R. A. Harley (2006), Influence of future climate and emissions on regional air quality in California, *J. Geophys. Res.*, *111*, D18303, doi:10.1029/2005JD006935.
- Tagaris, E., K. Manomaiphiboon, K.-J. Liao, L. R. Leung, J.-H. Woo, S. He, P. Amar, and A. G. Russell (2007), Impacts of global climate change and emissions on regional ozone and fine particulate matter concentrations over the United States, *J. Geophys. Res.*, *112*, D14312, doi:10.1029/2006JD008262.

- Tai, A., L. Mickley, D. Jacob, E. Leibensperger, L. Zhang, J. Fisher, and H. Pye (2012a), Meteorological modes of variability for fine particulate matter (PM_{2.5}) air quality in the United States: Implications for PM_{2.5} sensitivity to climate change, *Atmos. Chem. Phys.*, *12*(6), 3131–3145.
- Tai, A. P., L. J. Mickley, and D. J. Jacob (2010), Correlations between fine particulate matter (PM_{2.5}) and meteorological variables in the United States: Implications for the sensitivity of PM_{2.5} to climate change, *Atmos. Environ.*, *44*(32), 3976–3984.
- Tai, A. P., L. J. Mickley, and D. J. Jacob (2012b), Impact of 2000–2050 climate change on fine particulate matter (PM_{2.5}) air quality inferred from a multi-model analysis of meteorological modes, *Atmos. Chem. Phys.*, *12*(23), 11,329–11,337.
- Thishan Dharshana, K., S. Kravtsov, and J. D. Kahl (2010), Relationship between synoptic weather disturbances and particulate matter air pollution over the United States, *J. Geophys. Res.*, *115*, D24219, doi:10.1029/2010JD014852.
- Thomson, A. M., et al. (2011), RCP4.5: A pathway for stabilization of radiative forcing by 2100, *Clim. Change*, *109*(1–2), 77–94.
- Vautard, R. (1990), Multiple weather regimes over the North Atlantic: Analysis of precursors and successors, *Mon. Weather Rev.*, *118*(10), 2056–2081.
- Volz, A., et al. (2013), The CNRM-CM5.1 global climate model: Description and basic evaluation, *Clim. Dyn.*, *40*(9–10), 2091–2121, doi:10.1007/s00382-011-1259-y.
- Zhang, Y., X.-M. Hu, L. R. Leung, and W. I. Gustafson (2008), Impacts of regional climate change on biogenic emissions and air quality, *J. Geophys. Res.*, *113*, D18310, doi:10.1029/2008JD009965.